INFORMATION TO USERS

The most advanced technology has been used to photograph and reproduce this manuscript from the microfilm master. UMI films the text directly from the original or copy submitted. Thus, some thesis and dissertation copies are in typewriter face, while others may be from any type of computer printer.

The quality of this reproduction is dependent upon the quality of the copy submitted. Broken or indistinct print, colored or poor quality illustrations and photographs, print bleedthrough, substandard margins, and improper alignment can adversely affect reproduction.

In the unlikely event that the author did not send UMI a complete manuscript and there are missing pages, these will be noted. Also, if unauthorized copyright material had to be removed, a note will indicate the deletion.

Oversize materials (e.g., maps, drawings, charts) are reproduced by sectioning the original, beginning at the upper left-hand corner and continuing from left to right in equal sections with small overlaps. Each original is also photographed in one exposure and is included in reduced form at the back of the book.

Photographs included in the original manuscript have been reproduced xerographically in this copy. Higher quality 6" x 9" black and white photographic prints are available for any photographs or illustrations appearing in this copy for an additional charge. Contact UMI directly to order.

U·M·I

University Microfilms International
A Bell & Howell Information Company
300 North Zeeb Road, Ann Arbor, MI 48106-1346 USA
313/761-4700 800/521-0600

Order Number 9110569

Computer simulation of arterial blood flow

Stergiopulos, Nikolaos, Ph.D.

Iowa State University, 1990

U·M·I
300 N. Zeeb Rd.
Ann Arbor, MI 48106

Computer simulation of arterial blood flow

by

Nikolaos Stergiopulos

A Dissertation Submitted to the

Graduate Faculty in Partial Fulfillment of the

Requirements for the Degree of

DOCTOR OF PHILOSOPHY

Departments: Aerospace Engineering and Engineering Mechanics
Biomedical Engineering
Co-majors: Engineering Mechanics
Biomedical Engineering

Approved:

Signature was redacted for privacy.

Signature was redacted for privacy.

In Charge of Major Work

Signature was redacted for privacy.

Signature was redacted for privacy.

For the Major Departments

Signature was redacted for privacy.

For the Graduate College

Members of the Committee:

Signature was redacted for privacy.

Iowa State University
Ames, Iowa
1990

TABLE OF CONTENTS

LIST OF TABLES

LIST OF FIGURES

ACKNOWLEDGEMENTS

I am greatly indebted to Professor Donald F. Young. Throughout my studies at ISU, Professor Young has been for me a great teacher and an endless source of knowledge, encouragement, and support. My sincere gratitude also to Professor Thomas R. Rogge for his assistance and guidance.

My thanks to Professors David L. Carlson, Bruce R. Munson, and Theodore H. Okiishi for serving in my committee. My thanks are extended to the departments of Aerospace Engineering and Engineering Mechanics and Biomedical Engineering for all the help I received during my studies.

This work is dedicated to my lovely wife Soula and my wonderful son Constantinos. They made it all worth it.

NOMENCLATURE

a_o	wave propagation velocity
A	cross sectional area
A_o	cross sectional area at reference pressure
A_s	obstructed cross sectional lumen area
b_x	body-force vector component in the axial direction
B_1	wall shear stress model coefficient
c	wave propagation velocity
c_v	coefficient of viscous term in shear stress model
c_u	coefficient of inertia term in shear stress model
C'	arterial compliance
C'_o	linear compliance coefficient
C'_1	non-linear compliance coefficient
C'^{l}_{o}	modified linear compliance coefficient
C'^{l}_{1}	modified non-linear compliance coefficient
C'_T	volume compliance of terminal impedance
C'_{vol}	volume compliance of arterial segment
$C'_{vol,res}$	residual volume compliance
D	arterial diameter
E	Young's modulus of elasticity of arterial wall
$[K]$	global stiffness matrix
$[K_e]$	element stiffness matrix
K_t	coefficient of turbulence term in stenosis equation
K_u	coefficient of unsteady flow term in stenosis equation
K_v	coefficient of viscous term in stenosis equation
L	finite element length

L_s	length of stenosis
$\{N(x)\}$	shape function vector
p	pressure
$\{p\}$	nodal pressures vector
$\bar{p}$	mean pressure
p_e	external pressure
p_o	reference pressure
Q	flow
$\{Q\}$	nodal flows vector
$\bar{Q}$	mean flow
R_1	proximal resistance of terminal impedance
R_2	distal resistance of terminal impedance
R_p	Poiseuille resistance
R_T	total resistance of terminal impedance
S	seepage coefficient
t	time
U	instantaneous cross sectional average velocity
V_{art}	volume of arterial segment
$\vec{V}$	velocity vector
x	axial length coordinate
$X_{i,j}$	nodal coordinates
α	dimensionless frequency (Womersley alpha parameter)
β	experimental arterial elasticity constant
$\{\delta\}$	vector of unknown pressures and flows

Δt	time increment
Δx	spatial element length
λ	dimensionless velocity profile coefficient
λ_i	i^{th} eigenvalue of a matrix
μ	dynamic viscosity of the fluid
ν	kinematic viscosity of the fluid
ρ	fluid density
ψ	seepage through the arterial wall
ω	basic circular frequency of the pulse

CHAPTER 1. INTRODUCTION

Cardiovascular diseases and disorders are the leading causes of death in the developed and industrialized societies. Two of the most common cardiovascular diseases are *arteriosclerosis* and *atherosclerosis.* Arteriosclerosis relates to the loss of elasticity of the arterial wall through thickening, hardening, or calcification. Atherosclerosis relates to the lipid deposition in the subintimal layer of the artery, causing the development of localized inflammatory lesions called *atheromatous plaques* or simply *atheromas.* Atheromas often protrude into the lumen of the artery causing localized constrictions, usually termed *stenoses.* Stenoses are potentially harmful in two ways: a) their rough surface may cause blood clots to develop, resulting in the formation of embolus or thrombus, and b) the increased resistance to flow due to stenosis does not allow adequate blood supply to peripheral tissues (Guyton, 1976). Some additional characteristic examples of acute clinical conditions associated with cardiovascular disease include (Raines, 1972):

myocardial infarction in which a portion of the heart muscle becomes damaged because of interruption of its blood supply by atherosclerotic occlusion, acute thrombosis, or coronary artery embolism.

stroke in which the blood supply to portions of the brain is suddenly reduced by cerebral arterial occlusion or embolus.

gangrene in which the blood supply to a peripheral tissue mass is reduced due to arterial occlusion and the tissue dies.

The value of course of the early detection of the development of atherosclerotic lesions, where pharmacologic treatment can be used instead of expensive and complicated surgical procedures, cannot be overemphasized.

The diagnosis of arterial disease is often related to the effect of the arterial disease on the pressure and flow patterns and their deviations from what is normally found in circulation. Thus, a good understanding of the hemodynamics of normal and diseased arteries is of major importance. Although much of the work on arterial hemodynamics has been experimental (by means of in vivo experiments in humans and animals, and in vitro experiments in hydraulic circulatory models), computer models have also been used to model the systemic circulation and to study the various aspects of arterial blood flow.

Computer models offer some very attractive advantages over experimental work: they are relatively inexpensive, produce a great deal of information rapidly, and can be extremely versatile in modeling different types of flow conditions. The primary focus of this thesis is the development of a computer model of the human systemic circulation capable of modeling a wide range of physiological flows. Important model features include: multiple branching, non-linear elastic properties of the arterial wall, tapering, stenoses, different proximal and boundary conditions, and the effect of gravitational forces. In particular, the purpose of this study is to:

1. Develop a computer model for the human systemic circulation.

2. Evaluate the influence of the model parameters on the model performance.

3. Simulate cases of clinical significance.

CHAPTER 2. LITERATURE REVIEW

The concept of the circulation of blood was first established by William Harvey in 1628. Since then, numerous physical and mathematical models were developed aiming towards a realistic description of arterial flow. Some of these models will be briefly discussed here followed by a short review of various computer models previously used for arterial modeling.

Physical and Mathematical Models of the Systemic Circulation

Lumped parameter models

Hales, who was the first to make blood pressure measurements in 1733, was also the first to describe the elastic action of the arteries, that is, the storing of blood during systole and maintaining flow through passive contraction during the diastole. Otto Frank expanded on Hales' idea by introducing his *windkessel model* theory in 1899. The windkessel model was the first *lumped parameter* model that takes into account the resistive and compliant elements of the circulatory system. The electric analog of the windkessel model consists of a resistance and a capacitance combined in parallel, and the corresponding differential equation that relates pressure and flow is

$$Q = \frac{1}{k}\frac{dp}{dt} + \frac{p}{R} \tag{2.1}$$

where Q is the flow from the heart, p is the pressure throughout the system, and k is the elastic modulus of the windkessel (Skalak, 1972). The windkessel theory was used successfully to estimate the stroke volume of the heart (McDonald, 1974). The major fault of the windkessel theory is that it fails to account for wave propagation phenomena that take place in circulation. In fact, the windkessel theory assumes pressure changes travel at an infinite speed within the arterial system. Consequently, the windkessel model gives false pressure-flow relations during systole where propagation phenomena are important. During diastole, however, where pressure is almost established throughout the system and propagation phenomena are of less importance, the model predictions are closer to reality (Aperia, 1940). This assumption of infinite propagation speed also explains why the windkessel theory gives better results in cases of high pulse wave velocities, as for example in cases of stiffer arterial systems (due to arteriosclerosis or vasoconstriction), or in cases of short and stiff arterial systems of birds and fish (Skalak, 1972).

The concept of the windkessel model can be successfully applied to model small branches and their distal beds as well. This is sometimes done in terms of a modified windkessel lumped parameter model (Raines et al., 1974). The electrical analog of the modified windkessel consists of a two resistors R_1 and R_2 and a capacitor C_T placed in parallel with R_2, as shown in Figure 2.1.

In the electrical analogy, R_1 and R_2 represent the resistive components of the proximal and distal parts of the supplied beds, respectively, and C_T represents the total volume compliance of the distal bed. Therefore, the modified windkessel model takes into account the compliance of the distal beds, which is ignored in the case of a purely resistive impedance.

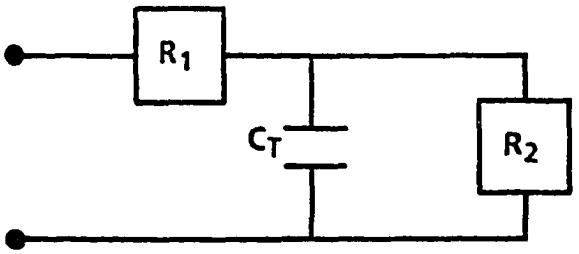

Figure 2.1: Electrical analog of the modified windkessel model

Modeling segmental flow

Attempts to describe mathematically the flow in an arterial segment go back as far as the eighteenth century, where two Swiss mathematicians, D. Bernoulli and L. Euler, attempted to apply the newly developed ideas of conservation of energy and momentum to describe blood flow phenomena. Euler was the first to formulate the mathematical model for flow in an arterial segment. His equations were valid for flow of an incompressible and inviscid fluid through an elastic conduit, and apart from the assumption of non-viscous flow this set of non-linear equations is identical to the equations used today. Euler suggested that this set of equations could be used to study pressure and flow wave transmission in the arterial system, but he failed to give closed form solutions to the problem.

The experimental work of a French physician named J. L. M. Poiseuille yielded one of the most famous equations in hemodynamics (and fluid mechanics in general), referred to as Poiseuille's law. Poiseuille was concerned with the pressure drop that

develops in the passage of blood through small blood vessels and capillaries. His observations on steady laminar flow through cylindrical, rigid conduits lead him to the development of Poiseuille's law (1846)

$$\frac{\Delta p}{l} = \left(\frac{8\mu}{\pi R^4}\right) Q \tag{2.2}$$

where $\frac{\Delta p}{l}$ is the pressure drop over a an arterial segment of length l, μ is the dynamic viscosity of the fluid, R is the internal radius of the artery, and Q is the volume rate of flow. The quantity inside the parenthesis (originally a constant in Poiseuille's law), is evaluated from the solution to Navier-Stokes equations (see below). Although Poiseuille's law is applicable only to steady and laminar flow, it has been widely used to model physiological flows. Its popularity relies mostly on the fact that is easy to use and understand, and provides a fairly accurate model that relates mean pressure and flow values to the frictional resistance of the arterial segment. The form of Equation 2.2 triggered the idea of the electrical analog, where pressure drop and flow can be related to the voltage drop and current through a resistance, R_p, of value

$$R_p = \frac{8l\mu}{\pi R^4} \tag{2.3}$$

The idea of the electric analog found many interesting applications, as for example in the construction of electrical models of the arterial system. Although electrical analogs of arterial segments often have a capacitance in parallel to account for the compliance of the arterial wall, Poiseuille type of resistance models were frequently used to form lumped resistance models of small peripheral beds.

Poiseuille's law modeled the effects of viscous resistance to flow, something that was missing from the Euler equations. The general equations of motion of a viscous fluid were developed initially by Navier in 1822 and by Stokes in 1845. These non-

linear differential equations, often referred to as the Navier-Stokes equations, are written in vector form as

$$\rho\left(\frac{\partial\vec{V}}{\partial t}+\vec{V}\cdot\vec{\nabla}\vec{V}\right)=-\vec{\nabla}p+\mu\nabla^2\vec{V}+\rho\vec{b} \tag{2.4}$$

and along with the continuity rquation

$$\vec{\nabla}\cdot\vec{V}=0 \tag{2.5}$$

express the conservation of momentum and mass, respectively. The non-linear form of the Navier-Stokes equations, as applied to the general case of arterial flow, prevents from any type of closed form, analytic solutions. Thus, researchers use certain simplifying assumptions that enable them to obtain analytic solutions for reduced forms of the Navier-Stokes equations. Witzig (1914) was the first to provide analytical solution of oscillatory motion in a cylindrical vessel but his results were not widely publicized. Other investigators arrived at similar solutions (Aperia, 1940; Iberall, 1950; Morgan and Kiely, 1954; Womersley, 1955a; Uchida, 1956). Womersley, with a series of papers published between 1955 and 1958, had a major impact on the development of modern hemodynamics. Based on the linearization of Equation 2.4, Womersley developed an analytic solution to the problem of oscillatory flow in straight, rigid tubes (1955a). Later he extended the analysis to include the effects of wall elasticity (1957). Womersley took advantage of the superposition principle that applies to linear systems to provide solutions only to harmonic oscillations. In case of arterial flow, where complicated waveforms exist, the prescribed waveforms can be broken down into their Fourier components and the solutions to each harmonic can be added to yield the complete solution to the problem. The well-known Womersley solution for

flow driven by a simple harmonic pressure gradient ($\Delta p(t) = A^* e^{i\omega t}$) is given by

$$u(r,t) = \frac{A^*}{i\omega\rho}\left[1 - \frac{J_o\left(r\alpha i^{\frac{3}{2}}\right)}{J_o\left(R\alpha i^{\frac{3}{2}}\right)}\right] e^{i\omega t} \tag{2.6}$$

where, u is the fluid velocity, r is the coordinate in the radial direction, $J_O(xi^{\frac{3}{2}})$ is a Bessel function of the first kind of order zero, and $\alpha = R\sqrt{\frac{\omega}{\nu}}$ is the dimensionless frequency, often called the Womersley parameter or the alpha parameter. Despite the series of assumptions used in the formulation of the problem, Womersley's solution proved to yield satisfactory predictions of velocity profiles and flow waveforms in arterial segments. Hale et al. (1955) performed experiments in dogs where the pressure gradient between two aortic locations and flow was measured. The flow waveform computed from the measured pressure gradient pulse compared reasonably well with the measured flow waveform. A complete discussion of Womersley's solution and its applications to arterial flow is given in McDonald (1974).

One-dimensional flow equations

The integration of the continuity and momentum equations over the cross section of the artery yields the following one-dimensional flow equations (Fox and Saibel, 1965)

$$\frac{\partial A}{\partial t} + \frac{\partial Q}{\partial x} + \psi = 0 \tag{2.7}$$

$$\frac{\partial Q}{\partial t} + \frac{\partial}{\partial x}\int u^2 dA = -\frac{A}{\rho}\frac{\partial p}{\partial x} + \frac{2\pi R\tau_w}{\rho} + Ab_x \tag{2.8}$$

where ψ is a seepage parameter representing the efflux through the walls per unit length (used in an attempt to model the effects of small branches) and τ_w represents

the shear stress acting at the inner wall. The form of Equations 2.7 and 2.8 provide a popular approach to arterial flow modeling (Streeter et al., 1963; Olsen and Shapiro, 1967; Anliker et al., 1971; Wemple and Mockros, 1972; Raines et al., 1974; Rumberger and Nerem, 1977; Rooz, 1980; Young et al., 1980; Porenta et al., 1986; Weerappuli, 1987; Balar et al., 1989).

The system of Equations 2.7 and 2.8 must be accompanied by an equation describing the distensible behavior of the arterial wall. A popular approach is to specify a function relating the changes in cross sectional area to changes in pressure, such as

$$A = A(p, x) \tag{2.9}$$

The simplest form of a pressure-area relation is one in which area varies linearly with pressure so that

$$A(p, x) = A_O + C'(p - p_O) \tag{2.10}$$

where, A_O is the cross sectional area at reference pressure p_O, and C' is the vessel compliance. The acceptance of such an area-pressure relation rests on the assumption that within the operational range of distending pressures a linear curve can provide fairly good approximations. This form of equation of state does not also introduce non-linearities in the final system of equations, and has been used in the past by several researchers (Snyder et al., 1968; Westerhof et al., 1969; Young et al., 1980).

It has been proven, however, through measurements in human and canine arteries that arterial pressure-area relationships are non-linear (Anliker et al., 1978; Mozersky et al., 1972; Bergel, 1961). It has been further suggested that the arterial compliance is inversely proportional to pressure ($C' = \frac{\partial A}{\partial p} = \frac{\beta}{p}$). Raines et al. (1974) integrated

this equation to arrive at the following logarithmic pressure-area relationship

$$A(p,x) = A_O(p_O,x) + \beta \ln \frac{p}{p_O} \tag{2.11}$$

where A_O is again the "normal" area obtained through angiographic measurements and β is an empirical quantity relating to the elastic properties of the artery.

Other researchers derived or proposed different forms of pressure-area relationships. Streeter et al. (1963) consider the artery as a thin-walled vessel made of incompressible elastic material (Poisson's ratio = 0.50) and derived the theoretical expression

$$A(p,x) = A_O(x)\left[1 - \frac{D_O(p-p_O)}{h_O E}\right]^{-1} \tag{2.12}$$

where h_O and D_O are the wall thickness and arterial diameter at reference pressure, p_O, respectively, and E is the effective elastic modulus.

Wemple and Mockros (1972) assumed an exponential relationship between the elastic modulus and the radius

$$\frac{E}{E_O} = \left[\frac{R}{R_O}\right]^{\beta} \tag{2.13}$$

to develop a different form of equation of state

$$\frac{p}{2a_O^2} = \frac{R_O}{R}\left[\frac{1}{\beta}\left[\left(\frac{R}{R_O}\right)^{\beta} - 1\right] + \frac{p_O}{2a_O^2}\right] \tag{2.14}$$

where β is a constant to be derived experimentally and a_O is the local wave speed.

Another form of exponential pressure-area relation was suggested by Rumberger and Nerem (1977)

$$A(p,x) = A_O(x)e^{\frac{p-p_O}{\rho c(p,x)c_O(p_O,x)}} \tag{2.15}$$

where c and c_O are the wave speeds at the distending pressure p and reference pressure p_O, respectively. The advantage of this p-A relationship is that it relies on the

experimental estimation of wave propagation speeds, c and c_o; parameters which are much easier to obtain than other compliance related quantities such as the effective modulus of elasticity, E, the wall thickness, h, etc.

The following quadratic relation for the equation of state was suggested by Rooz (1980)

$$A(x) = A_o(x) + C_o(p - p_o) + C_1(p - p_o)^2 \tag{2.16}$$

This form was not derived by theoretical analysis, rather, it is considered a convenient extension to the linear constitutive relation (Equation 2.10), capable of accounting for the non-linear properties of the arterial wall. The same form was used subsequently by several investigators (Rooz et al., 1982; Porenta, 1982; Porenta et al., 1986; Weerappuli, 1987; Balar et al., 1989).

The wall shear stress, τ_w, that appears in the right hand side of the one-dimensional momentum equation is an unknown quantity and therefore needs to be evaluated. By definition, the wall shear stress requires the knowledge of the velocity profile in the vicinity of the wall (which is in general unknown). Therefore, alternate, approximate methods for the evaluation of τ_w have been used in the past. A popular approach is to assume that the Poiseuille's law applies, so that

$$\tau_w = -\frac{4\mu}{\pi R^3} Q \tag{2.17}$$

(Raines et al., 1974; Rockwell et al., 1974; Rumberger and Nerem, 1977; Rooz, 1980; Young et al., 1980; Porenta, 1982; Rangarajan, 1983; Porenta et al., 1986). This approach effectively assumes that the velocity profile is parabolic at all times. Measurements reported in the literature show that the velocity profile, especially in the larger arteries, is rather blunt with steep gradients existing near the wall (Ling

et al., 1968; McDonald, 1974). McDonald (1974) suggested that, due to oscillatory flow, the induced steeper gradients at the wall result in approximately 50% increase in the flow resistance as compared to steady flow. To compensate for that, Raines et al. (1974) increased the value for the viscosity of blood in their calculations by 10%.

In an attempt to improve the wall shear stress approximation, Schaaf and Abbrecht (1972) used a formula derived from the solution to pulsating flow in an infinite, rigid, cylindrical tube:

$$\tau_w = \frac{8\mu}{D}U + \frac{\rho D(\lambda - 1)}{4}\frac{\partial U}{\partial t} \tag{2.18}$$

where $U = Q/A$ is the instantaneous cross sectional average velocity and λ is the momentum flux coefficient defined as

$$\lambda = \frac{1}{A}\int \frac{u^2}{U^2} dA \tag{2.19}$$

Schaaf and Abbrecht used the value of $\lambda = 4/3$, which corresponds to a parabolic velocity profile. However, when they set $\lambda = 1$, which drops the unsteady term off and effectively degenerates the shear stress model to that of Equation 2.17, they found little difference in their results. They even found little difference in their results when the viscosity was set zero, thus removing all frictional effects from the arterial system, except from the terminal impedances. Their overall conclusion was that the wall shear stress plays a relatively insignificant role in the pulse formation.

Wemple and Mockros (1972) also used a shear stress model that considers the oscillatory components of the flow. Their unsteady wall shear stress model was based on Womersley's solution and was of the form

$$\tau_w = B_1 Q + B_2 \frac{\partial Q}{\partial t} \tag{2.20}$$

where

$$B_1 = \pi\mu\alpha^2 \frac{\sin\epsilon_{10}}{AM_{10}} \tag{2.21}$$

$$B_2 = \frac{\pi\mu\alpha^2}{A\omega}\left(\frac{\cos\epsilon_{10}}{M_{10}} - 1\right) \tag{2.22}$$

and

$$M_{10}e^{i\epsilon_{10}} = 1 - \frac{2J_1(\alpha i^{\frac{3}{2}})}{\alpha i^{\frac{3}{2}} J_o(\alpha i^{\frac{3}{2}})} \tag{2.23}$$

The values for M_{10} and ϵ_{10}, as functions of the α parameter, are tabulated in McDonald (1974). Wemple and Mockros compared their computer results using the above shear stress model and one with shear stress set to zero, and concluded that the effect of wall shear stress is minimal.

Young and Tsai (1973b) also used Womersley's solution to oscillatory flow in a straight rigid tube to arrive at the relation

$$\tau_w = -\frac{\rho}{2\pi R}\left[\frac{8c_v\pi\mu}{\rho A}Q + (c_u - 1)\frac{\partial Q}{\partial t}\right] \tag{2.24}$$

which is similar to Equation 2.20. The semi-empirical coefficients c_v and c_u are functions of the α parameter and therefore can be evaluated precisely only in the case of purely harmonic flow.

Arterial Stenosis Models

Stenosis (from the Greek term for "narrowing") is a medical term used to describe a localized constriction in the artery. Stenoses are usually caused by the abnormal development of atheromatous plaques in the subintimal layer of the arterial wall, which subsequently protrude into the lumen of the artery, thus causing a narrowing

to the free passage of blood. Severe stenoses add significant resistance to flow and can be potentially harmful by preventing adequate blood supply to distal beds.

The hemodynamics of stenoses are a challenge to the analytical or numerical analyst, mainly because of the strong, geometry-induced non-linearities, and the presence of turbulence. Therefore, stenosis modeling relies mostly on experimental work. Young and Tsai (1973a,b) performed a series of experiments on steady and pulsatile flow through models of rigid axisymmetric and nonsymmetric stenoses. They found that the stenosis induced pressure drop, $\Delta p(t)$, can be approximated by the empirical formula

$$\Delta p(t) = \frac{K_v \mu}{D} U(t) + \frac{K_t \rho}{2} \left[\frac{A_o}{A_s} - 1\right]^2 |U(t)|U(t) + K_u \rho L_s \frac{dU(t)}{dt} \qquad (2.25)$$

where

A_o = the unobstructed cross sectional lumen area

A_s = the minimum cross sectional lumen area inside the stenosis

D = the diameter of unobstructed tube

K_v = empirical coefficient of viscous term

K_t = empirical coefficient of turbulence term

K_u = empirical coefficients of unsteady term

L_s = the length of stenosis

U = the instantaneous corss-sectional average velocity in the unobstructed tube

The first term in Equation 2.25 accounts for the pressure drop due to viscous action, the second term accounts for the turbulence and non-linear losses, and the third term accounts for the inertia effects due to unsteadiness of the flow. The appli-

cability of the stenosis model to arterial flow was investigated by Young et al. (1975) through in vivo experiments on dogs. Rigid, hollow, cylindrical plugs representing stenoses were introduced in the femoral arteries of the dogs, and flow and pressure drop across the stenoses were measured. It was found that Equation 2.25 yielded satisfactory predictions for the pressure drop. In a later study, Seeley and Young (1976) examined the effect of stenosis geometry on stenotic dynamics. They found that the coefficients K_t and K_u depend only slightly on geometry, and can be reasonably approximated with the constants 1.52 and 1.2, respectively, for the blunt-ended stenoses used in their study. The coefficient K_v, however, showed strong dependence on stenotic geometry. Through statistical analysis of the data, the empirical relation

$$K_v = 32\frac{0.83L_s + 1.64D_s}{D}\left(\frac{A_o}{A_1}\right)^2 \tag{2.26}$$

for K_v was developed where D_s is the diameter corresponding to area A_s. A complete review of the fluid mechanics of arterial stenoses is given by Young (1979).

Computer Models of the Circulation

Equations 2.7 and 2.8, along with one of the possible forms of the constitutive equation, constitute a system of first order non-linear differential equations. Even when the system is linearized, the solution usually requires the employment of a digital computer to carry out the computations.

Linearization of the governing equations results from dropping the convective acceleration term in the momentum equation and assuming that a linear pressure-area relationship (i.e., Equation 2.10) holds. If, in addition, the Poiseuille's friction term is used to model the wall shear stress (Equation 2.17), the resulting set of linear

equations takes the form

$$\frac{\partial p}{\partial x} = -RQ - L\frac{\partial Q}{\partial t} \tag{2.27}$$

$$\frac{\partial Q}{\partial x} = -Sp - C\frac{\partial p}{\partial t} \tag{2.28}$$

where $R = \frac{8\pi\mu}{A_o^2}$, $L = \frac{\rho}{A_o}$, and $Sp = \psi$ the seepage term, which is usually taken as zero. The above systems of equations is identical to those in transmission line theory, with pressure and flow being analogous to voltage and current, respectively. The fluid resistance R is analogous to electrical resistance, L to electrical inductance, and C is the analog of the electrical capacitance. Before the ready availability of digital computers, researchers took advantage of the analogy to construct electrical analog models of the arterial system and perform the computations directly on the analog computer (Snyder et al., 1968; Westerhof et al., 1969).

The advent of the digital computer gave researchers the option of using numerical techniques to obtain solutions to the linear set of equations (Equations 2.27 and 2.28) or even to the original set of non-linear equations (Equations 2.16, 2.8, and 2.9). A popular approach was to use the method of characteristics (Anliker et al., 1971; Wemple and Mockros, 1972; Schaaf and Abbrecht, 1972). Two other popular numerical methods used were the finite difference and the finite element method. Raines et al. (1974), in their computer model for the human leg, chose the finite difference method as a more convenient and economical method as compared to the method of characteristics. Raines et al. solved the non-linear set of equations to model certain cases of normal and diseased flow conditions in the human leg. Their results proved to be generally in good agreement with experimental measurements. The finite element method was also used successfully in modeling arterial flows (Rooz et al., 1982; Porenta et al., 1986; Weerappuli, 1987; Balar et al., 1989). Rooz et al. (1982) applied

the Galerkin method using linear isoparametric quadrilateral elements to transform the system of partial differential equations into a set of algebraic equations. Porenta et al. (1986) also utilized the Galerkin method, but he discretized the equations only in space to arrive to a system of ordinary differential equations which he subsequently solved by means of a standard ODE solver. Porenta et al. applied his method to Raines' leg model and found that both finite difference and finite element methods yield approximately the same results. Weerappuli (1987) and Balar et al. (1989) followed Porenta's approach, but their tests included models of the human arm and the uterine artery of the cow.

In this study both the finite element and the finite difference method are employed. The development of the mathematical model, as well the numerical analysis using both methods, is presented in the following two chapters.

CHAPTER 3. MATHEMATICAL MODEL OF ARTERIAL FLOW

Precise mathematical description of arterial flow is essentially an impossible task due to the complexity of the flow patterns, the non-linearities arising from the conduit geometry, the distensible nature of the arterial wall, and the rheological characteristics of blood, as well as the uncertainty of the boundary conditions. Thus, as discussed in the previous chapter many investigators have made use of simplified mathematical models to study various aspects of the arterial flow. While these simplified mathematical models varied considerably, from lumped parameter electrical analogues using linear transmission line theory equations to distributed parameters non-linear models, all provided considerable insight into the hemodynamics of the circulatory system, and proved capable of simulating to a certain extent, the characteristics of arterial flow. In this section a fully non-linear, distributed parameter model of the systemic arterial circulation is introduced. The model can accommodate multiple branching, non-linear wall properties, tapering, stenoses, different proximal and boundary conditions, as well as the effect of gravitational or inertial forces.

Governing Equations

The Navier-Stokes equations and the continuity equation can be used to describe flow within an arterial segment. The Navier Stokes equations, however, give a fine

description of the velocity field within the artery, a detail which in most cases is not required from a medical, or practical point of view. Instead, the cross sectional averaged continuity and x-momentum equations are often used, which relate the quantities of primary interest: the arterial pressure, p, and the flow rate, Q. The integrated, one-dimensional continuity and momentum equations are, respectively,

$$\frac{\partial A}{\partial t} + \frac{\partial Q}{\partial x} + Sp = 0 \tag{3.1}$$

$$\frac{\partial Q}{\partial t} + \frac{\partial}{\partial x}\left(\lambda \frac{Q^2}{A}\right) = -\frac{A}{\rho}\frac{\partial p}{\partial x} + \frac{2\pi R \tau_w}{\rho} + Ab_x \tag{3.2}$$

where τ_w is the shear stress at the arterial wall and λ is the momentum flux coefficient. Note that the evaluation of both τ_w and λ require a knowledge of the velocity profile over the cross section, which is unknown. The value of λ, however, is bounded between 1.0 (for completely flat velocity profile) and 4/3 (for parabolic profile). Theoretical analysis and measurements reported in the literature suggest that for pulsatile flow in major arteries the velocity profiles tend to be flat over a great portion of the arterial cross section, except for a small region near the wall where steep velocity gradients exist. Hence, a reasonable approximate value for λ is 1.0, which is the value used in the present study.

The wall shear stress is approximated using the following equation developed by Young and Tsai (1973b)

$$\tau_w = -\frac{\rho}{2\pi R}\left[\frac{8 c_v \pi \mu}{\rho A} Q + (c_u - 1)\frac{\partial Q}{\partial t}\right] \tag{3.3}$$

where c_v and c_u are the semi-empirical coefficients of the viscous and unsteady term, respectively. Both c_v and c_u are functions of the Womersley parameter, $\alpha = R\sqrt{\frac{\omega}{\nu}}$. Equation 3.3 with proper selection of coefficients c_v and c_u can match Womersley's

theoretical solution for flow in an infinitely long cylinder with rigid walls. Equation 3.3 is used in the present model because it offers two nice features: it relates the wall shear stress to the primary variable Q, and (if desired) it also can approximately account for inertia effects. It is recognized, however, that Equation 3.3 is valid for the case of harmonic flow (since coefficients c_v and c_u are functions of ω, the circular frequency of the particular harmonic), and its application in the general case of arterial flow is done only in an approximate manner.

The mathematical formulation of the problem is completed with the use of a constitutive relationship which relates the changes of the cross sectional area, $A(x,p)$, to the changes of the internal pressure, $p(x,t)$. The pressure-area relationship is chosen to be of the following form

$$A(x,p) = A_O(x)\left[1 + C_O'(p - p_O) + C_1'(p - p_O)^2\right] \tag{3.4}$$

where A_O is the cross sectional area of the artery that corresponds to reference pressure p_O, and C_O' and C_1' are the coefficients of linear and non-linear compliance respectively. The quadratic nature of the equation allows for the modeling of the non-linear properties of arterial wall, within the operational range of internal pressure. It is also flexible in the sense that it can approximate other proposed pressure-area relationships with proper selection of the coefficients C_O' and C_1'. An example of such an approximation is given in Chapter 6. Equation 3.4 allows for the variation of A_O, p_O, C_O' and C_1' along the artery (all variables can be functions of the axial coordinate x), but neglects the effect of 1) external pressure (assumed to be zero), 2) wall inertia, 3) neural control, and 4) viscoelastic wall properties.

The applicability of the governing equations to arterial flow relies on whether, or to what degree, the following assumptions are met (Weerappuli, 1987):

- An artery can be described as a straight, slightly tapered tube with a circular cross section.
- Arterial walls are thin, incompressible, elastic, and their material properties are approximately homogeneous over a relatively short segment.
- The vessel is totally constrained in the longitudinal direction.
- Blood can be treated as incompressible, homogeneous, isotropic, and Newtonian.
- The flow is laminar - except possibly at localized constrictions - and axisymmetric, and there are no secondary flows.
- The radial variation of the longitudinal velocity u_x is much greater than its longitudinal variation.
- The pressure does not vary along the radius.

These assumptions do not strictly hold for several cases of arterial flow, however, the set of Equations 3.1 and 3.2 have been repeatedly used in similar studies and proved to give a reasonable estimation to the conservation equations. A complete discussion of the validity of the above assumptions can be found in Weerappuli (1987).

Equation 3.4 can be differentiated with respect to time and substituted into the continuity equation (Equation 3.1) to yield

$$\frac{\partial Q}{\partial x} + A_o C_o \frac{\partial p}{\partial t} + A_o C_1 p \frac{\partial p}{\partial t} + Sp = 0 \tag{3.5}$$

where $C_o = C_o' - 2C_1' p_o$, and $C_1 = 2C_1'$. Substitution of the expression for the wall shear stress (Equation 3.3) into Equation 3.2 yields the following final form of the

momentum equation

$$c_u \frac{\partial Q}{\partial t} + \frac{\partial}{\partial x}\left(\lambda \frac{Q^2}{A}\right) + \frac{A}{\rho}\frac{\partial p}{\partial x} + B_1 Q - A b_x = 0 \qquad (3.6)$$

where $B_1 = \frac{8 c_v \pi \mu}{\rho A}$. Note that although the variable $A(x,t)$ has been eliminated from the continuity equation it still appears as an unknown coefficient in the modified momentum equation, which prevents the solution of Equations 3.5 and 3.6 for the variables p and Q. To overcome this difficulty, Equation 3.6 is further simplified by substituting the reference cross sectional area, $A_o(x)$ for the instantaneous cross sectional area $A(x,t)$, yielding the following final form of the momentum equation

$$c_u \frac{\partial Q}{\partial t} + \frac{\partial}{\partial x}\left(\lambda \frac{Q^2}{A_o}\right) + \frac{A_o}{\rho}\frac{\partial p}{\partial x} + B_1 Q - A_o b_x = 0 \qquad (3.7)$$

where now $B_1 = \frac{8 c_v \pi \mu}{\rho A_o}$. The system of equations, Equations 3.5 and 3.7, can now be solved for the variables $p(x,t)$ and $Q(x,t)$, given the proper initial and boundary conditions which are discussed below.

Initial and Boundary Conditions

Initial conditions

Although this is a time dependent problem, precise initial conditions cannot be imposed except at the proximal and distal boundaries. Fortunately, the viscous effects dampen out the discrepancies due to an incorrect initial pressure and flow distribution, and in the case of periodic flow the solution converges within two or three cycles.

Proximal and distal boundary conditions

Proximal boundary condition At the proximal end (the point of the arterial system closest to the heart) the pressure or the flow waveform is specified. In the present study only periodic flow is considered, hence, a convenient way to specify the proximal waveforms is in terms of their Fourier components. The problem, however, can be solved for any arbitrary time function of proximal pressure or flow.

Distal boundary condition For practical reasons small branches of the arterial model are terminated using a lumped-parameter impedance. The terminal impedance is thought to take into account the cumulative effects of the small vessels and microvasculature distal to the point of termination. From the mathematical standpoint, the nature of the terminal impedance gives rise to certain boundary conditions applied at the terminal sites, and thus, the mathematical formulation of the problem is closed and well posed. In the present study, the modified windkessel type of impedance is used (see Figure 2.1). The corresponding relationship between the pressure and flow at the termination point is

$$\frac{\partial Q}{\partial t} = \frac{1}{R_1}\frac{\partial p}{\partial t} + \frac{p}{R_1 R_2 C_T} - \left[1 + \frac{R_1}{R_2}\right]\frac{Q}{R_1 C_T} \tag{3.8}$$

where $R_1 + R_2 = R_T$, the total resistance of the terminal branch. The relationship requires that two additional parameters (R_1/R_T and C_T) besides R_T need to be estimated for every terminal branch. The major advantage of the model is that it accounts for both resistive and compliant effects of the distal vessels beyond the point of termination.

In the limiting case where $C_T = 0$, the modified windkessel model degenerates to a simple resistance, and in this case the corresponding boundary condition takes

the form

$$Q = \frac{p}{R_1 + R_2} = \frac{p}{R_T} \tag{3.9}$$

This boundary condition has been often used in the past, mainly because it is easy to implement, and because the total resistance of the terminal branch, R_T, can be obtained from mean flow measurements. The pure resistance boundary condition, however, takes into account only the resistive component of the lumped distal vessels and microvasculature.

Modeling of Branches and Stenoses

Model of arterial branching

A sketch of an arterial branching point is shown in Figure 3.1. Arterial branches cause complicated flow patterns and in the vicinity of the branch the governing equations do not strictly apply. Hence, a special model for the arterial branches should be employed. For the sake of simplicity, it is assumed that continuity of pressure and flow is preserved across the point of bifurcation. These conditions are specified mathematically as follows (in reference to Figure 3.1)

$$p_i = p_j = p_k \tag{3.10}$$

$$Q_i = Q_j + Q_k \tag{3.11}$$

Model of arterial stenoses

Stenoses are modeled using the empirical relationship

$$\Delta p(t) = \frac{4K_v\mu}{\pi D^3}Q(t) + \frac{K_t\rho}{2A_o^2}\left[\frac{A_o}{A_s} - 1\right]^2 Q^2(t) + \frac{K_u\rho L}{A_o}\frac{dQ(t)}{dt} \tag{3.12}$$

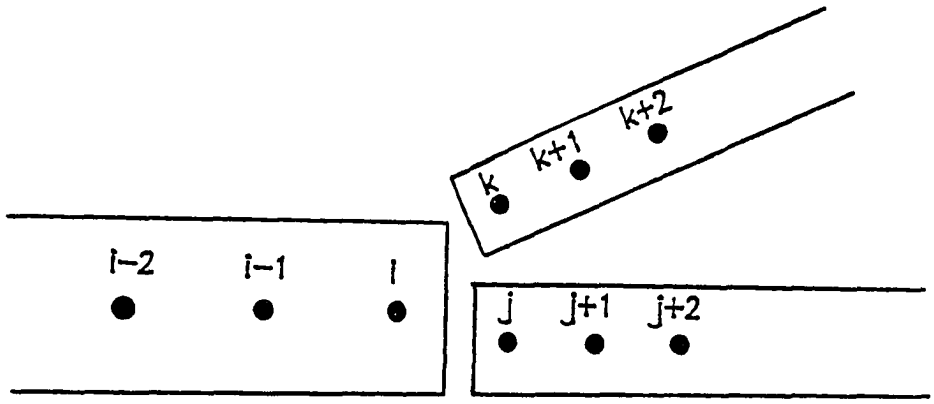

Figure 3.1: Schematic representation of an arterial branch

developed by Young and Tsai (1973b), where $K_v = 32\frac{0.83L_s - 1.64D_1}{D}\left(\frac{A_2}{A_1}\right)^2$. $K_t = 1.5$, and $K_u = 1.2$, are experimentally determined coefficients of the viscous, turbulent, and unsteady term, respectively. The term, L_s, represents the length of the stenosis. This equation is valid for rigid stenoses, and the corresponding continuity equation reduces to $\frac{\partial Q}{\partial x} = 0$ in the stenosis, which means that the instantaneous flowrate is constant through the stenosis.

The governing equations (Equations 3.5 and 3.7) along with the imposed boundary conditions and the special branch and stenoses models form a well posed mathematical problem described by a system of non-linear first-order partial differential equations. To solve the system of equations two standard numerical techniques, the finite difference method (FDM) and the finite element method (FEM), were employed. The development of both methods is discussed in the following chapter.

CHAPTER 4. NUMERICAL SOLUTIONS

Finite Difference Method

The first question that needs to be answered before the development of a particular finite difference scheme is whether an implicit or an explicit formulation should be employed. Implicit schemes offer the advantage of being unconditionally stable, and hence large time steps can be taken in the integration procedure, resulting in greater computational speed. The implicit schemes, however, require simultaneous solution of the whole system of equations as applied to each node of the arterial system, including the effects of branches and boundary conditions. Simultaneous solution to a system of equations can be computationally intense, unless the resulting matrix is banded (tri-diagonal or penta-diagonal) where efficient solution algorithms can be employed. In the case of arterial flow, the condition for tridiagonality or pentadiagonality is defeated due to the mathematical conditions imposed at the bifurcation points. As stated in Equations 3.10 and 3.11, pressure and flow at the distal end of the parent branch relates to pressure and flow at the proximal end of the daughter branches. The difference between the index values $j - i$ and $k - i$ which relates to the bandwidth of the matrix is arbitrary, depending on the number of nodes present in the daughter branches, and therefore is not limited to the convenient value of 1 or 2 (tridiagonal or pentadiagonal matrix respectively). Lagging the values from the

previous time step to achieve efficiency of the solution scheme would require small time steps to minimize the lagging error. Small time steps would defeat the purpose of employing an implicit scheme, so for the purposes of this study, an explicit scheme was developed.

Explicit schemes require solution of simple algebraic equations rather than a system of equations. Explicit schemes, however, often have stability constraints that result in small time steps which may hurt the computational efficiency of the method. The development of the finite difference equations used in the present study, as well as a comment on the stability of the method, is given below.

Development of finite difference equations

In order to employ the finite difference method each segment of the arterial tree needs to be discretized into a number of finite length elements. A typical arrangement for a three-segment arterial subsystem with the corresponding elements and nodes is shown in Figure 3.1. The differential equations are transformed into algebraic equations by approximating the partial derivatives with difference expressions. The quantities Δx and Δt represent the element length and time increment respectively.

Governing equations The governing equations, Equations 3.5 and 3.7, are written in the form

$$\frac{Q_i^n - Q^n{}_{i-1}}{\Delta x} + \left(A_o C_o + A_o C_1 p_i^n\right) \frac{p_i^{n+1} - p_i^n}{\Delta t} = 0 \qquad (4.1)$$

and

$$c_u \frac{Q_i^{n+1} - Q_i^n}{\Delta t} + \frac{\frac{\left(Q_i^n\right)^2}{A_o} - \frac{\left(Q^n{}_{i-1}\right)^2}{A_o}}{\Delta x} + \frac{A_o}{\rho} \frac{p_i{}_{+1}^n - p_i^n}{\Delta x} + B_1 Q_i^n - A_o b_x = 0 \tag{4.2}$$

where X_i^n denotes the value of the variable X at the node i and time step n. Note also that the no seepage was present in any of the arterial segments so the corresponding term was left out of Equation 4.1.

Equations 4.1 and 4.2 can be solved for the values of p_i^{n+1} and Q_i^{n+1} respectively to yield

$$p_i^{n+1} = p_i^n - \frac{\Delta t}{\Delta x \left(A_o C_o + A_o C_1 p_i^n\right)} \left[Q_i^n - Q^n{}_{i-1}\right] \tag{4.3}$$

and

$$\begin{aligned} Q_i^{n+1} \;=\; & \left[1 - \frac{B_1 \Delta t}{c_u}\right] Q_i^n - \frac{\Delta t A_o}{c_u \rho \Delta x} \left[p^n{}_{i+1} - p_i^n\right] \\ & - \frac{\Delta t}{c_u \Delta x} \left[\frac{\left(Q_i^n\right)^2}{A_o} - \frac{\left(Q_{i-1}{}^n\right)^2}{A_o}\right] + \frac{A_o b_x \Delta t}{c_u} \end{aligned} \tag{4.4}$$

Initial, boundary, and branch conditions The finite difference expressions developed for the governing equations apply to a generic interior point of an arterial segment. At the first and last node of each arterial segment the finite difference equations need to be modified to reflect the initial, boundary, or branch conditions.

At the proximal end of an arterial segment the equations become:

1. For the first segment of the arterial network when proximal pressure is prescribed

$$p_1{}^{n+1} = p(t) \tag{4.5}$$

and

$$Q_i^{n+1} = \left[1 - \frac{B_1 \Delta t}{c_u}\right] Q_i^n - \frac{\Delta t A_o}{c_u \rho \Delta x} \left[p^n{}_{i+1} - p_i^n\right] + \frac{A_o b_x \Delta t}{c_u} \tag{4.6}$$

When proximal flow is prescribed

$$Q_1^{n+1} = Q(t) \tag{4.7}$$

and

$$p_i^{n+1} = p_i^n - \frac{\Delta t}{\Delta x \left(A_o C_o + A_o C_1 p_i^n\right)} \left[Q^n{}_{i+1} - Q_i^n\right] \tag{4.8}$$

2. For any subsequent arterial segment (see Figure 3.1)

$$p_j^{n+1} = p_i^{n+1} \tag{4.9}$$

and

$$Q_i^{n+1} = \left[1 - \frac{B_1 \Delta t}{c_u}\right] Q_i^n - \frac{\Delta t A_o}{c_u \rho \Delta x} \left[p^n{}_{i+1} - p_i^n\right] + \frac{A_o b_x \Delta t}{c_u} \tag{4.10}$$

At the distal end of each arterial segment the pair of governing equations is modified according to the following:

1. When the segment bifurcates (in reference to Figure 3.1)

$$p_i^{n+1} = p_i^n - \frac{\Delta t}{\Delta x \left(A_o C_o + A_o C_1 p_i^n\right)} \left[Q_i^n - Q^n{}_{i-1}\right] \tag{4.11}$$

and

$$Q_i^{n+1} = Q_j^{n+1} + Q_k^{n+1} \tag{4.12}$$

2. When the segment terminates with a lumped-parameter impedance

$$p_i^{n+1} = p_i^n - \frac{\Delta t}{\Delta x \left(A_o C_o + A_o C_1 p_i^n\right)} \left[Q_i^n - Q^n{}_{i-1}\right] \tag{4.13}$$

and

$$Q_i^{n+1} = \left[1 - \frac{\Delta t}{R_1 C_t} \left[1 + \frac{R_1}{R_2}\right]\right] Q_i^n + \frac{p_i^{n+1} - p_i^n}{R_1} + \frac{\Delta t}{R_1 R_2 C_T} p_i^{n+1} \tag{4.14}$$

Stability of finite difference scheme

A complete stability analysis on the full set of non-linear differential equations is not possible through analytical methods. Even if the system of equations is linearized, the stability analysis that includes the effect of proximal and boundary conditions reduces to the evaluation of the eigenvalues of a 2xN matrix, N being the number of nodes in the arterial system. This again is a difficult task, beyond the scope of this study. For the purposes of the numerical analysis presented here, an approximate stability criterion based on the linearized set of governing equations (Equations 2.27 and 2.28) is developed. If the friction and the seepage terms are dropped, the above equations can be written in matrix form as

$$\frac{\partial\{\delta_e\}}{\partial t} + [A]\frac{\partial\{\delta_e\}}{\partial x} = 0 \tag{4.15}$$

where

$$\{\delta_e\} = \begin{Bmatrix} p \\ Q \end{Bmatrix} \tag{4.16}$$

and

$$[A] = \begin{bmatrix} 0 & \frac{1}{A_o C_o'} \\ \frac{A_o}{\rho} & 0 \end{bmatrix} \tag{4.17}$$

The condition for stability for the finite difference scheme used is (Anderson et al., 1984)

$$\frac{\Delta t}{\Delta x}\lambda_{max} \leq 1 \tag{4.18}$$

where λ_{max} is the maximum eigenvalue of matrix $[A]$. The eigenvalues of $[A]$ are

$$\lambda_{1,2} = \pm\frac{1}{\sqrt{\rho C_o'}} \tag{4.19}$$

Therefore, the approximate stabilty criterion is

$$\Delta t \leq \frac{1}{\sqrt{\rho C_o'}} \Delta x = \frac{1}{a_o} \Delta x \tag{4.20}$$

where $a_o = \sqrt{\rho C_o'}$ the local wave propagation velocity (see also Chapter 5, Equations 5.3 and 5.7).

The stability criterion defines a maximum allowable time step depending essentially on the elastic properties of the artery and the spacing of the computational nodes. For the range of C_o' values used in the model (see Chapter 5) Δt_{max} is in the neighborhood of 0.0005-0.001 sec. This is roughly the stability range that was empirically found to apply for the complete set of non-linear equations. It was also found empirically that the convective acceleration term requires an upwind differencing scheme like the one in Equation 4.2 to maintain stability.

Finite Element Method

The approach followed in the development of the finite element model was similar to the one by Weerappuli (1987). The domain was discretized only in space, retaining continuity in time for the variables p and Q. One-dimensional linear elements with two degrees of freedom (p and Q) at each node were used, so that within a typical element

$$p(x,t) = [N(x)]\{p(t)\} \tag{4.21}$$

and

$$Q(x,t) = [N(x)]\{Q(t)\} \tag{4.22}$$

where, $N(x)$

$$N(x) = \left[\frac{X_j - x}{L} \qquad \frac{x - X_i}{L}\right] \tag{4.23}$$

is the linear shape function vector, and $\{p(t)\}$ and $\{Q(t)\}$

$$\{p(t)\} = \left[p_i(t) \qquad p_j(t)\right]^T \tag{4.24}$$

$$\{Q(t)\} = \left[Q_i(t) \qquad Q_j(t)\right]^T \tag{4.25}$$

are the element pressure and flow nodal vectors respectively. The quantities X_i and X_j are the spatial coordinates of the i^{th} and j^{th} nodes of the element, and L is the element length.

The Galerkin method was then applied to the governing equations to yield the element equations. According to the Galerkin method, the residual is multiplied by the shape functions and integrated over the element length to yield the element equations. Hence, the continuity equations becomes

$$\int_{X_i}^{X_j} [N]^T \{\frac{\partial Q}{\partial x} + A^e C_o \frac{\partial p}{\partial t} + A^e C_1 p \frac{\partial p}{\partial t} + Sp\} dx = 0 \tag{4.26}$$

where the average value of the cross sectional area of each element, A^e, is used instead of the x-dependent cross sectional area, $A_o(x)$, to ease the integration process. Proceeding in a similar fashion, the Galerkin method applied to the momentum equation yields

$$\int_{X_i}^{X_j} [N]^T \{c_u \frac{\partial Q}{\partial t} + \frac{\partial}{\partial x}\left(\lambda \frac{Q^2}{A^e}\right) + \frac{A^e}{\rho}\frac{\partial p}{\partial x} + B_1 Q - A^e b_x\} dx = 0 \tag{4.27}$$

The integration of Equations 4.26 and 4.27 is carried out to the point where the element equations are specified in a compact matrix form. The details of the

mathematical procedure can be found in Appendix A. After assemblage of the element equations, the final system of equations was expressed in matrix form as

$$\frac{d\{\delta\}}{dt} = [K]\{\delta\} \tag{4.28}$$

where $\{\delta\} = \left[p_1, Q_1, \ldots, p_N, Q_N\right]^T$ is the global vector of the nodal values, $[K]$ is the global stiffness matrix. Equation 4.28 represents a system of 2xN non-linear first order differential equations, N being the number of nodes in the network.

The initial, branch, and boundary conditions as well as modeling stenoses are conceptually the same as in the finite difference case, the only significant difference being that the corresponding equations are given in terms of the time derivatives of p and Q instead of p and Q themselves. A discussion of the formulation of these conditions can be found in Weerappuli (1987). The final system of ODE's was solved using LSODES, a numerical solver for stiff differential equations.

Numerical Solution

A FORTRAN-77 code was written for both the finite difference and the finite element method. The codes are listed in Appendices B and C, respectively. The code lines which are not in standard FORTRAN-77 language and are software dependent (i.e., Microsoft Fortran for the FDM and Vax Fortran for the FEM) are marked with an asterisk.

The finite difference code was run on a Zenith Z-386 SX microcomputer, equipped with a 387 math co-processor. For the 239-node arterial system (presented in the next chapter) and a time step of $\Delta t = 0.001$ sec, the execution time was 143 sec. The solution was carried over two cycles (2 sec), so that the system of 2x239=478

algebraic equations was evaluated 2000 times within that period of time. It interesting to note that for this size of arterial network, real-time computing would require a computer $\frac{143}{2} \simeq 70$ times faster than the one used here. Computers with this capability are readily available today.

CHAPTER 5. PHYSIOLOGICAL MODEL

A literature search for a complete and concise set of data for the geometric and elastic properties of the arterial tree failed to provide satisfactory results. Certain sections of the vascular tree of particular medical interest (i.e., the coronary arteries, the aorta, etc.) or sections more accessible to measurements (i.e., upper and lower limbs) had their parameters measured and reported more frequently than other arterial segments. Geometric data were in general easier to find, but direct estimates of the elastic properties and the peripheral resistances were most difficult to obtain.

A common source of physiological data for many analog or computers models of the arterial tree (Snyder et al., 1968; Westerhof et al., 1969; Schaaf and Abbrecht, 1972; Avolio, 1980; Sud and Sekhon, 1986) was the data compiled by Noordergraaf et al. (1963) and subsequently modified by Westerhof et al. (1969). The arterial model of the current study is based primarily on the data published by Westerhof et al. (1969). The model of the arterial system consists of fifty-five arterial segments which are shown schematically in Figure 5.1. The proximal end of the arterial system is the root of the ascending aorta immediately distal to the aortic valve, but the system does not include the coronary arteries. The original model also did not include the internal iliac arteries which are major arteries of the human leg, hence, these two arteries were added in the present model. The geometric, elastic, and peripheral resistance data

presented below are considered representative of a healthy young adult, and will be referred to as the control case data.

Geometrical Data

The geometrical properties of the arterial segments specified were: 1) the length of the arterial segment, 2) the proximal and distal cross sectional area, and 3) the orientation of the arterial segment. The geometrical data are tabulated in Table 5.1.

The cross sectional area of each segment is assumed to vary linearly between the proximal and distal values. Although it has been found that the area may vary in a non-linear fashion along arterial segments (see for example Raines et al., 1974) the ease in the construction of the model overweighs the small discrepancies due to the linearity assumption, and the errors resulting from this assumption are generally thought to be small.

The orientation of the arterial segments is also given in Table 5.1. The arterial segments are projected on a two-dimensional mid-sagittal plane, and their orientation is defined by the angle between the longitudinal axis of the artery and a reference horizontal axis running from right to left. The assumptions made here are 1) the arterial segments are straight and 2) the person is laying or in an upright standing position with upper and lower limbs straight. The data were obtained form Sud and Sekhon (1986) with small modifications due to incompatibilities in the arterial segments defined.

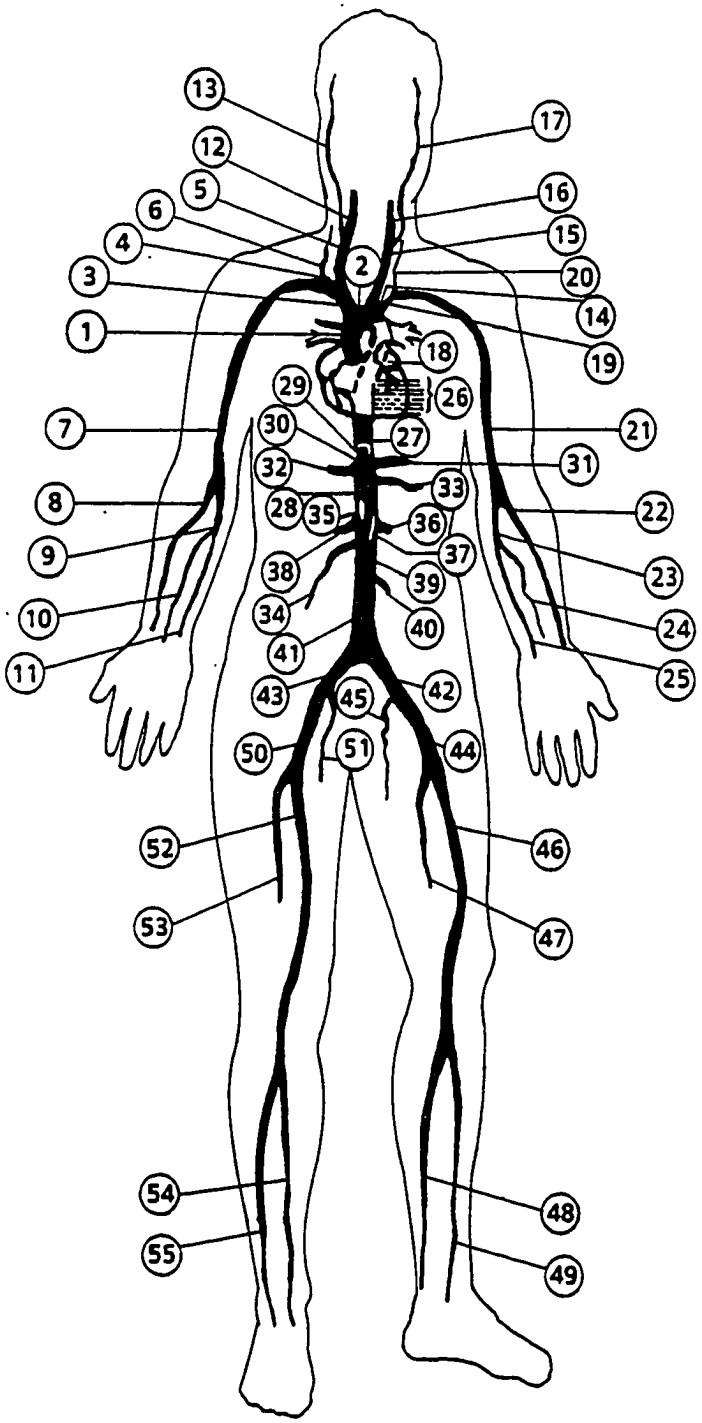

Figure 5.1: Model of the human arterial system

Table 5.1: Physiological data for the arterial model

Seg.	Name	Length (cm)	Prox. R (cm)	Distal R (cm)	Angle (deg)	Vol. compl. ($10^{-6}\frac{cm^5}{dyne}$)
1	Ascending Aorta	4.0	1.470	1.440	90	104.400
2	Aortic Arch A	2.0	1.120	1.120	0	29.600
3	Innominate	3.4	0.620	0.620	135	13.500
4	R. Subclavian A	3.4	0.423	0.423	180	5.600
5	R. Carotid	17.7	0.370	0.370	90	21.360
6	R. Vertebral	14.8	0.188	0.183	120	1.682
7	R. Subclavian B	42.2	0.403	0.236	240	33.870
8	R. Radial	23.5	0.174	0.142	240	1.877
9	R. Ulnar A	6.7	0.215	0.215	240	1.110
10	R. Interosseous	7.9	0.091	0.091	240	0.090
11	R. Ulnar B	17.1	0.203	0.183	240	2.210
12	R. Internal Carotid	17.7	0.177	0.083	90	0.943
13	R. External Carotid	17.7	0.177	0.083	135	0.943
14	Aortic Arch B	3.9	1.070	1.070	0	52.100
15	L. Carotid	20.8	0.370	0.370	60	25.100
16	L. Internal Carotid	17.7	0.177	0.083	90	0.943
17	L. External Carotid	17.7	0.177	0.083	45	0.943
18	Thoracic Aorta A	5.2	0.999	0.999	270	59.700
19	L. Subclavian A	3.4	0.423	0.423	45	5.600
20	Vertebral	14.8	0.188	0.183	60	1.682
21	L. Subclavian B	42.2	0.403	0.236	300	33.870
22	L. Radial	23.5	0.174	0.142	300	1.877
23	L. Ulnar A	6.7	0.215	0.215	300	1.110
24	L. Interosseous	7.9	0.091	0.091	300	0.090
25	L. Ulnar B	17.1	0.203	0.183	300	2.210
26	Intercostals	8.0	0.200	0.150	0	3.000
27	Thoracic Aorta B	10.4	0.675	0.645	270	47.600
28	Abdominal Aorta A	5.3	0.610	0.610	270	20.400
29	Celiac A	1.0	0.390	0.390	0	1.360
30	Celiac B	1.0	0.200	0.200	0	1.000
31	Hepatic	6.6	0.220	0.220	315	2.300
32	Gastric	7.1	0.180	0.180	450	1.510
33	Splenic	6.3	0.275	0.275	0	3.740
34	Superior Mesenteric	5.9	0.435	0.435	225	10.400

Table 5.1 (Continued)

Seg.	Name	Length (cm)	Prox. R (cm)	Distal R (cm)	Angle (deg)	Vol. compl. ($10^{-6}\frac{cm^5}{dyne}$)
35	Abdominal Aorta B	1.0	0.600	0.600	270	4.000
36	L. Renal	3.2	0.260	0.260	0	1.670
37	Abdominal Aorta C	1.0	0.590	0.590	270	3.800
38	R. Renal	3.2	0.260	0.260	0	1.670
39	Abdominal Aorta D	10.6	0.580	0.548	270	33.900
40	Inferior Mesenteric	5.0	0.160	0.160	270	0.792
41	Abdominal Aorta E	1.0	0.520	0.520	270	3.500
42	R. Common Iliac	5.8	0.368	0.350	315	4.580
43	L. Common Iliac	5.8	0.368	0.350	225	4.580
44	L. External Iliac	14.4	0.320	0.270	315	15.620
45	L. Internal iliac	5.0	0.200	0.200	270	3.300
46	L. Femoral	44.3	0.259	0.190	270	13.640
47	L. Deep Femoral	12.6	0.255	0.186	315	1.130
48	L. Posterior Tibial	32.1	0.247	0.141	270	2.206
49	L. Anterior Tibial	34.3	0.130	0.130	270	0.842
50	R. External Iliac	14.4	0.320	0.270	225	15.620
51	R. Internal iliac	5.0	0.200	0.200	270	3.300
52	R. Femoral	44.3	0.259	0.190	270	13.640
53	R. Deep Femoral	12.6	0.255	0.186	225	1.130
54	R. Posterior Tibial	32.1	0.247	0.141	270	2.206
55	R. Anterior Tibial	34.3	0.130	0.130	270	0.842

Elastic Properties

The equation of state requires a way of relating the changes of arterial cross sectional area to the changes of intraluminal pressure. The concept of arterial compliance, C, is introduced, where

$$C = \frac{\partial A(p,x)}{\partial p} \tag{5.1}$$

In general the arterial compliance varies with location within the arterial tree and is a function of the distending pressure, p. The values for the arterial compliance used in the present study were obtained from those reported by Westerhof et al. (1969). Westerhof et al. recognized the fact that elastic tapering is present in the arterial system, that is, Young's modulus of elasticity increases from the aorta to the periphery. Due to lack of sufficient data Westerhof et al. assumed that:

1. for the main arterial trunk, upper arms and legs, and lower part of the carotid artery, $E = 4 \times 10^6 \frac{g}{cm \times s^2}$,
2. for the middle part of legs, arms, and head, $E = 8 \times 10^6 \frac{g}{cm \times s^2}$, and
3. for the lower part of legs and arms, $E = 16 \times 10^6 \frac{g}{cm \times s^2}$

The volume compliance of each arterial segment was then computed using the equation

$$C_{vol} = \frac{\Delta V_{art}}{\Delta p} = L\frac{\Delta A}{\Delta p} = L\frac{3\pi r^2(a+1)^2}{E(2a+1)} \tag{5.2}$$

where V_{art} is the intraluminal arterial segment volume, L is the length of the arterial segment, and $a = \frac{r}{h}$ is the ratio of the internal radius to wall thickness. The tabulated values for the volume compliance of each segment are given in Table 5.1.

Considering the subcase of a linear constitutive relation, Equation 3.4 is written as

$$A(x) = A_O(x)\left[1 + C'_O(p - p_O)\right] \tag{5.3}$$

Differentiation with respect to pressure yields

$$C = A_O C'_O \tag{5.4}$$

so that the linear compliance coefficient, C'_O can be evaluated as

$$C'_O = \frac{C_{vol}}{LA_O} \tag{5.5}$$

Since C'_O was considered constant within the arterial segment, the average segmental value of A_O was used in the evaluation of C'_O.

The evaluation of the non-linear compliance coefficient, C'_1, cannot be done directly unless the specific shape of the pressure-area curve is known. Porenta et al. (1986) suggested that an indirect estimate of C'_1 can be obtained by assuming that the following pressure-area relationship proposed by Streeter et al. (1963) applies

$$A(p,x) = A_O(x)\left[1 - \frac{D_O(p - p_O)}{h_O E}\right]^{-1} \tag{5.6}$$

The above equation can be expanded in a Taylor series to yield

$$A(p,x) = A_O(x)\left[1 + \left(\frac{1}{\rho a_O^2}\right)(p - p_O) + \left(\frac{1}{\rho a_O^2}\right)^2 (p - p_O)^2\right] \tag{5.7}$$

where $a_O = \sqrt{\frac{h_O E}{D_O \rho}}$ is the wave speed as approximated by the Moens-Korteweg equation. Comparison with the original constitutive relation (Equation 3.4) suggests that $C'_1 = \left(C'_O\right)^2$, which is the relationship used to complete the constitutive model of the present study.

Terminal Impedances

Terminal impedances are represented by modified windkessel models. This representation requires a knowledge of three parameters: 1) the total resistance, R_T, 2) the ratio of the proximal resistance, R_1, to total resistance, R_T, and 3) the terminal compliance, C_T.

The evaluation of the total resistance is the easiest of the three parameters to estimate because it is defined as the ratio of the mean pressure to mean flow through the terminal branch. Yet, a consistent set of data for the arterial system under consideration was not found in the literature. The values used in the current study were obtained from Schaaf and Abbrecht (1972), and are tabulated in Table 5.2.

The ratio of the proximal to total terminal resistance, $\frac{R_1}{R_T}$, reflects the relative significance of the resistive elements of the lumped vessels closer to the point of termination as compared to the total resistive elements of the proximal and distal smaller vessels and microvasculature. Attempts have been made in past studies to estimate $\frac{R_1}{R_T}$ based on certain hypotheses, as for example minimization of the reflection coefficient, by Raines et al. (1974). In the present study such hypotheses are not posed, rather a somewhat arbitrary value of 0.2 for the resistance ratio is assigned to all terminal impedances. This value was close to the one estimated by Raines et al. for the human leg and measured by Weerappuli (1987) for the hindlimb of the dog, and is thought to be reasonable in the sense that the biggest part of total resistance (80%) is attributed to the effect of the small-diameter, highly-resistive distal microvasculature.

The terminal compliance, C_T, which in effect accounts for the compliant characteristics of the lumped distal vessels is also a quantity difficult to estimate, and

Table 5.2: Terminal impedance data

Segment	Total resistance $(\frac{Ns}{m^5})$	Terminal compliance $(\frac{m^5}{N})$
6	0.60100E+10	0.30955E-10
8	0.52800E+10	0.35235E-10
10	0.84300E+11	0.22069E-11
11	0.52800E+10	0.35235E-10
12	0.13900E+11	0.13384E-10
13	0.13900E+11	0.13384E-10
16	0.13900E+11	0.13384E-10
17	0.13900E+11	0.13384E-10
20	0.60100E+10	0.30955E-10
22	0.52800E+10	0.35235E-10
24	0.84300E+11	0.22069E-11
25	0.52800E+10	0.35235E-10
26	0.13900E+10	0.13384E-09
31	0.36300E+10	0.51251E-10
32	0.54100E+10	0.34389E-10
33	0.23200E+10	0.80191E-10
34	0.93000E+09	0.20005E-09
36	0.11300E+10	0.16464E-09
38	0.11300E+10	0.16464E-09
40	0.68800E+10	0.27041E-10
45	0.79360E+10	0.23443E-10
47	0.47700E+10	0.39003E-10
48	0.47700E+10	0.39003E-10
49	0.55900E+10	0.33281E-10
51	0.79360E+10	0.23443E-10
53	0.47700E+10	0.39003E-10
54	0.47700E+10	0.39003E-10
55	0.55900E+10	0.33281E-10

few values of the terminal compliances are reported in the literature. In principle, one needs to measure simultaneously pressure and flow pulses at the point of termination and estimate the value of C_T' using statistical methods. In this study the values for the terminal compliance were estimated in the following approximate and indirect way: First, the residual volume compliance of the arterial system was estimated. The total volume compliance of the arterial system was taken to be $1.0 \frac{\text{ml}}{\text{mm Hg}}$ (Burton 1965). The volume compliance for the arterial segments in the model is found by summing up the volume compliances of each segment, and this summation yields a value of $0.835 \frac{\text{ml}}{\text{mm Hg}}$. Therefore, the residual volume compliance is $C_{vol,res}' = 0.165 \frac{\text{ml}}{\text{mm Hg}}$. It was then assumed that the the residual compliance was distributed among the terminal branches in proportion to their mean flow, i.e.,

$$C_{T_i}' = C_{vol,res}' \frac{\overline{Q_i}}{\overline{Q_{total}}} = C_{vol,res}' \frac{R_{total}}{R_{T_i}}$$

where R_{total} is the total resistance of the arterial system. The total resistance is calculated by summing up the resistances of the arterial network. The values of the calculated terminal compliances, expressed in the SI system of units ($\frac{m^5}{N}$), are listed in Table 5.2.

The physiological model is completed by defining the rheological properties of blood. Blood was considered a Newtonian fluid having a constant dynamic viscosity of 0.0045 $\frac{Ns}{m^2}$, and constant density of 1050 $\frac{kg}{m^3}$. An input data file which includes all the model parameters corresponding to the control case is given in Appendix D. Several programs runs were made to evaluate the overall performance of the model and to determine its effectiveness in modeling normal and diseased states of arterial flow. The results of these runs are presented in the following chapter.

CHAPTER 6. COMPUTER SIMULATION OF ARTERIAL FLOW

Based on the physiological model data given in the previous chapter several computer runs were made to simulate arterial blood flow. The results were analyzed and compared (when possible) with experimental data to determine the overall effectiveness of the model in modeling normal and diseased states of arterial flow.

Control Case

The control case is defined as the case for which a "normal" pressure or flow waveform is used as input at the proximal end, no stenoses are present, and the system is not subjected to inertial or gravitational forces. The control case serves two purposes: 1) it provides a measure for the evaluation of the model by comparing control case results with normal flow measurements found in the literature, and 2) it provides a reference point for comparing the results of other computer simulations, where some of the model parameters are altered in an attempt to examine their influence on pressure and flow characteristics.

For most of the results presented in this chapter, a flow waveform is specified at the proximal end. Pressure waveforms also could be used as proximal boundary conditions, although it was difficult to generate the flat, zero-flow portion of diastolic flow at the proximal end with this boundary condition. The flow waveform used

Table 6.1: Fourier coefficients for the proximal flow waveform

Harmonic	Cosine term $(\frac{m^3}{s})$	Sine term $(\frac{m^3}{s})$
0	0.86393E-4	0.00000E+0
1	-0.88455E-4	0.13368E-3
2	-0.52515E-4	-0.12280E-3
3	0.86471E-4	0.22459E-4
4	-0.26395E-4	0.22693E-4
5	-0.12987E-4	0.22398E-5
6	0.20133E-5	-0.22315E-4
7	0.70896E-5	0.10065E-4
8	0.32577E-5	-0.21066E-5
9	-0.56573E-5	0.90633E-5
10	-0.19302E-5	-0.85422E-5

as input for the control case was taken from Nichols et al. (1977). The Fourier components of the pulse are given in Table 6.1

Comparisons with experimental measurements were made in terms of 1) pressure and flow waveform shapes at various locations, and 2) aortic input impedance.

Pressure and flow wave shapes

A typical set of computed pressure and flow waveforms is given in Figures 6.1 and 6.2. The four output locations selected were at the root of the ascending aorta, at the distal end of the brachial artery (immediately before the bifurcation point), at the abdominal aorta between the celiac and the superior mesenteric, and at the distal end of the left femoral artery (immediately before the tibial bifurcation). The computed waveforms exhibit the following general characteristics which are commonly found in the systemic circulation:

- There is a significant amplification of the pressure pulse (although the mean pressure is dropping) as the pulse propagates along the vascular tree. This phenomenon is more pronounced in the arteries of the upper and lower limbs. The flow pulse, however, is damped and the mean flow is reduced as a direct effect of branching.

- The diacrotic notch (inscisura) is dampened quickly (not present in the abdominal aorta pressure pulse) resulting in a smoother peripheral pressure pulse. Peripheral pressure pulses exhibit a secondary hump (often referred to as a reflection wave) following the end of systole.

- Flow pulses along the main aortic trunk, and continuing to the main arteries of the limbs, exhibit regions of flow reversal (back flow) during a small fraction of the cycle.

- There is a definite time delay as the pressure and flow pulses travel to the periphery. The foot-to-foot time delay between the ascending aorta and the femoral artery is 0.155 seconds, which compares favorably with values reported in the literature.

- There is a phase shift between pressure and flow waveforms which is related to the characteristics of the distal arterial network. The computed flow waveforms reach their peak values before the corresponding pressure waves and this characteristic is in accordance to experimental observations where flow is found to lead pressure (McDonald, 1974).

The shapes of the pressure and flow waveforms were generally in good agreement with experimental measurements. Figure 6.3 shows typical waveforms measured at

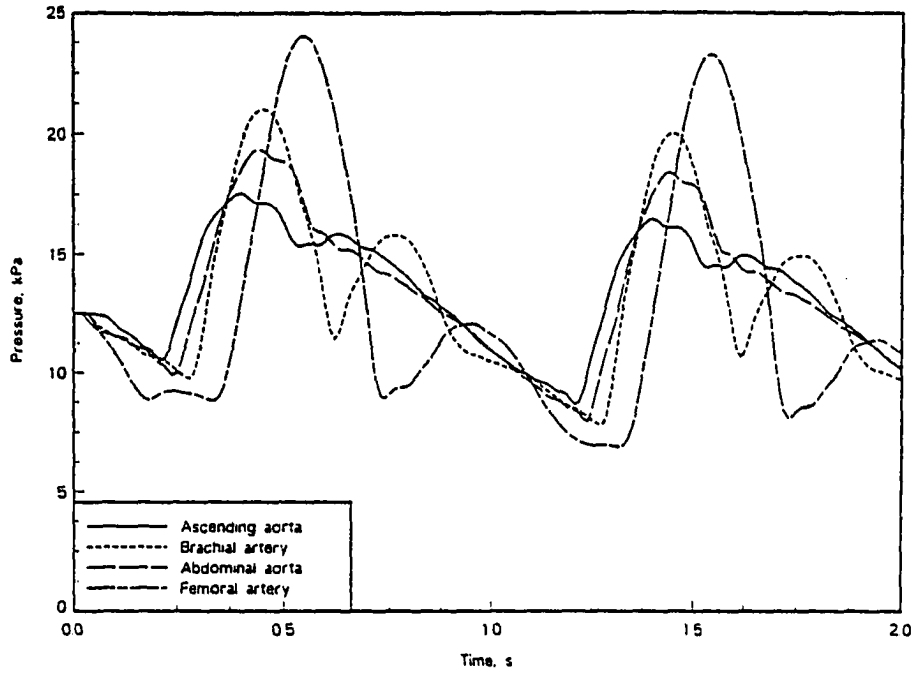

Figure 6.1: Pressure waveforms for the control case

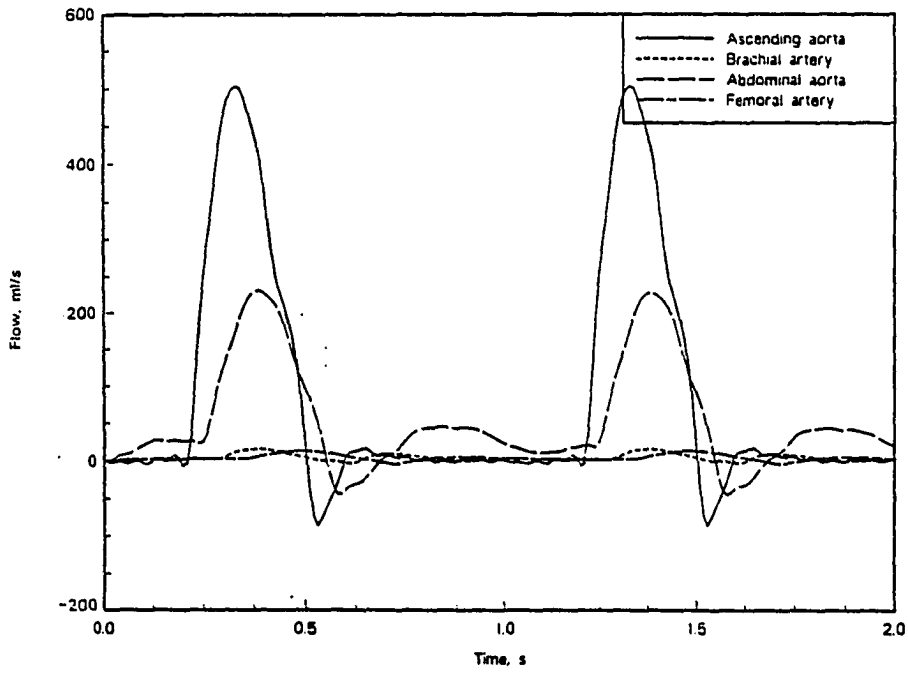

Figure 6.2: Flow waveforms for the control case

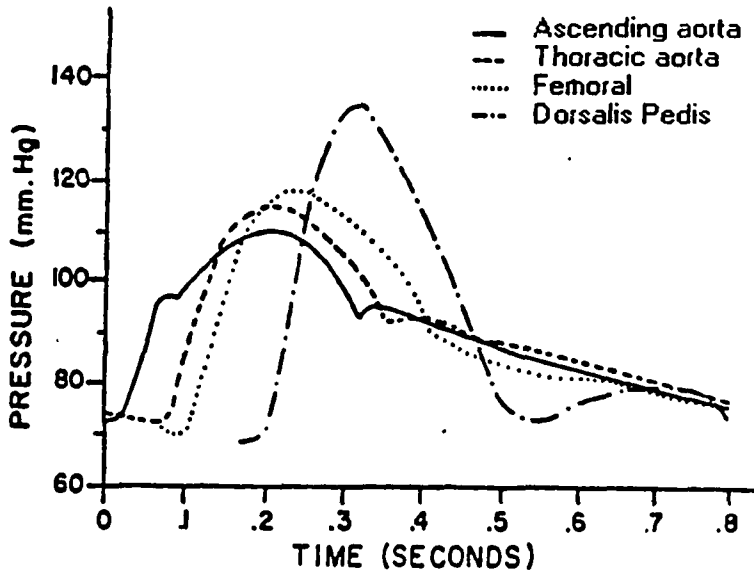

Figure 6.3: Typical measured pressure waveforms. From Guyton. (1976)

different locations of the arterial tree. The comparison can be only qualitative in nature. but the agreement in shape between the model predictions and the measured waveforms can be considered satisfactory. Deviations between measured and predicted waveforms certainly exist. as for example the not so sharp diacrotic notch on the predicted pressure waveform in the ascending aorta or the over-pronounced secondary pressure wave in the brachial artery. These deviations are to a degree expected and are mainly attributed to: 1) incompleteness in the physical description of the arterial tree (only major arteries included), 2) errors in estimated model parameters. and 3) uncertainty in branch and boundary conditions (important determinants of the reflection waves).

Figure 6.4 shows the predicted pressure waveforms from a computer model by Avolio (1980). The computer model was based on the transmission line theory equations. Comparison with the present numerical model predictions show that the trends

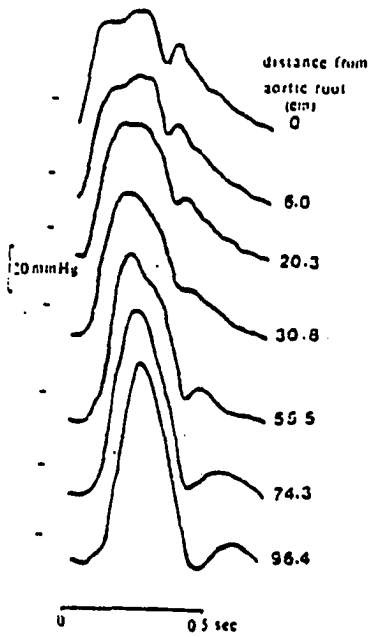

Figure 6.4: Computer generated pressure waveforms along the arterial tree, as given by Avolio (1980)

in the arterial pulse formation are similar, despite the differences in the computational method, governing equations, boundary conditions, and model characteristics.

Aortic input impedance

The aortic input impedance, Z, is calculated by analyzing the pressure and flow waveforms at the root of the ascending aorta into their Fourier components. Then, by definition, the magnitude of the i^{th} harmonic of the aortic impedance is calculated as

$$|Z_i| = \frac{|p_i|}{|Q_i|} \tag{6.1}$$

and the phase as

$$\phi_{Z_i} = \phi_{p_i} - \phi_{Q_i} \tag{6.2}$$

where $|p_i|$, $|Q_i|$, ϕ_{p_i}, and ϕ_{Q_i} are the magnitudes and the phases of the i^{th} harmonic of the pressure and flow waveforms, respectively. From the medical standpoint, input impedance indicates the characteristics of the distal arterial bed, and in the case of the aortic input impedance the characteristics of the whole arterial tree, as well as the output load on the left ventricle. A typical graph of the magnitude and phase versus frequency of the human ascending aorta input impedance is shown in Figures 6.5 and 6.6. The magnitude of the impedance at zero frequency reflects the total resistance of the system (mean pressure over mean flow). Although the shape of the magnitude and phase curves can vary from individual to individual there are some characteristics common to all experimental findings: The impedance magnitude drops rapidly within the first two harmonics and oscillates slightly thereafter. Averaging the values of the impedance magnitude at higher frequencies (i.e., 2 to 10 Hz) gives the value of the *characteristic impedance*. For the human, the average normal value of the characteristic impedance is 74 dyne-s/cm^5 with a standard deviation of approximately 15 dyne-s/cm^5 (Milnor, 1982). In the first few harmonics the phase is negative supporting the well established fact that at low frequencies flow leads pressure. The minimum phase value ranges between -1 and -2 rad with a typical value of approximately -80 degrees. The phase curve crosses to positive values at approximately the point of minimum impedance. The point of crossing however as well as the behavior of the phase curve at higher frequencies is not well established.

In the present study, the impedance at the ascending aorta was calculated by expressing the pressure and flow waveforms in terms of Fourier series and performing a straightforward complex number division to yield the magnitude and phase of the input impedance. The procedure gives discrete values of magnitude and phase at

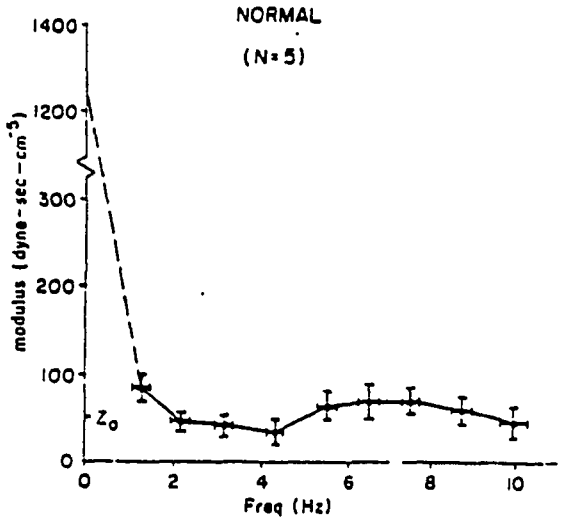

Figure 6.5: Experimental aortic impedance modulus. From Nichols et al. (1977)

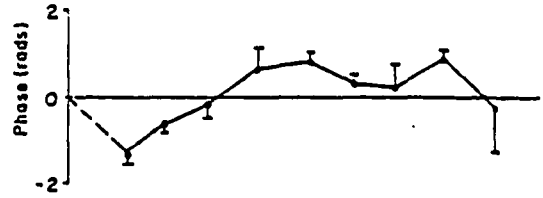

Figure 6.6: Experimental aortic impedance phase. From Nichols et al. (1977)

each harmonic, but, in principle, a continuous curve can be obtained by varying the fundamental frequency of the driving pulse. The results are shown in Figures 6.7 and 6.8.

The predicted impedance modulus reflects quite well the impedance characteristics. Shown on non-dimensional scale, the modulus drops steeply in the first two harmonics and then levels out oscillating slightly at the higher harmonics. Although the oscillations are smaller in magnitude than commonly observed, the value of the characteristic impedance ($0.07 \times Z_O$) is in good agreement with the published data. The predicted impedance phase curve does show a significant negative portion for the lower harmonics, however, the minimum value (-140 deg) is lower than the usual range of minimum found in the literature. The curve also crosses to the positive values before the third harmonic which is in the lower extreme of the usual range. The source(s) for these discrepancies in the phase difference between the pressure and flow pulse are not easily accounted for. Errors could be due to the pressure-area relationship used, as well as due to viscoelastic effects which are present in real arteries, but are not included in the present model. Perhaps another source of error is the particular numerical scheme used to obtain the solution. When applied to propagation phenomena, first-order finite difference schemes, like the one utilized in the present study, tend to exhibit predominantly dispersive errors (Anderson et al., 1984). Dispersive errors translate to phase errors in the pressure and flow waveforms and hence in the phase of input impedances. The question of whether this hypothesis is correct or not could be resolved if a higher order scheme (for example a second order scheme) is applied to the same arterial model and the improvement over the present results assessed.

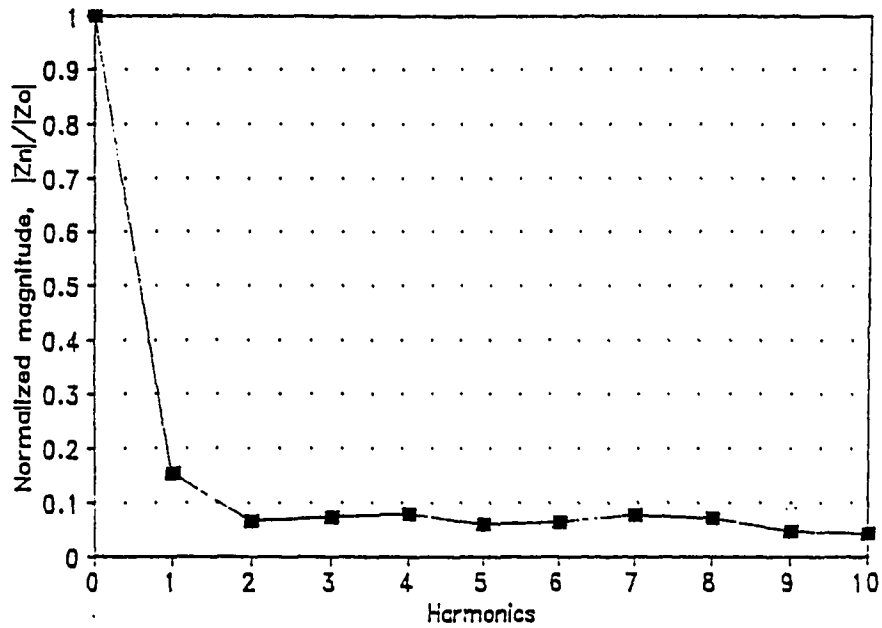

Figure 6.7: Model prediction of aortic impedance modulus

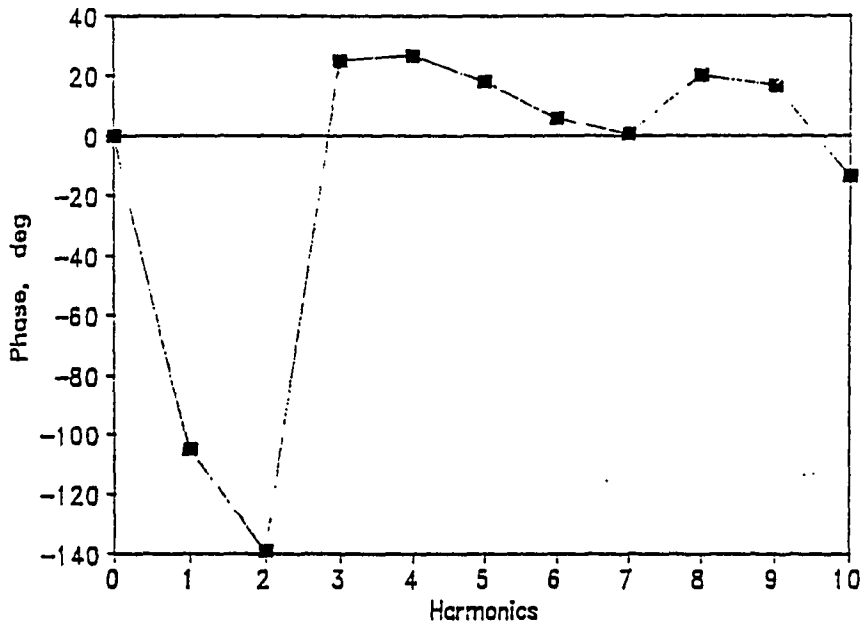

Figure 6.8: Model prediction of aortic impedance phase

Flow input versus pressure input

For an open arterial system, like the one under consideration, the question of whether flow or pressure should be prescribed at the proximal end is not easily answered. From the mathematical standpoint it makes no difference which one of the two primary variables is prescribed, nor does it matter from the computational standpoint. To illustrate that point and also check the integrity of the numerical solution scheme, two solutions were obtained: one where flow is prescribed at the proximal end, and a second one where pressure is prescribed at the proximal end. The proximal pressure for the second run was obtained from the converged solution of the first run. The results of these runs in terms of prescribed and calculated pressures and flows at the proximal end are shown in Figures 6.9 and 6.10.

The results indeed show that the two solutions are identical once convergence is achieved, and therefore either pressure or flow can be used as the proximal condition. The results also show that it takes approximately two to three cycles before the effects of the erroneous initial conditions are totally damped out. After that point the solution virtually repeats itself and the procedure is assumed converged.

In this study, flow was used as a proximal condition for most cases studied. It was found that using pressure as the proximal condition, and without any other condition imposed on the proximal flow, the zero-flow portion of the ascending aortic flow that takes place during the diastole was not accurately resolved. Rockwell (1969) also showed preference toward flow proximal condition since this condition appeared to yield more satisfactory results (rather than prescribing the pressure and computing the flow). The selection of the type of proximal condition can be critical in special cases of arterial flow, as for example in the case of +Gz loading (gravitational or

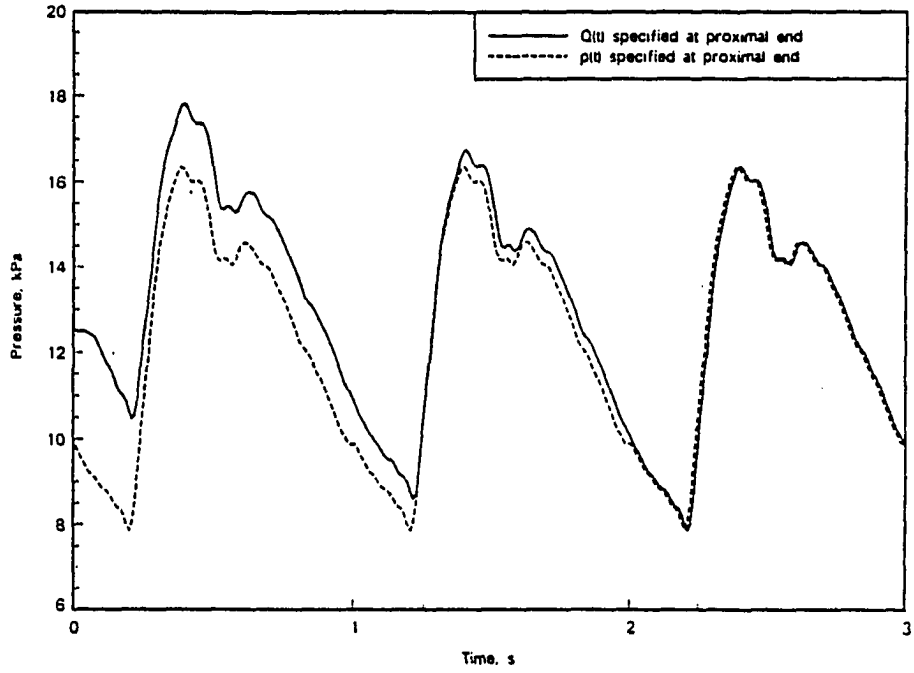

Figure 6.9: Prescribed and predicted pressure waveforms at the proximal end (root of ascending aorta)

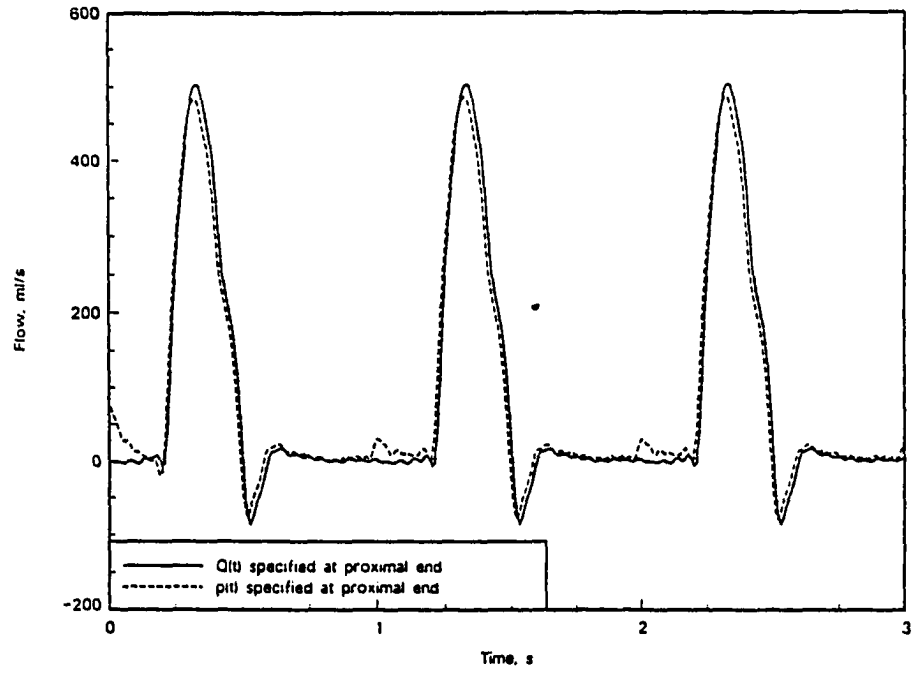

Figure 6.10: Prescribed and predicted flow waveforms at the proximal end (root of ascending aorta)

inertial forces with a head-to-foot direction). It is clear that if a normal arterial pressure pulse is applied at the onset of large +Gz loading the amount of flow through the aorta can be unreasonably large since no essential restrictions on the amount of flow were imposed. The question of the proper proximal condition was not intended to be within the scope of this thesis. It is recognized, however, that it is of importance in the modeling of arterial systems and further investigation is required before the matter is completely resolved.

Model Evaluation

During the development of the model certain assumptions and simplifications were imposed to ease and complete the mathematical formulation of the problem. In particular, certain mathematical models were selected for the wall shear stress, the boundary conditions at the terminal sites, and the pressure-area relationship. Some tests to evaluate how the above assumed models affect the overall performance of the model were run, and the results are presented below. The results of a test regarding the significance of the convective acceleration (non-linear term) are also included.

Effect of wall shear stress model

The mathematical model for the wall shear stress was

$$\tau_w = -\frac{\rho}{2\pi R}\left[\frac{8c_v\pi\mu}{\rho A}Q + (c_u - 1)\frac{\partial Q}{\partial t}\right] \tag{6.3}$$

The coefficient of the viscous term, c_v, and the coefficient of the unsteady term, c_u, are functions of the Womersley parameter α, and can be selected so that they can match the theoretical solution for harmonic flow in an infinite, straight, rigid tube of

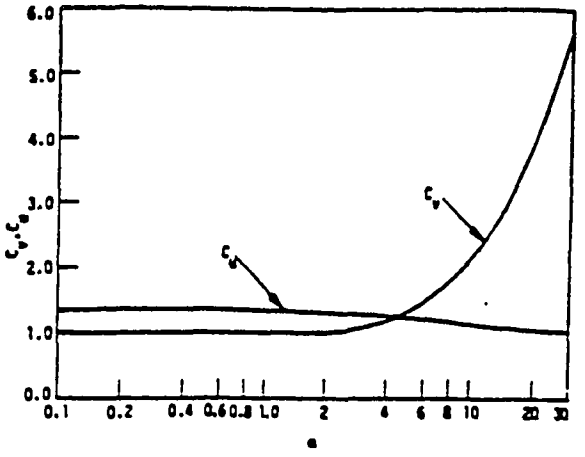

Figure 6.11: Coefficients of the shear stress model for simple harmonic flow in a straight rigid tube. From Young and Tsai (1973b)

constant diameter. For a simple harmonic motion the variation of c_v and c_u with α is shown in Figure 6.11.

It is clear that the shear stress model proposed cannot be strictly applied to arterial flow unless the conditions implied by the theoretical solution (straight, rigid tube of infinite length) are satisfied. But even if these conditions are relaxed, the solution is not valid since arterial flow is at best a periodic flow which can be described approximately by a Fourier series expansion. Hence, there is no unique set of c_v and c_u coefficients. From Figure 6.11 it is noted that the value of c_u is bounded between $4/3$ (for $\alpha = 0$) and 1 (for $\alpha = \infty$). The coefficient c_v has approximately the value of 1 for $\alpha \leq 3$ but then it increases rapidly for higher α values. In the present study both coefficients were set equal to one. However, with the wide range of α values found in the systemic circulation, it is of interest to investigate the effect that the

values assigned to coefficients c_v and c_u have on the solution. Two runs were made: one in which c_u obtained its highest possible value ($c_u = 4/3$) with $c_v = 1$, and one in which $c_v = 2$ and $c_u = 1$, which can be thought as representative of a range of high α values ($\alpha \geq 10$), normally found in large arteries (ascending or descending aorta, etc.). The results were compared with the reference case ($c_v = 1$, $c_u = 1$), and are shown in Figures 6.12 and 6.13.

Comparisons between the computed pressure and flow waveforms were made at two locations: in the abdominal aorta (seg. # 28), which is typical of a large artery, and in the femoral artery (seg. # 52), which is representative of a smaller size artery. Figures 6.12 and 6.13 show that the shear stress effects were rather minimal in the abdominal aorta, but they were significant in the femoral artery. This observation is in accordance with the physics of the problem: in smaller arteries, the wall shear stress is a strong function of the local radius, and the smaller the radius the higher the magnitude of the shear stress, whereas, at the same time, the inertia effects are rather small. In larger arteries, although high shear stresses may develop due to plug-like central core flows, they are relatively small when compared to inertia forces. Since the femoral artery has an internal radius of less than half of that of the abdominal aorta, it is not unexpected that the shear stress effects are more pronounced in the femoral artery. The results also show that the pressure waveforms in the femoral artery are more affected than the flow waveforms. Raising the value of c_u from 1 to 4/3 does not significantly affect the magnitude of pressure and flow, but it tends to shift both waveforms to the right. These effects were expected since c_u is the coefficient of the inertia term which can affect the phase of the waveform but carries no dissipative power to affect the magnitude of the pulse. Raising the value

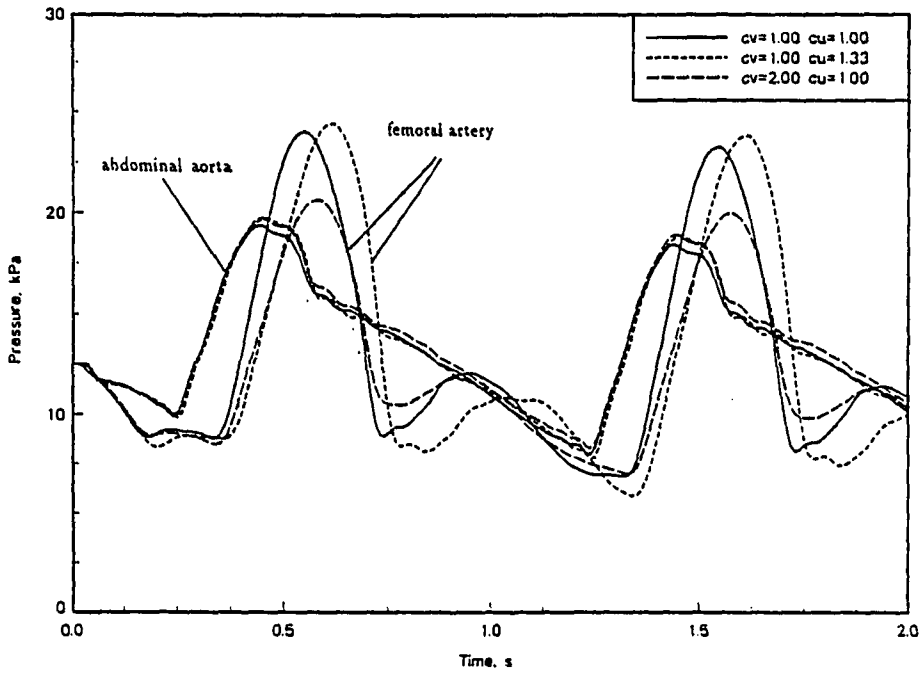

Figure 6.12: Calculated pressure waveforms in the abdominal aorta and the femoral artery for different cases of wall shear stress coefficients

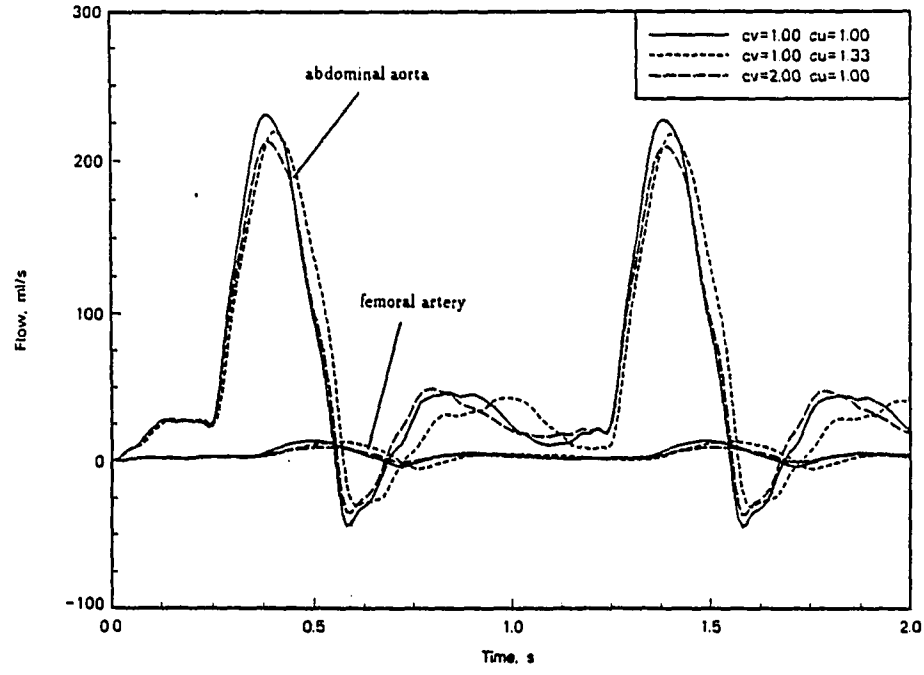

Figure 6.13: Calculated flow waveforms in the abdominal aorta and the femoral artery for different cases of wall shear stress coefficients

of the viscous coefficient c_v, however, raises the dissipation term proportionally with a subsequent reduction in the pressure and flow magnitudes. This effect was more pronounced in the pressure waveform. Raising c_v appears to have no effect on the phase of both pressure and flow. It should be noted that raising the value of c_v by a factor of 2 is equivalent to raising the viscosity of blood by the same factor. This is of course a quite unreasonable correction to be used throughout the arterial system and was done only for demonstrational purposes. Values of $c_v = 2$ are quite unlikely to be found in the smaller size peripheral arteries, although are possible in large arteries like the aorta, especially in the case for higher frequency pulsations. Thus, putting emphasis on the results for the abdominal aorta, it is concluded that the wall shear stress does not affect arterial flow significantly. This observation is in accordance to other computer model findings (Schaaf and Abbrecht, 1972; Wemple and Mockros, 1972; Raines et al., 1974).

Since the relative importance of the wall shear stress was concluded to be small, the specific selection of c_v and c_u values was of minor importance, and thereby, for simplicity both values were taken to be 1. In this case, the shear stress model (Equation 3.3) degenerates to that of Poiseuille type of flow (Equation 2.17).

Effect of boundary conditions

The imposed distal boundary conditions depend on the type of lumped parameter impedance used at the terminal branches. In the present model the lumped parameter impedance of choice was the modified windkessel model, which was introduced in Chapter 2. The modified windkessel model yields a rather complex boundary condition, which is described by Equation 3.8. Another popular approach

to boundary conditions is that of a pure resistive type of impedance at the terminal sites, which in turn yields a much simpler relation between terminal pressure and flow, as described by Equation 3.9. Since the use of the modified windkessel requires the knowledge of two additional parameters, C_T and R_1/R_T (which are hard to estimate), it is of interest to compare the solutions based on the modified windkessel type of boundary condition to those based on the pure resistance terminal condition. The comparison between the computed pressure and flow waveforms is done at two locations: in the abdominal aorta and in the femoral artery. The results are presented in Figures 6.14 and 6.15.

The results suggest that the change in the impedance model had minimal effect on the pressure and flow waveforms in the abdominal aorta, which is representative of a large artery in the main arterial trunk. The change in the impendance model, however, seemed to have some effect on the pressure and flow in the femoral artery, which is representative of a medium size peripheral artery. The pure resistance model, which lacks the additional compliance present in the modified windkessels (through the terminal compliance, C_T) tended to yield less smooth pressure and flow curves. The pure resistance model also seems to amplify the reflection waves, as the secondary hump in the pressure and flow pulse appears more pronounced. A more significant effect of the pure resistance model, which again relates to the lack of compliance in the model, is the amplification of the pressure pulse (increase in the maximum pressure and decrease in the minimum pressure). A similar, well established, phenomenon takes place in arteriosclerosis (hardening of arteries), where the compliance of arteries decreases resulting in a peak-to-peak amplification of the pressure pulse. This phenomenon will be discussed in a later section.

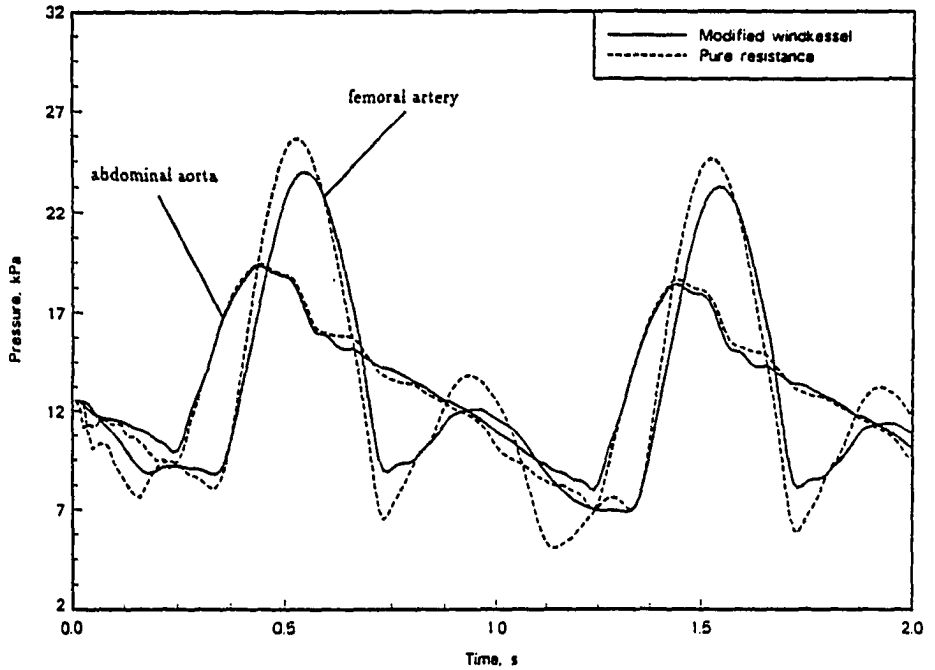

Figure 6.14: Calculated pressure waveforms in the abdominal aorta and the femoral artery for the modified windkessel and pure resistance type of boundary conditions

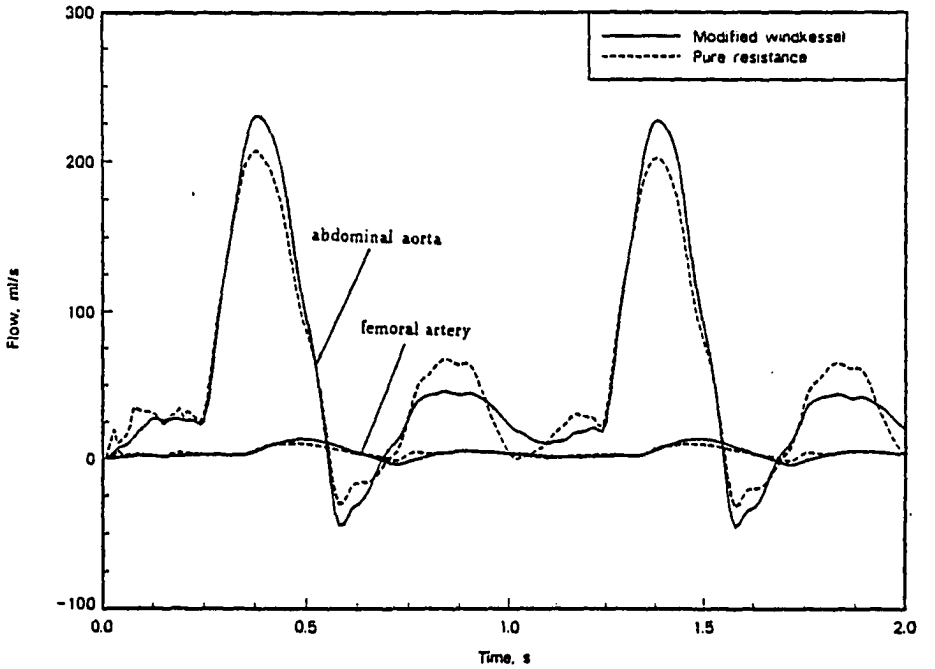

Figure 6.15: Calculated flow waveforms in the abdominal aorta and the femoral artery for the modified windkessel and pure resistance type of boundary conditions

The modified windkessel type of impedance has been suggested by several investigators as an improvement over the pure resistance model in the sense that this model is capable of yielding more realistic boundary conditions at the termination points (Raines et al., 1974; Porenta et al., 1986; Weerappuli, 1987). The nature of the model, however, requires certain hypotheses to be posed for the evaluation of its parameters. The results presented above suggest that although there can be some improvement in the model performance by using more appropriate boundary conditions, the improvement on a large scale model is certainly within the range of errors inherent in the model (due to the uncertainty of the various model parameters). Hence the practicality using a sophisticated lumped parameter model, at the time where basic model parameters (such as arterial diameters and compliances) are not precisely known is rather questionable. The search for the appropriate boundary conditions in a circulatory model, however, is an important subject in arterial modeling, as it is an important building block for the ultimate arterial model.

Effect of pressure-area relationship

The pressure-area relation used in the construction of the model is

$$A(x) = A_O(x)\left[1 + C_O'(p - p_O) + C_1'(p - p_O)^2\right] \tag{6.4}$$

The quadratic term was included to provide flexibility in the modeling of non-linear arterial pressure-area relationships. Non-linear pressure-area relationships proposed in the literature can generally be approximated accurately by series expansion and truncating the terms of third or higher order (Porenta et al., 1986). Three test cases using different types of p-A relationships were made to assess their effect on the computed pressure and flow waveforms. In the first case only the linear term

of Equation 6.4 was maintained. This naturally results in a linear p-A relation as shown in Figure 6.16. Although it is well established that the arterial pressure-area relation is non-linear, a linear p-A relationship has often been used in the past on the basis that in the operational range of pressures, a linear curve can be a fairly good approximation. For the second case the quadratic term was retained and evaluated as explained in section 5.2. Under the adoption of the pressure-area relation proposed by Streeter et al. (1963) (Equation 5.6), it turns out that the compliance coefficient of the quadratic term is evaluated as $C_1' = (C_o')^2$. This relationship demands that the second compliance coefficient, C_1', is always positive, and as a consequence of that, the effective compliance of the arterial segments increases as the distending pressure increases. Experimental observations, however, suggest that arteries tend to be stiffer at higher transmural pressures, and hence the coefficient C_1' should more likely be negative (Bergel, 1961). This is indeed the case in the third case in which the following pressure-area relation proposed by Raines et al. (1974)

$$A(p,x) = A(p_O,x)\left[1 + K \ln \frac{p}{p_O}\right] \tag{6.5}$$

is used. This logarithmic type of relationship can be expanded in series, and comparison with Equation 6.4 yields $C_o' = K/p_O$ and $C_1' = -K/(2p_O^2)$ (Porenta, 1986). In terms of C_o' (which is kept the same for all three runs for purposes of comparison), C_1' is evaluated as

$$C_1' = \frac{-C_o'}{2p_O} \tag{6.6}$$

p_O being the reference distending pressure taken as 97 mm Hg for all arterial segments. The above relationship indicates that C_1' is negative. As a consequence, the effective compliance of the arterial segments decreases with increase in pressure making the

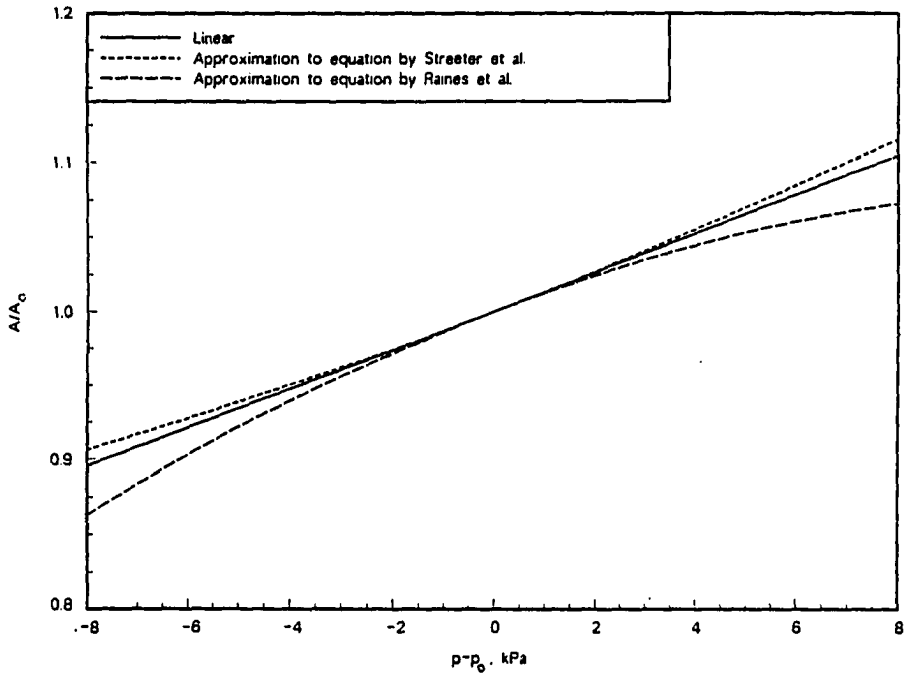

Figure 6.16: Comparison of the three different pressure-area relationships as applied to the femoral artery

artery stiffer at higher distending pressures. These trends are shown graphically for the femoral artery in Figure 6.16.

The computed pressure and flow waveforms at the femoral artery corresponding to different p-A relationships are plotted in Figures 6.17 and 6.18, respectively. The waveforms show that the differences were not very significant and were pronounced mostly at the peak values. The patterns of the pressure waveforms, however, demonstrate nicely the functional dependence of pressure propagation on the effective arterial compliance. The calculated pressure waveform based on the logarithmic p-A relationship peaks up more than the other two as expected, since at higher pressures the artery becomes stiffer and amplification of the pulse takes place (see later section for a discussion on the effect of the arterial compliance of pressure waveforms). At

lower pressures the effect of the negative quadratic term makes the artery less stiff (more compliant) than the other two, and the diastolic pressure is kept at higher values. The dependence of the wave speed on the arterial compliance which relates to the proposed p-A relation is also nicely demonstrated in Figure 6.17. For the case of the logarithmic p-A relationship the artery becomes stiffer at higher distending pressures, and hence, in accordance to Moens-Korteweg equation, the wave speed increases. Thus, as the pressure propagates from the aorta to the periphery, the peak pressure should travel faster for the case of the logarithmic relationship, resulting in a relative phase shift between the three curves. The same phenomenon is responsible for the relative skewness of the "logarithmic" pressure pulse as compared to the other two pulses. It is noteworthy that this type of skewness on the systolic pressure is evident in some of the pressure pulses reported in the literature (O'Rourke and Taylor, 1966).

Effect of convective acceleration

To assess the importance of the non-linear convective acceleration term in the momentum equation, tests were made in which the convective acceleration term was dropped. The results in terms of computed pressure and flow waveforms in the abdominal aorta and femoral artery together with results of the "normal" case are plotted in Figures 6.19 and 6.20.

The results suggest that the effects of the convective acceleration are minimal for the abdominal aorta. Even in the femoral artery where some tapering exists, the effects are rather small. The neglect of the convective acceleration term tends to suppress slightly the pressure peak. For the femoral artery the drop is approximately

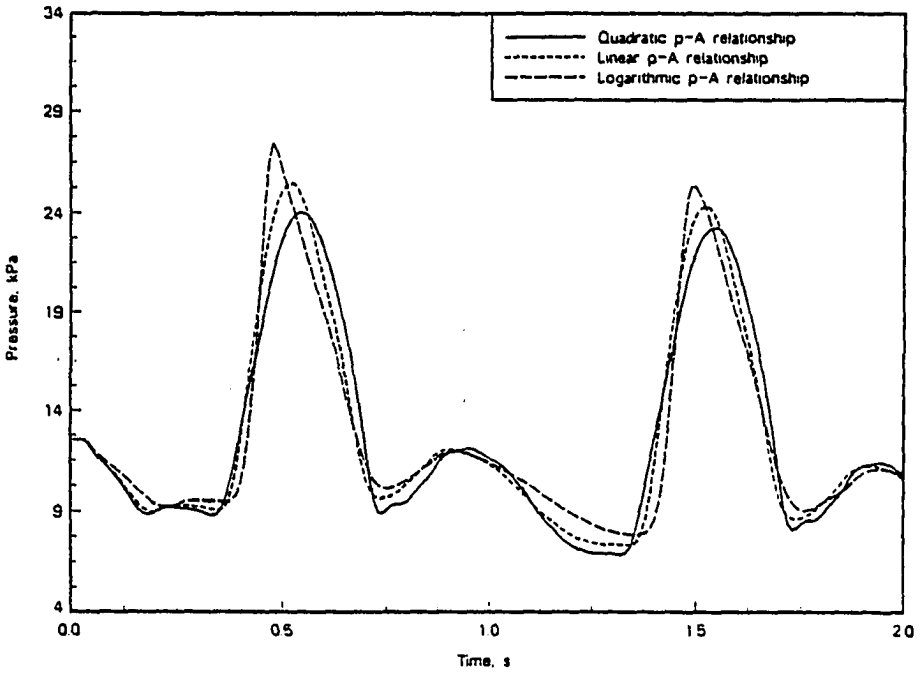

Figure 6.17: Comparison of pressure waveforms in the femoral artery for different pressure-area models

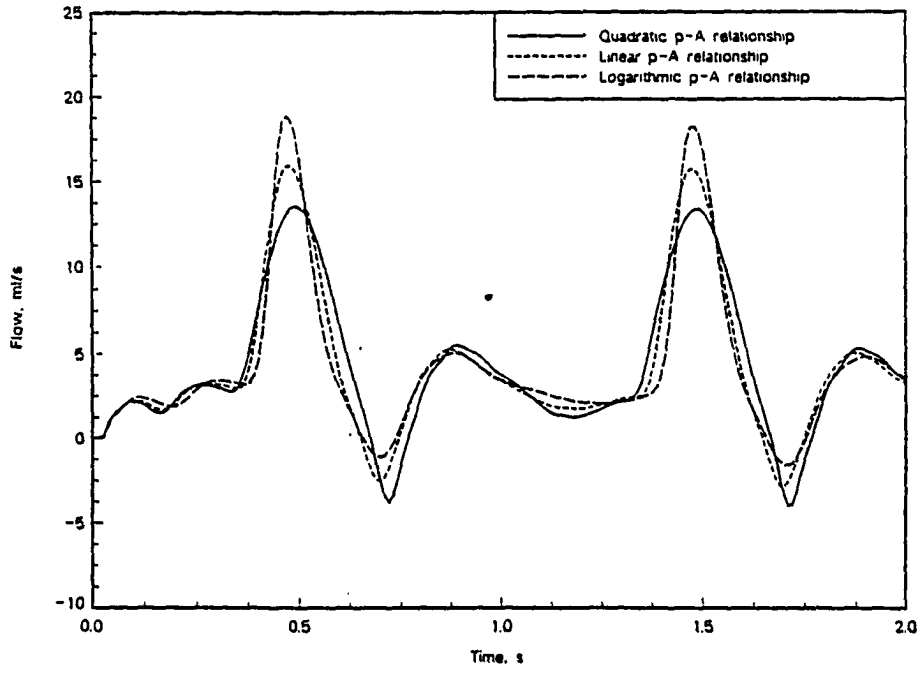

Figure 6.18: Comparison of flow waveforms in the femoral artery for different pressure-area models

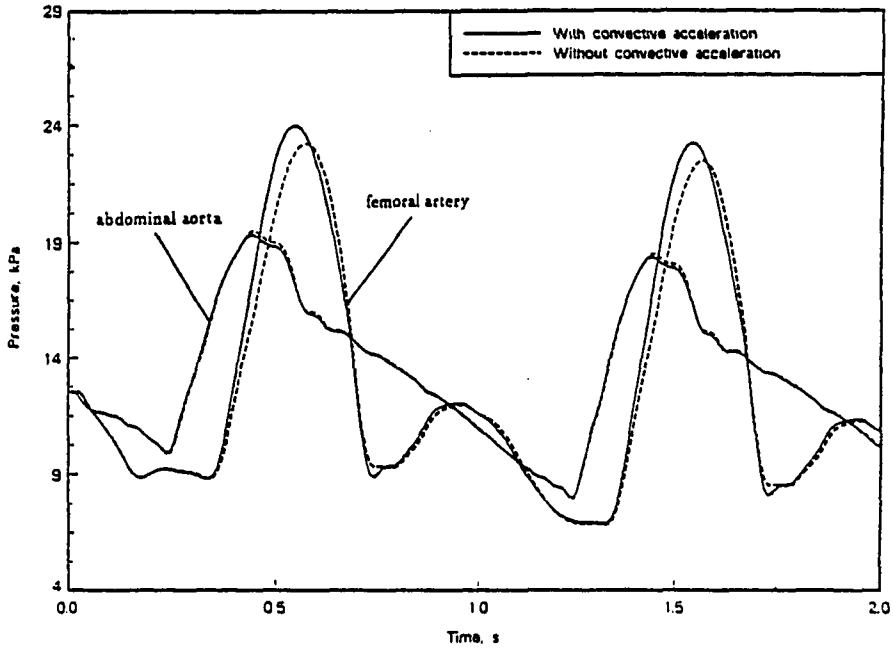

Figure 6.19: Comparison of pressure waveforms in the abdominal aorta and the femoral artery for the normal case and for the case where convective acceleration was omitted

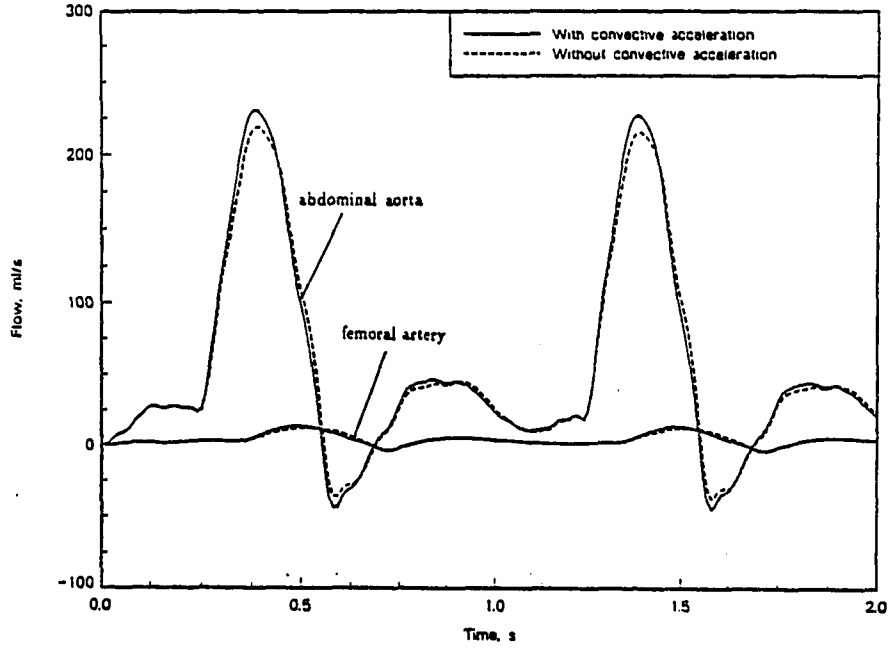

Figure 6.20: Comparison of flow waveforms in the abdominal aorta and the femoral artery for the normal case and for the case where convective acceleration was omitted

5 mm Hg. Raines et al. (1974) also reported a drop of approximately 3 mm Hg for the femoral artery of their leg model, concluding that convective acceleration effects are of minor importance.

Finite Element Versus Finite Difference Model

All the results presented so far were obtained with the finite difference method. The finite element method developed in Chapter 4 provides an equally powerful approach for the development of an arterial flow model. To compare the finite element and the finite difference schemes, the solution to a model of the human arm was considered. The human arm model was adopted from Balar et al. (1989). The model includes the brachial artery and its two major branches, the radial and ulnar artery. Details of the construction of the arm model can be found in Balar et al. (1989). Pressure and flow waveforms were computed using the finite element and the finite difference scheme at two locations: at the proximal end (beginning of brachial artery) and at the distal end (end of radial artery). The results are compared in Figures 6.21 and 6.22.

Figures 6.21 and 6.22 show that both methods yield essentially the same results. There is a minor phase shift between the pressure waveforms and a relatively small error in the magnitude of the peak pressure and flow. These discrepancies are attributed mainly to the differences in truncation and approximation errors between the two methods. Despite these small errors, the results of this test suggest that both methods yield similar solutions, and therefore both methods are suitable for the modeling of arterial blood flow.

The finite element model includes all the features of the finite difference model,

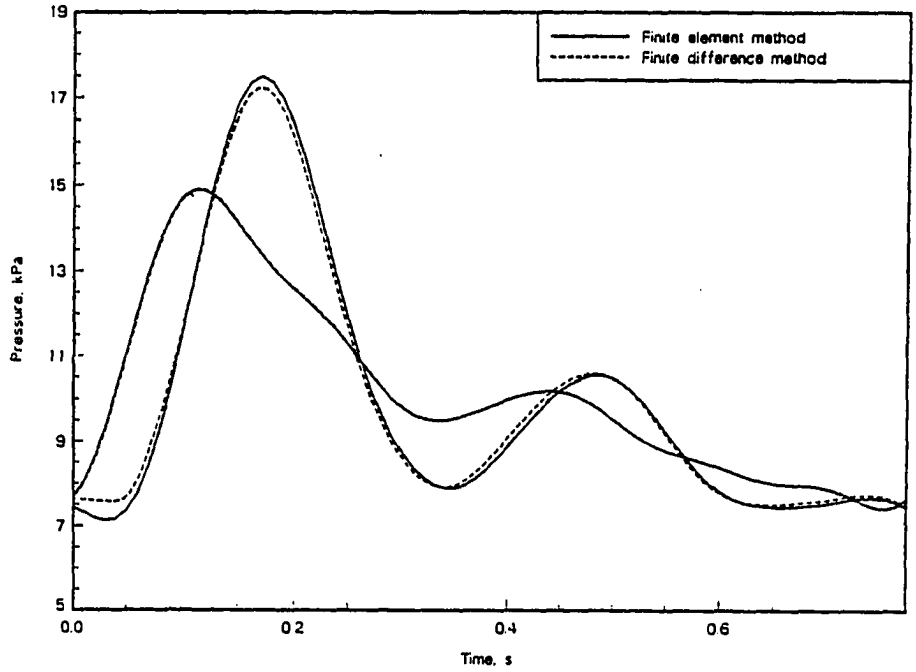

Figure 6.21: Computed pressure waveforms using the finite element and the finite difference scheme for the arm model

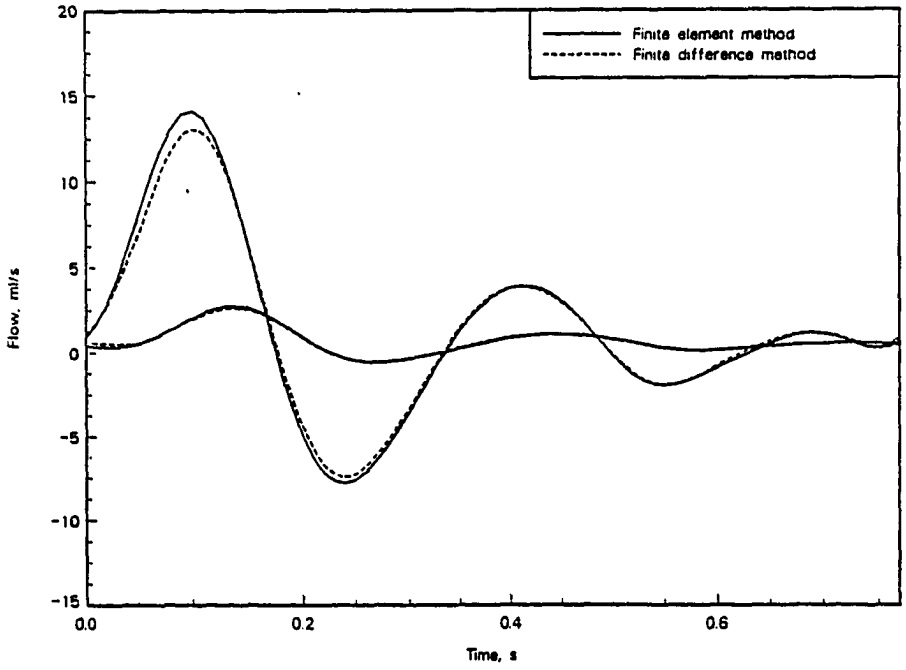

Figure 6.22: Computed flow waveforms using the finite element and the finite difference scheme for the arm model

and, as demonstrated above, provides stable solutions for smaller and less complicated arterial networks as for example models of the human arm and leg. However, the application of the finite element method to the complete circulatory model failed to give converged solutions. The solution started to exhibit oscillations at a certain point during the integration procedure and continued to increase exponentially. The same behavior was noticed by Weerappuli (1987), who used the same technique to model flow in the human arm, leg, canine leg, and the utirine artery of the cow. Weerappuli applied a moving average smoothing techique to eliminate the "numerical noise". Since the solution to the final set of ordinary differential equations was carried by an external equation solver (LSODES subroutine of the ODE package), it was hard to locate the source of the numerical instabilities. The development of a stable finite element model of the arterial circulation is of course of particular interest, and it is recommended as a future project.

CHAPTER 7. CASES OF CLINICAL SIGNIFICANCE

An important reason for the development of a computer model of the circulation is to use the model to study cardiovascular diseases and other circulatory phenomena of medical interest. A reliable computer model can provide valuable information about different aspects of certain circulatory diseases or disorders, without resorting to expensive, impractical, or sometimes impossible in vivo experimental procedures. Some potential applications of the circulatory system models include:

- Study of the effect of rigid or compliant stenoses on regional blood flow. The study can include the effect of stenoses on the pulsatility of flow as well as the potential diagnostic value of the pressure and flow waveforms.
- Study of the effect of cardiac valve disease on cardiac output and peripheral pulse formation. As in the case of stenoses the diagnostic value of the affected pressure and flow waveforms can be explored.
- Study of the effect of corrective procedures, such as arterial bypass grafts on blood flow.
- Study the effect of shunts, anastomoses, and collateral vessels on blood flow.
- Study of the effect of arteriosclerosis on the peripheral pulse formation. Evaluation of the role of the various systemic parameters that contribute to the

development of arteriosclerosis.

- Study of the coronary and cerebral circulation. The arterial networks that carry blood to these vital organs have specialized features (e.g., cardiac-phase dependent peripheral resistance for the coronary circulation), and their mechanisms can be explored through computer simulation.

- Study of the effect of gravitational or acceleration forces on blood flow.

Some of the above cases of potential clinical significance are examined in this section. In particular, the computer model is used to simulate: a) the effect of arterial stenoses, b) the effect of aortic stenosis c) the effect of arterial compliance and peripheral resistance on arteriosclerosis and hypertension, and d) the effect of gravitational forces on blood flow.

Effect of Arterial Stenoses

Two cases of arterial stenoses are studied: 1) a stenosis is placed in the abdominal aorta (segment # 39), which is representative of a large size artery of the main arterial trunk, and 2) a stenosis is placed in the right femoral artery (segment # 50), which is representative of a medium size peripheral artery. The length of the abdominal stenosis was chosen to be 1.5 cm, giving a length to diameter ratio of 1.6, and the length of the femoral stenosis was chosen to be 2 cm giving a length to diameter ratio of 4.8. The approximate location of the stenoses is shown in Figure 7.1.

The mathematical model that relates the net pressure drop across the stenosis to flow is given by Equation 3.12. This relationship was developed for blunt, rigid stenoses, although, the results are expected to be approximately the same for rigid

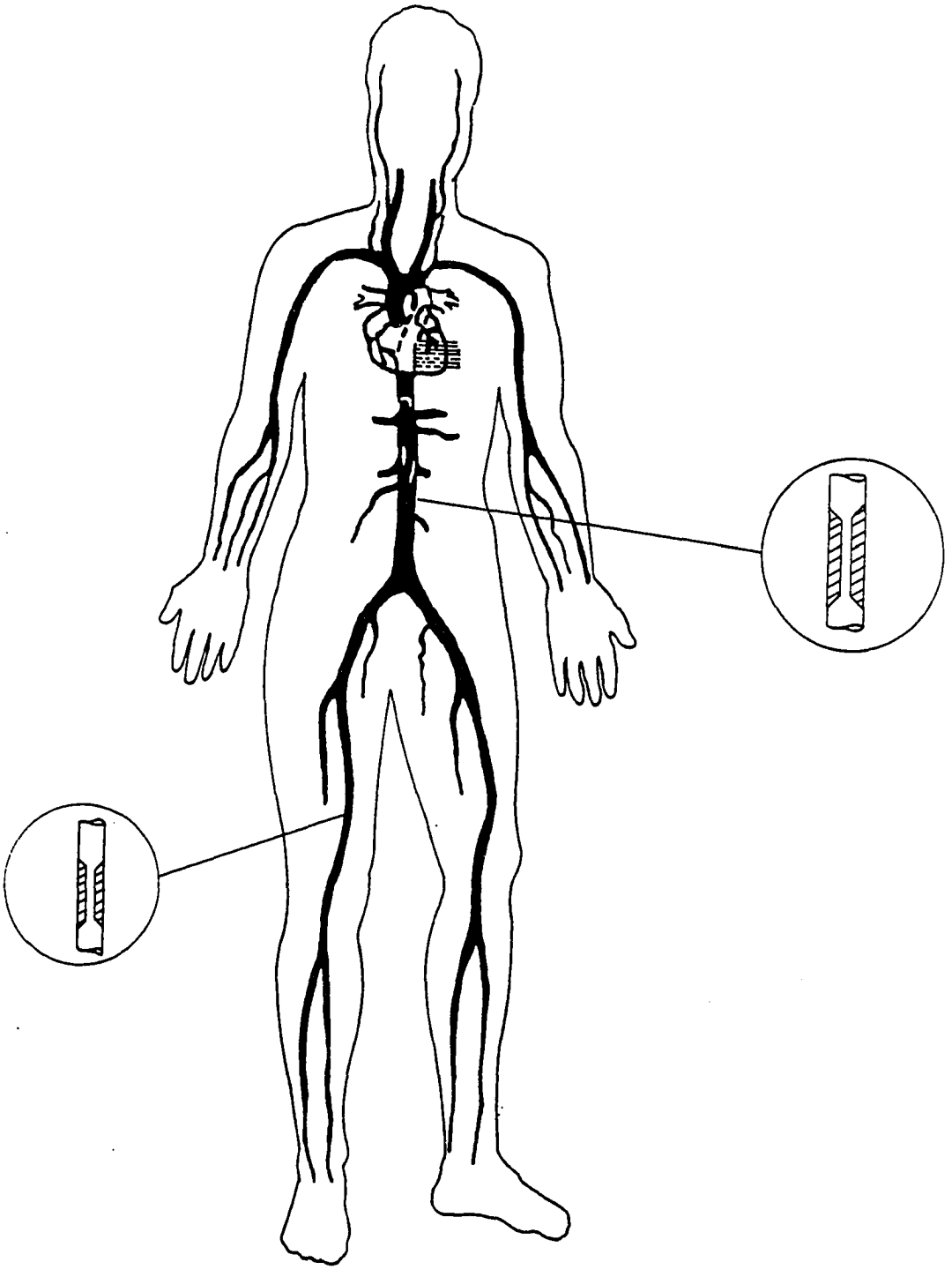

Figure 7.1: Location of arterial stenoses

stenoses of different shapes (Young et al., 1975; Seeley and Young, 1976). Dynamic or compliant stenoses which can provide mechanisms of arterial collapse are not modeled in this study.

The effect of stenoses on circulatory flow is viewed from two different perspectives: 1) the effect on regional blood flow (mean flow through the stenosed segment), and 2) the effect on the pulsatility of the flow (influence on the shape of pressure and flow waveforms upstream and downstream of the stenosis). The effect of stenosis on regional blood flow relates to the medical concern for the adequate blood supply of the distal peripheral beds, whereas, the effect of stenosis on the pulsatility of the flow relates to the potential diagnostic value of the stenosis-induced changes in pressure and flow waveforms. The results are described below.

Effect of stenosis on regional blood flow

The effect of the stenosis severity on the mean flow through the stenosis was checked for two cases: one, in which no compensation for the increased resistance occurs (all distal resistances remain unchanged), and one, in which all distal resistances are reduced to model the effect of compensatory mechanisms (vasodilation). For the case with vasodilation the reduction in the total resistance, R_T, was assumed uniform at all the distal peripheral beds supplied by the stenosed artery, at 20% of the original value. The results for the case of the abdominal and the femoral artery stenosis are shown in Figures 7.2 and 7.3, respectively.

The results show that for the case of normal peripheral resistance the effect of the stenosis on mean flow becomes important only after about an 80% reduction in cross sectional area for the abdominal aorta and 75% area reduction in the femoral

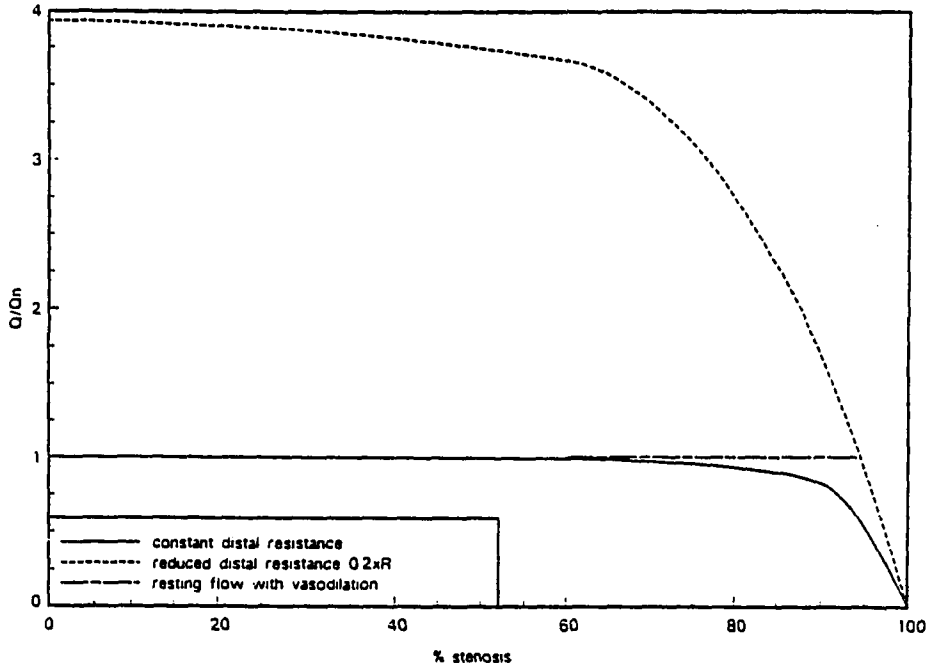

Figure 7.2: Effect of abdominal stenosis on regional mean blood flow

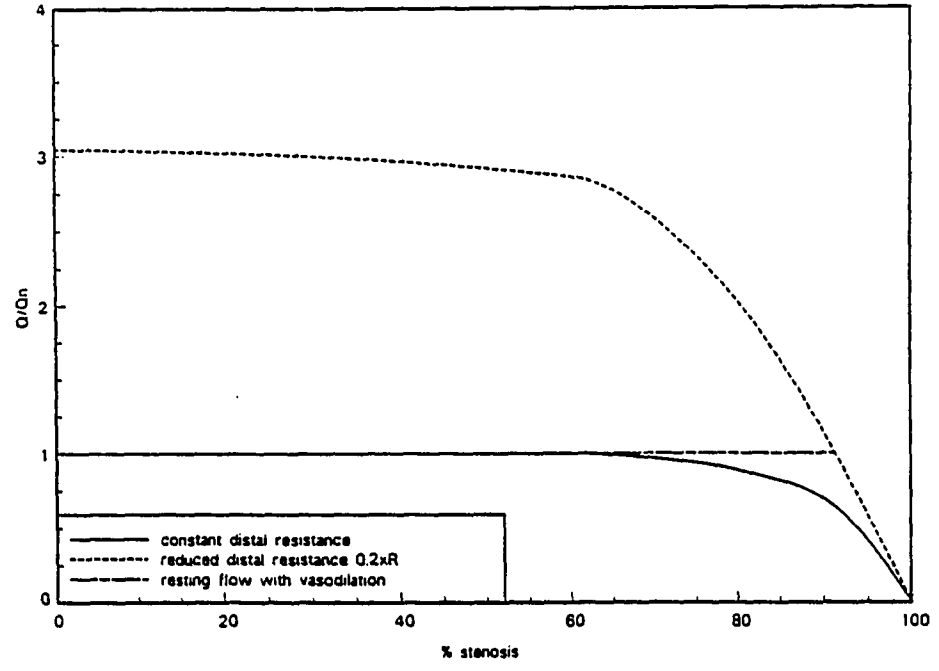

Figure 7.3: Effect of femoral stenosis on regional mean blood flow

artery. Beyond the critical stenosis areas noted, the effect of the stenosis increases dramatically with the percent area reduction, and eventually leads to total occlusion (no flow) at 100% area reduction. When distal vasodilation takes place, the effects of stenosis on flow become noticeable at lower percent area reductions. However, the effect of stenosis still remains small until it reaches a severity of approximately 60%. The increased hemodynamic severity of the stenosis at higher flow rates is a well established clinical phenomenon(Young et al., 1977). From a physical standpoint, the dependence of stenotic severity on flow rate is attributed to the second, non-linear term of Equation 3.12. The Q^2 term suggests that the resistance due to stenosis (pressure drop across the stenosis over flow) depends linearly on flow, and therefore the stenosis severity increases at elevated flows.

In reality the resting flow through a stenosed artery is not likely to follow the solid line shown on the graph. The body can sense the reduction in perfusion and respond with distal vasodilation to maintain normal flow (dotted line). The degree of vasodilation (reduction in peripheral resistance) needed for a particular artery is of course a function of the stenosis severity. As an example of that, Figure 7.2 suggests that for a 94% stenosis in the abdominal aorta, a reduction of approximately 80% in the total terminal resistance of all distal peripheral beds would be required to maintain normal flow. By the same token, 80% reduction in distal terminal resistances would be able to maintain normal flow in a femoral artery, only if the stenosis severity was less than 92%. Further increase in stenosis severity (ie., 95% stenosis) with the same degree of vasodilation would result in a reduction on mean flow, as indicated on the corresponding point on the dashed-line. In any event, the point made by the above graphs is that once the maximum vasodilation has been reached, there is

a critical severity of stenoses beyond which any increase in stenosis severity would result in reduction of mean flow. The particular value of the critical stenosis appears to be a function of the stenosis location as well as the degree of maximum distal vasodilation.

Effect of stenosis on the pulsatility of the flow

The presence of stenosis affects not only the mean pressure and flow values, but also the shape of pressure and flow waveforms. As a typical example, the pressure and flow waveforms at the distal right posterior tibial (ankle) are plotted for different degrees of stenoses placed in the abdominal aorta (Figures 7.4 and 7.5) and in the femoral artery (Figures 7.6 and 7.7).

The results show that for resting flow the effect of a mild stenosis (60% area reduction) on pressure and flow waveforms is negligible. As the severity of the stenosis increases significant changes in both pressure and flow waveforms take place. In particular, the peak values of pressure and flows are dampened by the presence of stenosis. This effect is most noticeable for the 90% stenosis for which the two distinct pressure peaks (systolic pressure and reflection wave) have been dampened to a large plateau of slightly decreasing pressure (Figures 7.4 and 7.6). During diastole, however, when the flow drops to low levels, the effect of a stenosis on pressure is expected to be small, and that is consistent with the results shown in Figures 7.4 and 7.6. For the flow waveforms, the presence of stenoses affects not only the maximum but also the minimum flow values. Again, this effect is more pronounced for the 90% stenosis where the region of maximum (systolic) flow and the region of minimum (negative) backflow have been dampened to approximately the mean flow value (Figures 7.5

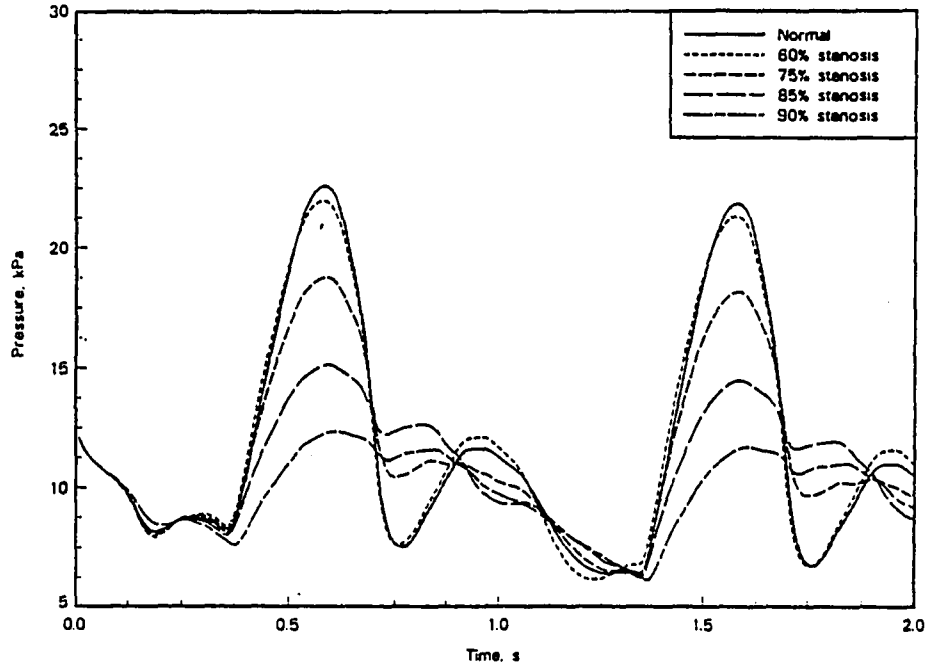

Figure 7.4: Effect of severity of abdominal stenosis on R. posterior tibial pressure waveforms

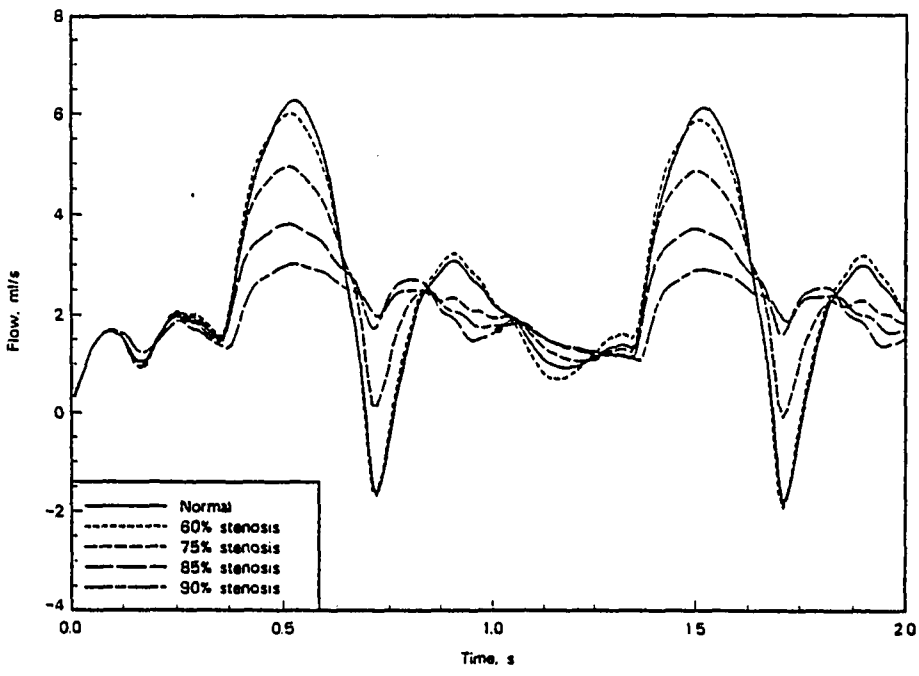

Figure 7.5: Effect of severity of abdominal stenosis on R. posterior tibial flow waveforms

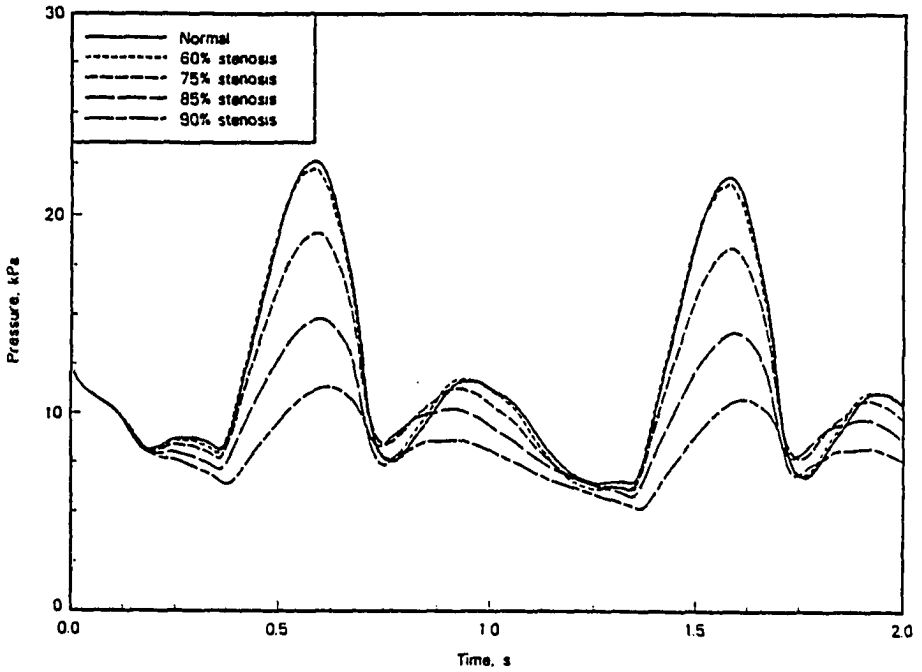

Figure 7.6: Effect of severity of femoral stenosis on R. posterior tibial pressure waveforms

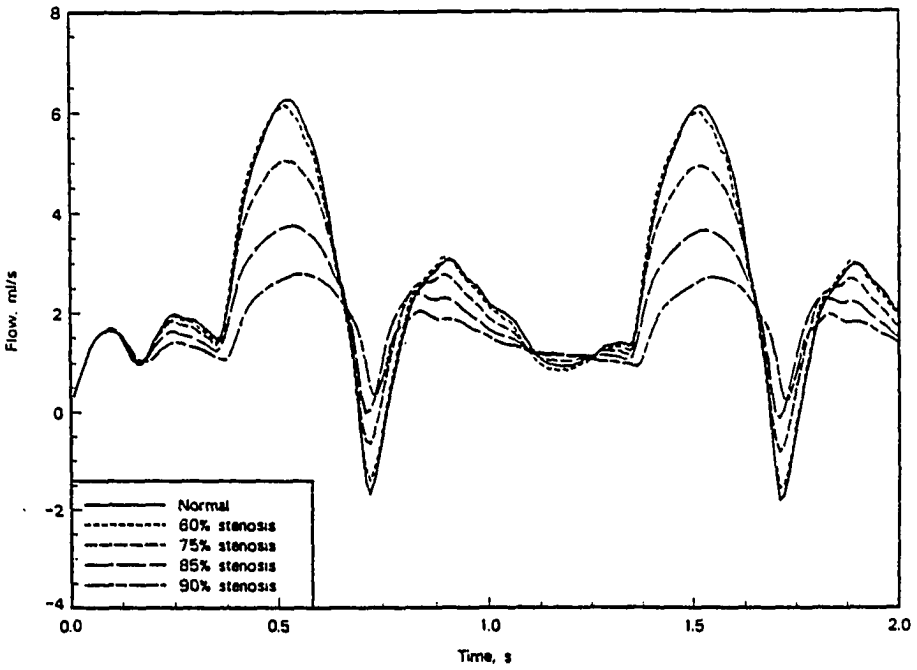

Figure 7.7: Effect of severity of femoral stenosis on R. posterior tibial flow waveforms

and 7.7). These findings are consistent with the results of other computer simulations (Porenta et al., 1986; Avolio, 1980; Balar, 1989) as well as in vivo experimental measurements reported in the literature (Giddens et al., 1977; Young et al., 1977).

The effect of stenoses on the detailed shape of the waveforms is not widely used as a diagnostic tool because of the large variation in the pulse shapes and the difficulty associated with the measurements. Instead, other, easier to obtain and interpret non-dimensional indices, that relate to pressure and flow waveforms are often used clinically to diagnose the presence of stenoses. A commonly used diagnostic index is the pulsatility index, PI (Gosling et al., 1971; Evans et al. , 1980), which is defined as the ratio of peak to peak flow to the mean flow so that

$$PI = \frac{Q_{max} - Q_{min}}{\bar{Q}} \tag{7.1}$$

The major advantage of the pulsatility index is that it can be measured non-invasively with an ultrasonic flowmeter.

To assess the influence of stenoses on the pulsatility index, two different stenoses, one placed in the abdominal aorta and one placed in the right femoral artery were studied. The pulsatility index was calculated from the computed flow waveforms at two locations: one just distal to the stenosis, and the other at the distal end of the right posterior tibial artery. The variation of PI, (normalized to the value at 0% stenoses, PI_n), with the stenosis severity is plotted in Figures 7.8 and 7.9.

The results show that at resting flow conditions the pulsatility index remains essentially unaffected by the presence of a mild stenosis (up to approximately 60%). Beyond the 60% stenosis, any increase in stenosis severity results in a significant decrease in the value of the pulsatility index. The decrease appears to be more abrupt for the case of the abdominal stenosis. The shape of the curves corresponding

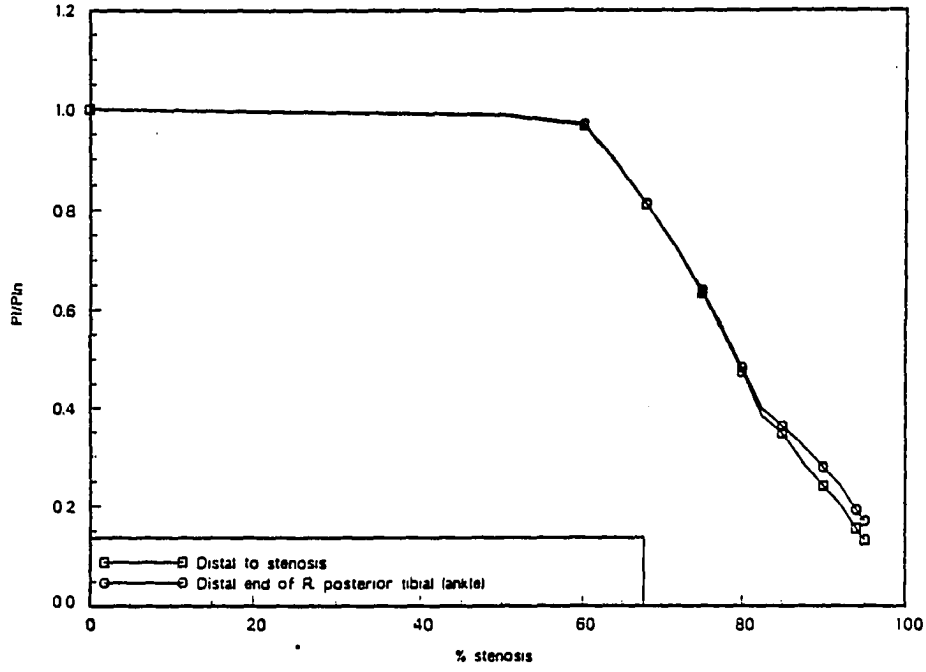

Figure 7.8: Effect of abdominal stenosis severity on pulsatility index

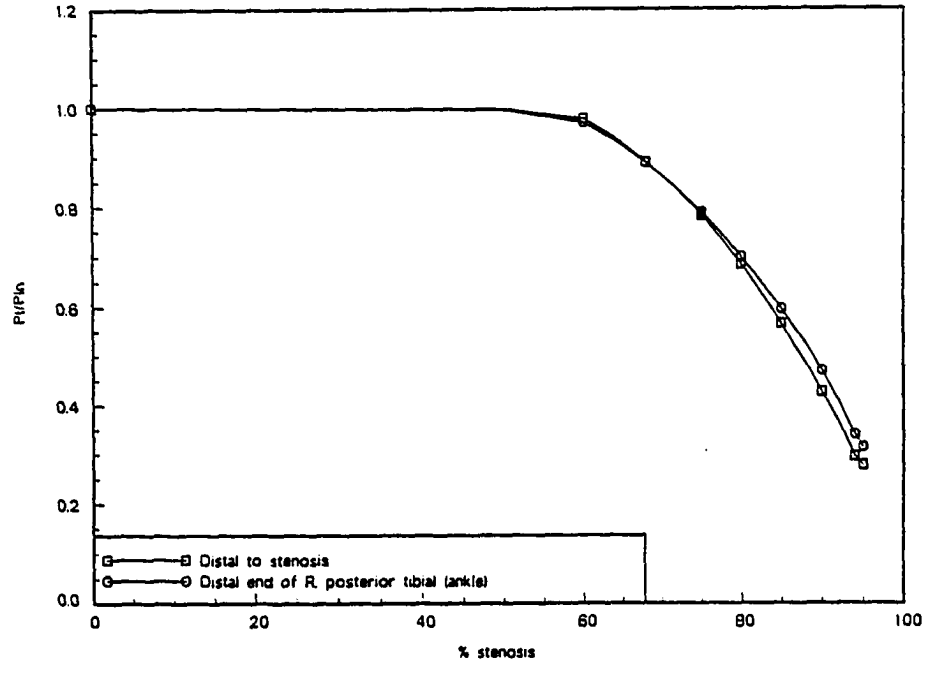

Figure 7.9: Effect of femoral stenosis severity on pulsatility index

to the two distal locations (immediately distal to stenosis and approximately at the ankle) is practically the same, which suggests that the pulsatility index is affected the same at all points distal to the stenosis. The results are presented up to severity of 95%, since beyond that point and especially close to total occlusion (100% stenosis) the PI is ill defined. Clinical observations do show that the PI is strongly affected by the presense of severe stenoses, so that PI index variation is proposed as a useful diagnostic tool.

An example of the clinical use of the PI is shown in Figure 7.10. This figure shows flow pulses at various sites in the legs of a patient with a severe stenosis in the left femoral artery. The flow pulses distal to stenosis are altered significantly, and in a way that is qualitatively the same as predicted by the computer model (i.e., flattening of the pulse - no flow reversal). It is also interesting to note that the two pulsatility indices distal to stenosis are affected at approximately the same scale when normalized to the pulsatility indices of the "normal" right leg (at the knee $\frac{PI}{PI_n} = \frac{1.3}{5.5} = 0.236$ and at the ankle $\frac{PI}{PI_n} = \frac{0.3}{1.5} = 0.200$). Although Gosling et al. did not quantify the severity of the stenosis they did state that it was a rather severe one, close to a complete block. These values are similar to those predicted from the model since a PI ratio of 0.2 requires a stenosis with severity greater than 95%, which indeed is close to complete block.

Another non-dimensional index used in the diagnosis of atherosclerotic disease, is the ratio of systolic pressure to a reference systolic pressure. The reference systolic pressure is assumed not to be affected by the stenosis (not distal to it), and usually, for convenience, is taken as the brachial systolic pressure. The cases of abdominal and femoral stenoses are considered again. The results are presented in terms of

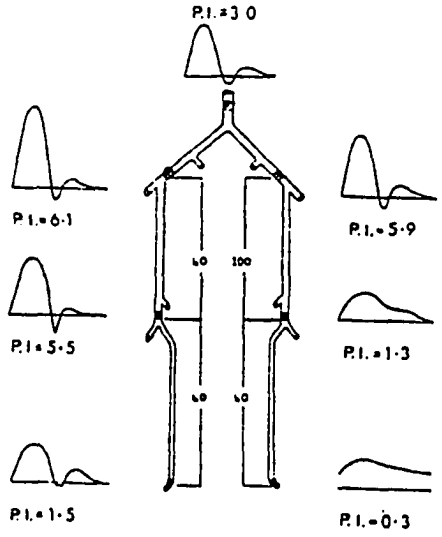

Figure 7.10: Effect of stenoses on PI. From Gosling et al., 1971

the variation of the normalized systolic pressure with the degree of stenosis severity. For purposes of comparison with published data, the results are reported at three locations: upper thigh, knee, and ankle. The corresponding graphs are shown on Figures 7.11 and 7.12. For the case of a stenosis in the abdominal aorta, the effect of the stenosis on the systolic pressure in the three leg locations (thigh, knee, and ankle) is uniform. The normal systolic pressure (at 0% stenosis) ranges between 1.1 to 1.2 times the systolic brachial pressure, and remains approximately at the same level until a stenosis severity of about 60%. After that point, the systolic pressure decreases rapidly to the limiting value of zero at total occlusion (100%).

The same behavior is observed for the case of a stenosis in the femoral artery. The interesting deviation is the curve that represents the systolic pressure variation in the upper thigh. As opposed to the knee and ankle, the upper thigh is located proximal to stenosis, and hence, the systolic pressure is little affected by the stenosis.

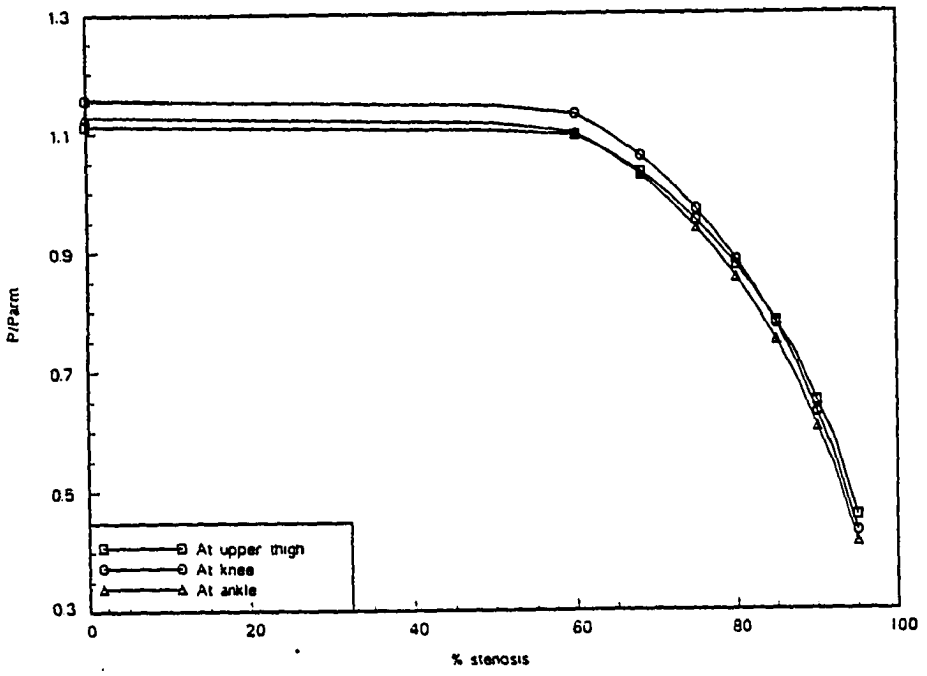

Figure 7.11: Effect of abdominal stenosis severity on systolic pressure

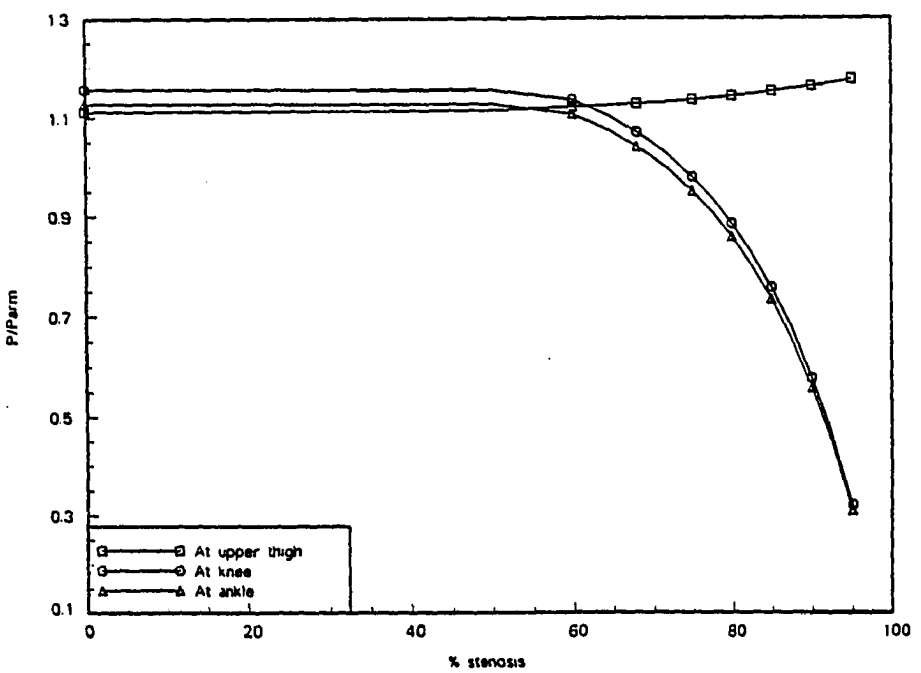

Figure 7.12: Effect of femoral stenosis severity on systolic pressure

As the figure shows, the systolic pressure, rather than dropping, increases slightly with the increase in percent stenosis. Although it is to a degree speculative, the increase in systolic pressure is mainly attributed to reflections caused by the stenotic impedance (Farrar et al., 1979).

The results related to the systolic pressure ratio are in qualitative agreement with the results of Fronek et al. (1973) who used the segmental systolic pressure index to study and compare groups of normal subjects with groups of patients with aortoiliac and femoropopliteal vascular occlusive disease. Fronek et al. did not provide estimates of the stenotic severities, rather they gave their results in terms of group average values. The normalized systolic pressure values for the upper thigh, knee, and ankle were for the normal subjects 1.34, 1.26, and 1.08, respectively, and for the patients with aortoiliac disease 0.720, 0.698, and 0.571, respectively. The experimental data show more variation than the computer model predictions, although the results are similar to the predicted values. Also, for the case of femoropopliteal obstruction, the experimental values for the thigh, knee, and ankle were 1.265, 0.728, and 0.513, respectively. Overall, the results of the model are in good agreement with the experimental values, and show that the systolic pressure is altered significantly by the presense of severe stenosis, and that it can be a convenient indicator for both the presense and the location of the stenosis.

Effect of Aortic Stenosis

Aortic stenosis is one of the common heart valve diseases, and refers to a pathologic condition in which the aortic valve does not open fully during the systolic ejection of blood from the left ventricle into the aorta. A diseased aortic valve with

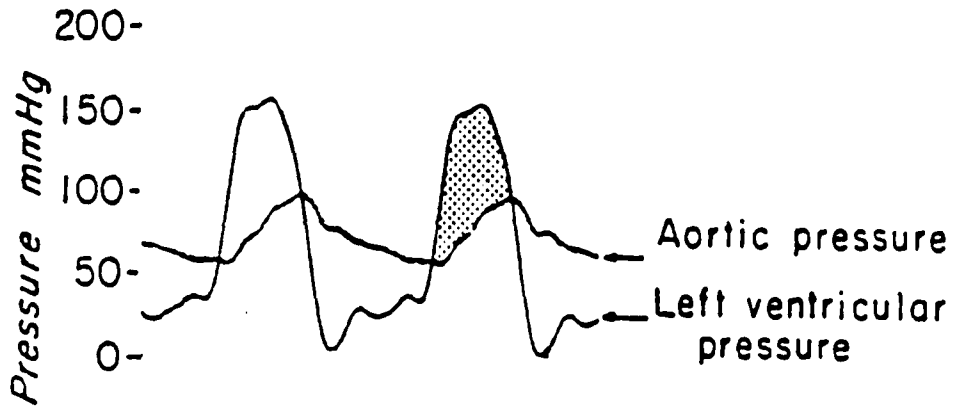

Figure 7.13: Left ventricular and aortic pressure pulses for the case of severe aortic stenoses. From Blackmon and Murray, 1970

reduced orifice size creates an increased resistance to flow. The situation becomes critical, and clinical signs start to develop, when the aortic valve orifice area is reduced from a normal range of 2.5 to 3.5 cm^2 to a range of 0.5 to 1.0 cm^2 (Blackmon and Murray, 1970). In such cases of severe aortic stenoses the resistance to flow is large, and significant pressure gradients develop across the valve. The peak pressure differences between the left ventricle and the aorta may reach or sometimes exceed 100 mm Hg. A typical left ventricular and aortic pressure pulse showing the large pressure gradient across the stenosed aortic valve is shown in Figure 7.13.

The increased work load on the left ventricle due to aortic stenosis leads to myocardial hypertrophy. For most cases, cardiac output remains normal at rest, but in exercise the output can be restricted, especially if the aortic stenosis is severe. Clinical symptoms of severe aortic stenoses include: fatigue and dyspnea for younger

individuals, and syncope, angina pectoris, and heart failure for older individuals. Aortic stenosis is a major life-threatening disease and naturally there is great medical interest in the diagnosis and evaluation of this disease.

Before the catheterization of the left heart became a routine procedure, one of the methods for diagnosis was based on the induced abnormalities of the arterial pulse contour (Wright et al., 1956). The aortic stenosis creates an aortic pressure pulse which is characterized by a reduced amplitude and a slower systolic pressure rise (reduced dp/dt), as seen in Figure 7.13. Peripheral pressure pulses are also changed from the normal case. In an attempt to assess the diagnostic value of the pressure pulse contour, Wright et al. (1956) studied central and peripheral pressure pulses in normal individuals and individuals with aortic stenosis. Typical pressure pulses from each group are shown in Figures 7.14 and 7.15.

From the analysis of their experimental measurements, Wright et al. concluded that in the case of severe aortic stenosis the following characteristic changes are observed: (1) the usual striking differences between the central and peripheral pressure pulse contours (due to pressure amplification) are diminished; (2) the buildup time is prolonged in all pulses; (3) unusual anacrotic pauses are often seen on the radial and on the central pulse, and, (4) the radial systolic pressure, unlike the normal, is commonly a few millimeters of mercury less than the simultaneously recorded central systolic pressure. These changes can be seen in Figure 7.15.

To examine the effectiveness of the model in simulating the effects of aortic stenosis, the model was run using as proximal condition two different aortic pressure waveforms: a normal pressure waveform and one typical of aortic stenosis (taken from Figure 7.13). Figure 7.16 shows the two input pressure waveforms as well

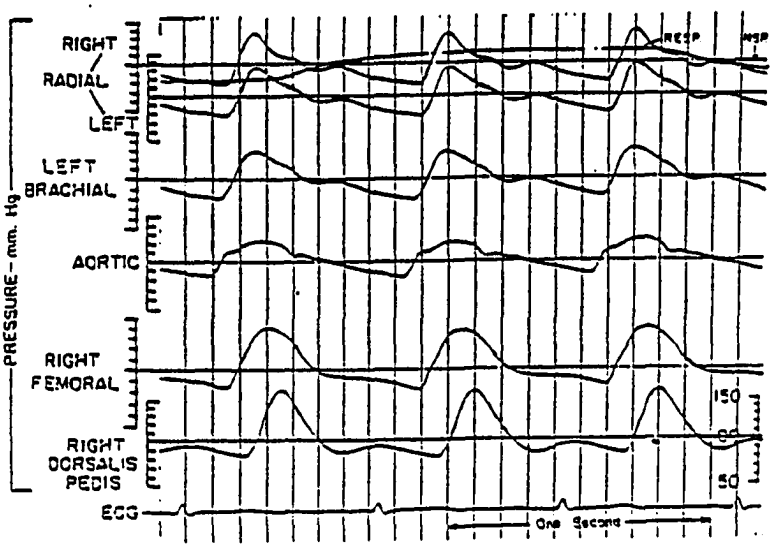

Figure 7.14: Normal central and peripheral pressure pulses. From Wright et al. (1956)

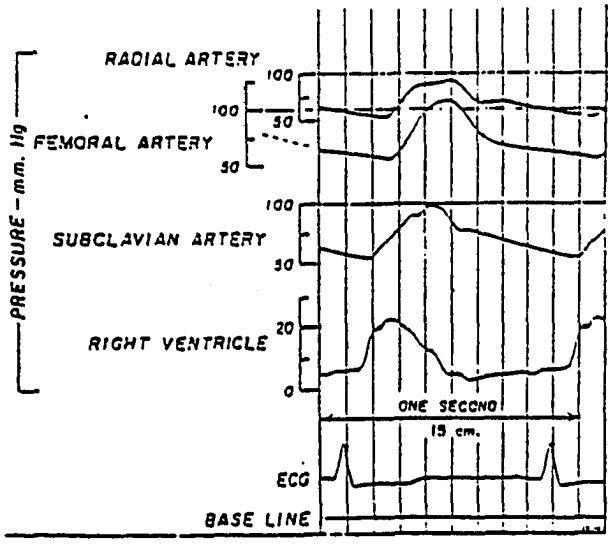

Figure 7.15: Central and peripheral pressure pulses for severe aortic stenosis. From Wright et al. (1956)

as the corresponding predicted femoral artery pressure waveforms. The comparison clearly supports the experimental observations: the systolic pressure of the peripheral pulse in the normal case is much greater than the systolic pressure in the aorta, whereas in presence of aortic stenosis the systolic pressure in the femoral artery is only slightly higher than the aortic one. The time for systolic rise in pressure is prolonged (approximately 32% longer) when compared to the normal case. The same prolongation in the buildup time is evident for the radial pressure pulses which are compared in Figure 7.17. Surprisingly enough, the model also predicts that, in the case of aortic stenosis, the systolic pressure in the radial artery is slightly less than the systolic pressure in the aorta. In further support of the experimental findings, the diseased radial pressure waveform exhibits a small anacrotic pause as well as a flat region around the peak value (see Figure 7.15 for comparison).

The above results suggest that severe stenoses alter the characteristics of central and peripheral pressure pulses. These changes may possess enough information to be used for the diagnosis of aortic stenosis. The computational findings also suggest that the computer model can capture aortic stenosis effects on the pressure waveforms in a satisfactory manner.

Effect of Arterial Compliance and Peripheral Resistance on Arteriosclerosis and Hypertension

Arteriosclerosis, as the name implies, is a pathologic condition which relates to the hardening (sclerosis) of the arterial wall. As a person gets older, the arterial walls change their composition, losing elastic and muscular tissues to more fibrous tissue. Often, calcified plaques also develop, resulting in a greatly reduced arterial

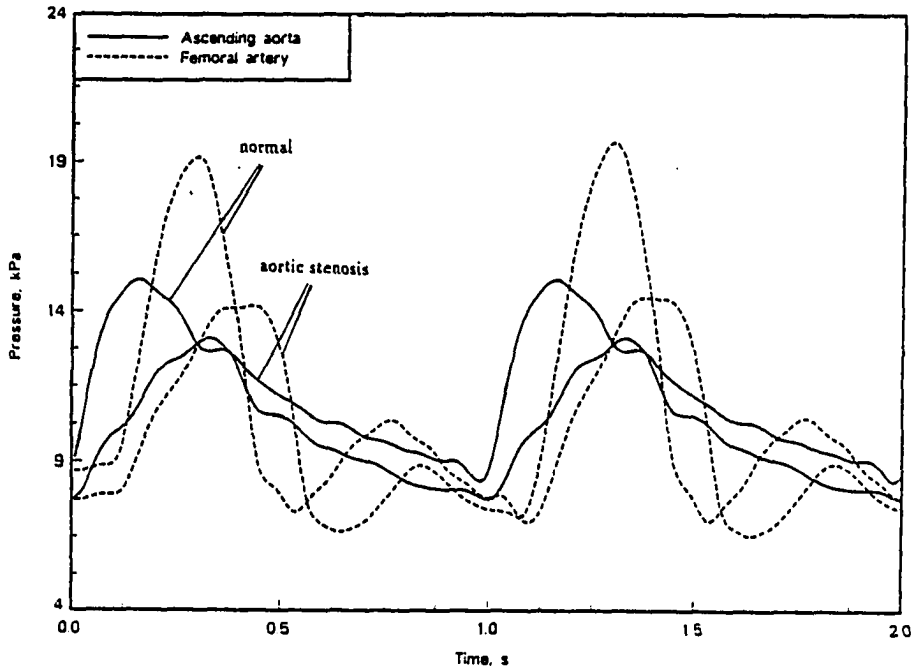

Figure 7.16: Computed aortic and femoral pressure waveforms for normal flow and flow in the presence of severe aortic stenosis

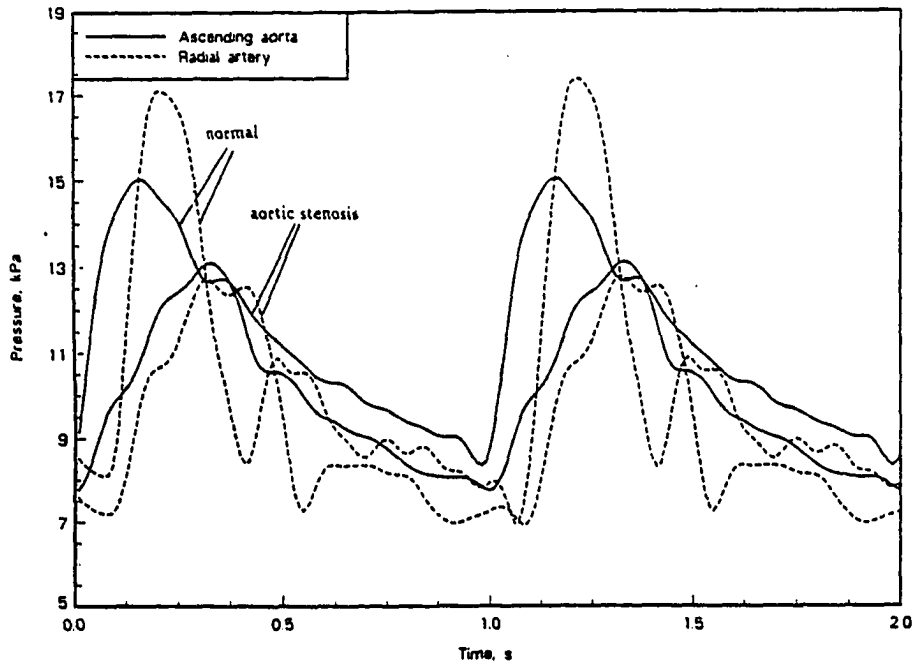

Figure 7.17: Computed aortic and radial pressure waveforms for normal flow and flow in the presence of severe aortic stenosis

compliance (Guyton, 1976). With the loss of elasticity the vessels cannot expand and recoil as freely to the pressure changes produced by the pumping action of the heart. Consequently, the pressure pulse is not buffered, rising high during the systole and falling at lower levels during the diastole. This rise in systolic pressure due to loss of elasticity (and indirectly due to aging) is sometimes termed old age hypertension (Westerhof et al., 1968). To simulate the effects of arteriosclerosis, the arterial compliance is reduced by 33% and 50%, while at the same time peripheral resistances were kept unchanged. The comparison between the normal and the arteriosclerotic pressure pulses in the femoral artery is shown in Figure 7.18. The results show that as the arterial distensibility decreases, the systolic pressure increases and the diastolic decreases. This phenomenon is well established for patients where compliance is reduced due to arterial calcification (Raines et al., 1974). The same observations were made in the aortic pressure pulses of patients with arteriosclerosis (Bard, 1961).

The decrease in arterial compliance has a direct effect on the wave propagation speed. If the arterial compliance were to be reduced by 50%, then according to Moens-Korteweg equation, the pulse wave velocity should be increased by approximately 25%. This is indeed the case here, where the time delay between the normal pulse and the one of 50% reduced compliance is approximately 0.043 seconds. Hence the foot-to-foot time delay between the ascending aorta and the femoral artery has been reduced from 0.155 seconds to $0.155 - 0.043 = 0.112$ seconds, a reduction in time of approximately 28%. This result is close to the linear theory estimate of 25% reduction in time, and the relatively small difference can be attributed to the effect of the non-linear compliance (pressure-area relationship) employed by the model.

Essential hypertension, which translates to high blood pressure of unknown ori-

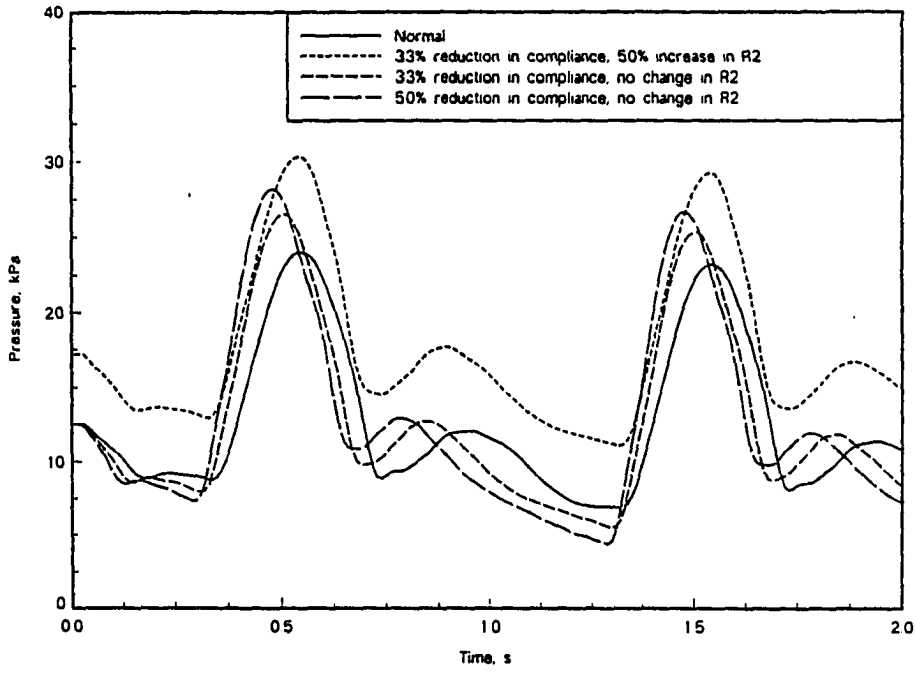

Figure 7.18: Comparison of computed pressure waveforms in the femoral artery for different values of arterial compliance and peripheral resistance

gin (Guyton, 1976), is characterized by generalized vasoconstriction. Essential hypertension is often attributed to renal or neurogenic activity (Bard, 1961). To simulate the effects of essential hypertension, all total peripheral resistances were increased by 40%, through a 50% increase in all the values of R_2, which are conceivably most responsive to neural and humoral control (R_1 values were not increased). This was done for the case of 33% decrease in arterial compliance, and the results are shown in Figure 7.18. As the figure suggests, in essential hypertension the total pressure pulse is shifted upwards, resulting in an increase in systolic, diastolic, and mean pressure. This is in contrast with the old age hypertension where mean pressure was virtually unaffected by the changes in compliance and the diastolic pressure decreased rather than increase. The increase in peripheral resistance seems to increase the effect of distal reflections, as can be judged by the augmentation of the secondary hump (reflection wave) of the pressure pulse. All the above observations are in good agreement with previous similar studies (Raines et al., 1974).

The increase in systemic blood pressure with age often combines the effect of arteriosclerosis (hardening of arteries) along with a mild form of essential hypertension (Guyton, 1976). A graph of the typical variation of the systolic, diastolic, and mean pressure with age is shown in Figure 7.19.

The graph shows that after the body is fully developed (age $\geq$ 20), there is a slight increase in diastolic and mean pressure, as well as a more significant increase in systolic pressure with age. As mentioned earlier, decrease in compliance alone would result in reduced diastolic pressure, whereas increase in peripheral resistance would increase systolic and diastolic pressure in proportion, none of which is the case here. Hence, the variation in pressures shown in Figure 7.19 supports the aforementioned

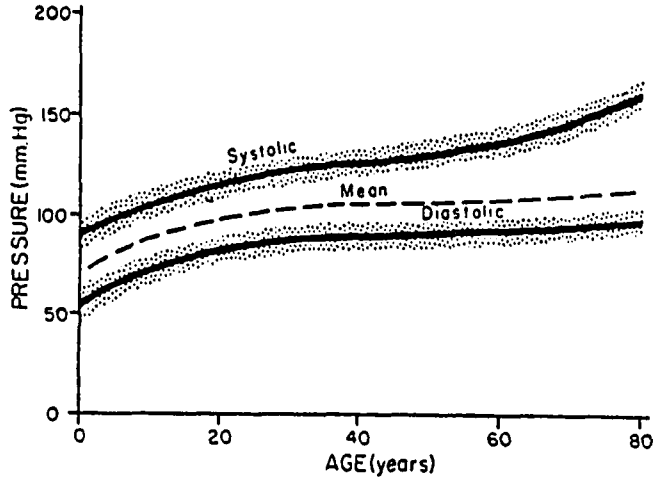

Figure 7.19: Changes in systolic, diastolic, and mean pressure with age. From Guyton, 1976.

hypothesis that arteriosclerosis is accompanied by essential hypertension to form a typical old age pressure pulse.

To get a first estimate of the order of changes in arterial compliance and peripheral resistance necessary to reproduce Figure 7.19. the computer model was utilized in the following manner: first, the relative change of systolic and diastolic pressure as compared to reference age of 20 was recorded off the graph. Then, by means of trial and error, the compliance (C'_0) and peripheral resistance (R_T) of the model were altered until the relative changes in the computed systolic and diastolic pressures in the aorta match the graph value. This procedure was done for ages 40, 60, and 80 (note that for ages less than 20 years the present adult model may not be representative), and the results are shown in Figure 7.20.

The results presented in Figure 7.20 are more of qualitative rather than quantitative value. The results, however, do indicate the importance of the changes in both compliance and peripheral resistance in the formation of the arteriosclerotic pulse.

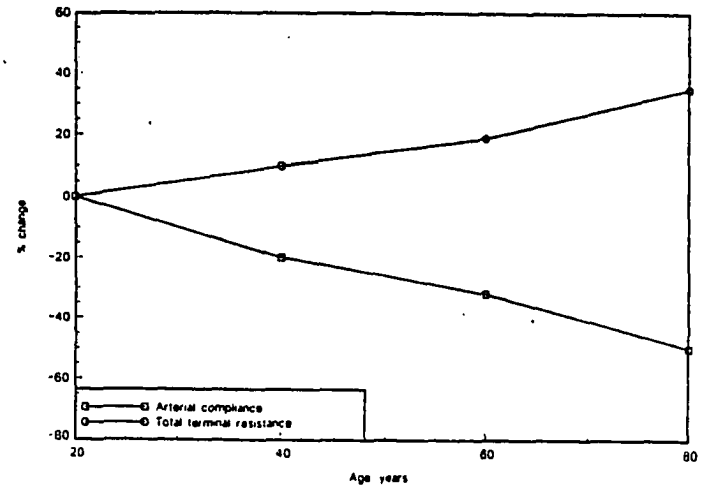

Figure 7.20: Relative change in arterial compliance and peripheral resistance with age

Effect of Gravitational Forces

The cases of arterial flow considered so far assume the human body as being at rest in a prone (horizontal) position, and free of acceleration or gravitational effects. In an upright position, the circulatory system will be affected by the gravitational field and the pressure distribution in the arterial system will be modified accordingly to reflect the effect of the pressure head. Moreover, the body can be subjected to high accelerations (as in the case of high speed aircraft maneuvers) with dramatic effects on the distribution of pressure and flow in arterial system. Perhaps the case that has received the most medical attention is that of high or sustained $+Gz$ loading. The designation "$+Gz$ loading" refers to the case in which, due to body position or motion, the body is subjected to a gravitational or inertial force that has a head-to-foot direction. An example of a $+Gz$ load is the force that a person standing in an elevator feels when the elevator starts accelerating upward. It is common practice

to characterize the intensity of +Gz forces in multiples of the earths gravitational force. For example, a person standing upright is said to be subject to 1 +Gz force. Important consequences of high +Gz loading include: low pressure and reduction in perfusion in the head vessels, blood pooling and increase in pressure toward the lower extremities, or even cardiac arrythmias or ischemias (Burton et al., 1974).

Although the majority of the research related to the effect of acceleration forces is experimental (usually performed on a centrifuge), computer models have also been used to study the effects of acceleration on arterial blood flow (Jaron et al., 1984; Sud and Sekhon, 1986). Jaron et al. developed a multi-element arterial model using equations similar to those presented by Snyder et al. (1968). The Jaron et al. cardiovascular system model included a model of the left heart, a lumped pulmonary model, a lumped systemic venous bed model, as well as control mechanisms for the heart rate, the venous compliance, and the stroke volume. A closed cardiovascular model along with a proper control system is required for the modeling of +Gz loading, where massive autoregulatory responses are expected with the onset of +Gz stress (Erickson et al., 1976; Vettes et al., 1980; Jaron et al., 1984).

In the present study the cardiovascular model is open (i.e., no venous system, pulmonary system, or heart), and lacks control mechanisms that could influence various circulatory parameters such as heart rate, peripheral resistance, etc. Thus, the model in its present form cannot handle cases of high +Gz loading for which the system's responses to the stress load are of major importance. The inclusion of the body force term in the momentum equation of the mathematical model was done merely for showing the capability of the model to handle such terms, and as first step for a future development of a closed, dynamically controlled model of the

cardiovascular system. However, for demonstrational purposes, three different types of acceleration loads are considered: a) 1g at 270 degrees (direction head-to-foot), b) 2g at 270 degrees, and c) 2g at 315 degrees (load vector pointing at 45 degrees down and to the left). The indicated angle is measured between the acceleration vector and a reference axis which is perpendicular to the longitudinal axis of the body and is running from right to left. The results are presented in terms of pressure and flow waveforms in the femoral artery, and are shown in Figures 7.21 and 7.22 respectively.

As expected, the extra pressure head created increases the pressure levels in proportion to the G-load. Specifically, the pressure head is determined by the dot product of the G-load vector and the position vector (defined as the vector from the root of the ascending aorta to the arterial point under consideration). Hence, the angle between the G-load vector and the position vector is of major importance in determining the pressure head. This is shown clearly in Figure 7.21 where the application of a 2g load at 315 degrees (45 degrees off the head-to-foot direction) results in a reduced pressure head as compared to a 2g load at 270 degrees (2 +Gz load).

The increase in pressure in the lower extremities will increase the amount of flow proportionally, since the peripheral resistances are assumed to remain constant. This effect is shown in Figure 7.22. In reality, the peripheral resistances in the legs will respond quickly to the flow increase by means of active vasoconstriction, and therefore shortly after the onset of the application of a G-load the peripheral resistances are expected to be different than those used in obtaining Figures 7.21 and 7.22. At best, the results presented here are indicative of the pressure and flow distribution immediately after the application of the G-load and before any

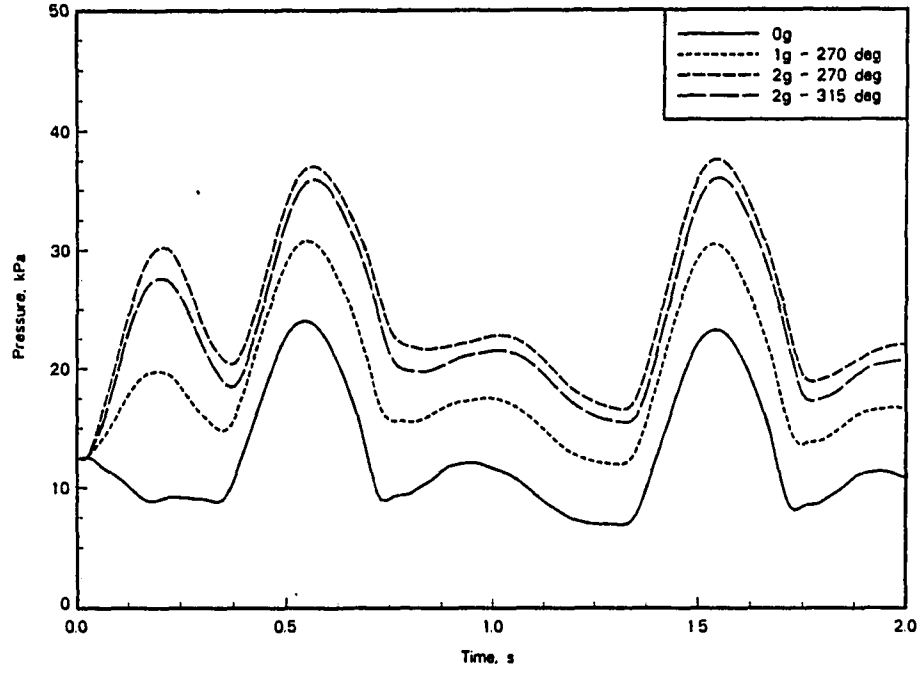

Figure 7.21: Effect of acceleration loads on L. femoral artery pressure waveforms

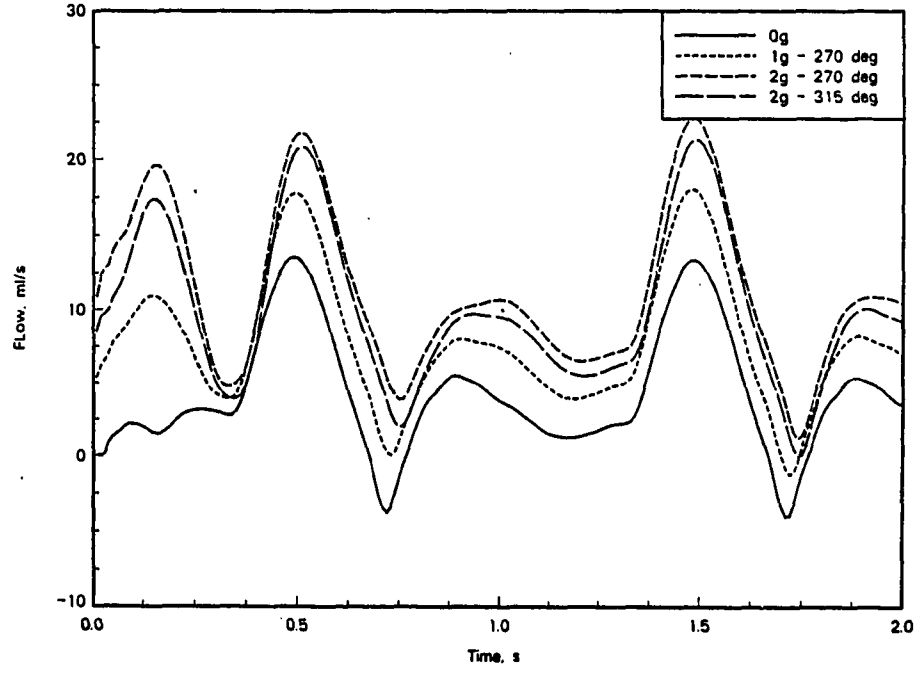

Figure 7.22: Effect of acceleration loads on L. femoral artery flow waveforms

Table 7.1: Systolic pressure, mean pressure, and mean flow at the distal end of the R. external carotid artery for different +Gz loads

+Gz load	Systolic pressure (kPa)	Mean pressure (kPa)	Mean flow (ml/s)
0	17.8	12.3	0.876
1	11.8	6.4	0.446
2	5.8	0.3	0.002

body imposed compensation takes place. Although these results are of some value, the major point made here is to recognize that accurate modeling of cardiovascular responses to acceleration loads requires the development of a circulatory system model which includes appropriate control mechanisms.

The effect of +Gz loading on the main arteries that supply blood to the brain are of special importance since +Gz induced lack of perfusion is associated to loss of peripheral vision, loss of central vision, and loss of conciousness. As a typical example of the effect of gravitational forces on flow to the head, the flow in the right external carotid artery under conditions of 0, 1, and 2 +Gz loads is considered. The pressure and flow waveforms at approximately the eye level (distal end of segment #17) are plotted in Figures 7.23 and 7.24.

As expected the effects of gravitational loads on blood flow to the head are opposite of the effects on flow to the lower extremities. Both pressure and flow are lowered significantly and in proportion to the +Gz loads. The corresponding systolic pressure, mean pressure, and mean flow is given in Table 7.1

As in the case of flow to the leg, the model predictions for the pressure and flow seem to overestimate the effect of gravitational forces. For a 2 +Gz load, the systolic pressure at the distal end of the right external carotid (eye level) drops to 5.8 kPa which is equivalent to 44 mm Hg. Shubrooks et al. (1973) report minimum

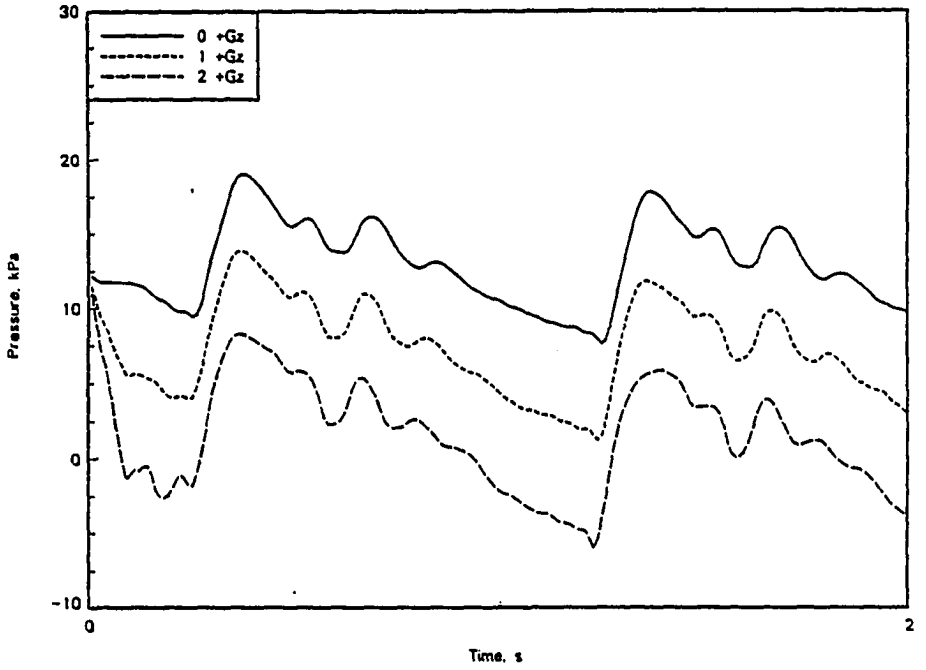

Figure 7.23: Effect of acceleration loads on R. external carotid artery pressure waveforms

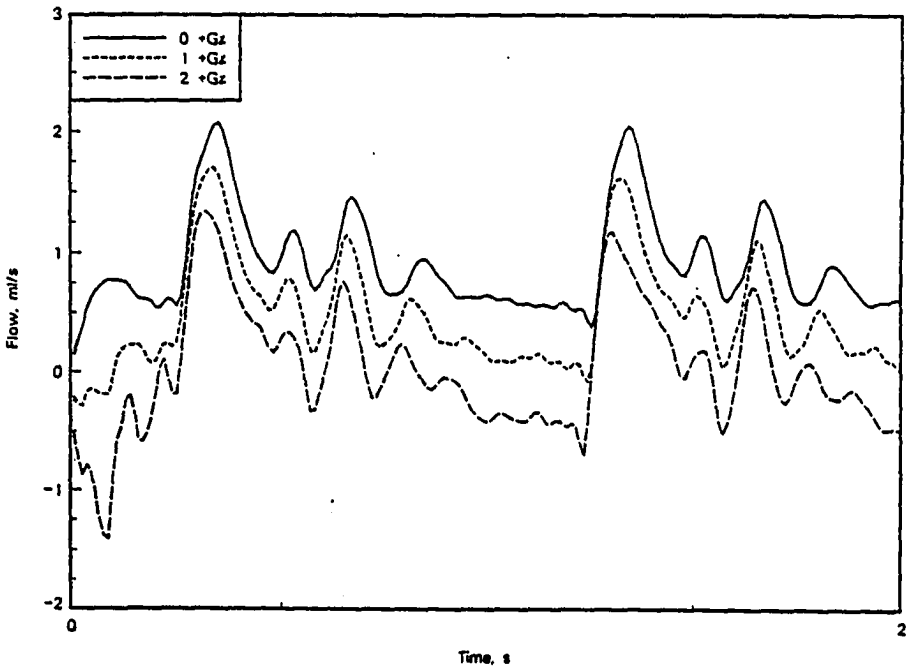

Figure 7.24: Effect of acceleration loads on R. external carotid artery flow waveforms

systolic pressure of 40 mm Hg at eye level but for the much higher load of 3.7 +Gz. This minimum systolic pressure value occurred in the early stage of the acceleration, and eventually, due to compensatory mechanisms, the systolic pressure rose to higher levels. The model also predicts almost zero flow through the external carotid artery for a 2 +Gz load. Experimental findings suggest that flow ceases at higher +Gz loads. It is interesting, however, to note that flow ceases when systolic pressure at eye level is approximately 50 mm Hg, a value which compares well with experimental findings (Sandler et al., 1977).

CHAPTER 8. CONCLUSIONS

The principal objective of this work was the development of a computer model of the human systemic circulation. The model is based on the one-dimensional flow equations. The required physiological data were obtained from the literature, and when not available through indirect estimations. The model was used to simulate several cases of normal and diseased arterial flow, from which the following major conclusions can be drawn:

- It is possible to use the computer model to study the arterial circulation. The model appears to simulate well many of the important characteristics of pressure and flow waveforms throughout the circulatory system.

- The model accommodates special features such as multiple branching, non-linear pressure-area relationships, vessel tapering, different forms of boundary conditions, stenoses, and inertia/gravitational forces, all of which contribute to the improvement and versatility of the model.

- Inclusion of non-linearities due to pressure-area relationship and convective acceleration seem to improve the model performance. The selection of the pressure-area relationship appears to be more influential, while convective acceleration effects are important only at higher flow rates. Frictional effects are

of minor importance.

- The use of a modified windkessel model as lumped parameter impedance at terminal sites is an improvement over the pure resistance model.

- The model can be used to study various types of cardiovascular disease. Simulated conditions of arteriosclerosis and atherosclerotic plaques leading to vascular obstructions demonstrate the capability of the model to simulate the effects of the disease on circulatory dynamics. In arteriosclerosis, the pressure pulse is altered considerably. In atherosclerosis, the presence of a severe obstruction can limit flow to peripheral beds despite the action of compensatory mechanisms. Severe obstructions cause significant alterations in pressure and flow characteristics.

- The model can be also used to study the hemodynamics of heart valve disease. Simulation of aortic stenosis showed that peripheral pulses are markedly different than the normal pulses, so that it may be feasible to use these pulses for diagnostic purposes.

- Although the inclusion of the body force terms presents no special difficulty in the mathematical and numerical formulation of the model, it is believed that the model will not give accurate results for high $+Gz$ flows unless the necessary control mechanisms are included.

- Both finite element and finite different methods can be used to yield valid and comparable solutions to the problem. The finite difference scheme was conditionally stable, and always converged if the stability criterion was met.

The finite element scheme exhibited oscillations and did not converge when it was applied to the complete arterial system.

The present arterial flow model can be improved in several ways. With regard to physiological modeling the model could be modified to include collateral flow and anastomoses, with possible extensions to the study of bypass grafts. Pressure-area relationships could be modified to account for the viscoelasticity of the arterial wall. Distal lumped parameter impedances could be modified to account for inertial effects. For the numerical analysis, a higher order scheme could be developed to improve the accuracy of the solution. Ideally the scheme should be free of numerical oscillations and instabilities. Further investigation of the use of the finite element technique for the complete circulation should be undertaken.

All the above possibilities represent steps towards a better and more accurate model of the arterial circulation, none of which will be of any practical value unless the plethora of parameter data necessary to describe the circulation becomes available. The reliability of such a computer model is, of course, as good as the reliability of the model parameters used. Hence, the importance of complete, consistent, and reliable sets of physiological data cannot be overemphasized. Hopefully, with the continuous improvement of the measuring techniques, these data will be available to the researcher, so that a computer model of the complete circulation will be both a reliable and a useful tool.

BIBLIOGRAPHY

Anderson D. A., J. C. Tannehill, and R. H. Pletcher. 1984. Computational fluid mechanics and heat transfer. Hemisphere Publishing Co., New York.

Anliker, M., R. L. Rockwell, and E. Ogden. 1971. Nonlinear analysis of flow pulses and shock waves in arteries. ZAMP 22:217-246.

Anliker, M., J. C. Stettler, P. Niederer, and R. Holenstein. 1978. Prediction of shape changes of propagation of flow and pressure pulses in human arteries. Pages 15-34 *in* R. D. Bauer and R. Busse, eds. The arterial system: Dynamics, control theory and regulation. Springer Verlag, Berlin.

Aperia, A. 1940. Hemodynamical studies. Skand. Arch. Physiol. Suppl. 83:1-230.

Avolio, A. P. 1980. Multi-branched model of the human arterial system. Med. and Biol. Eng. and Comp. 18:709-718.

Balar, S. D. T. R. Rogge, and D. F. Young. 1989. Computer simulation of blood flow in the human arm. J. Biomechanics 22:691-697.

Bard, P. 1961. Regulation of the systemic circulation. Page 191 *in* P. Bard, ed. Medical physiology. Mosby, St. Louis.

Bergel, D. H. 1961. The static elastic properties of the arterial wall. J. Physiol. 156:445-457.

Blackmon, J. R., and J. A. Murray. 1970. Valvular heart disease. Pages 469-505 *in* R. F. Rushmer ed. Cardiovascular dynamics. W. B. Saunders Co., Philadelphia.

Burton, A. C. 1965. Physiology and biophysics of the circulation. Year book Medical Publishers, Chicago.

Burton, R. R., S. D. Leverett, and E. D. Michaelson. 1974. Man at high sustained +Gz acceleration: A review. Aerospace Med. 45(10):1115-1136.

Erickson H. H., H. Sandler, and H. L. Stone. 1976. Cardiovascular function during sustained +Gz stress. Aviat. Space Environ. Med. 47(7):750-758.

Evans, D. H., W. W. Barrie, M. J. Ascher, S. Bentley, and P. R. F. Bell. 1980. The relationship between ultrasonic pulsatility index and proximal arterial stenosis in a canine model. Circ. Res. 46(4):470-475.

Farrar, D. J., H. D. Green, and D. W. Peterson. 1979. Noninvasively and invasively measured pulsatile haemodynamics with graded arterial stenosis. Cardiovascular Research 13:45-57.

Fox, E. A., and E. Saibel. 1965. A formulation of the problem of flow through tubes. Proceedings 4th International Congress on Rheology, 4:125-133.

Frank, O. 1899. Die grundform des arterielennen pulses. Erste abhandlung. Mathematische analyse. Z. Biol. 37:483-526.

Fronek, A., K. H. Johansen, R. B. Dilley, and E. F. Bernstein. 1973. Noninvasive physiologic tests in the diagnosis and characterization of peripheral arterial occlussive disease. The American Journal of Surgery 126:205-214.

Giddens, D. P., R. F. Mabon, and R. A. Cassanova. 1977. Measurements of distorded flows distal to subtotal vascular stenoses in the thoracic aortas in dogs. Circulation Research 39:112-119.

Gosling, R. G., G. Dunbar, D. H. King, D. L. Newman, C. D. side, J. P. Woodcock, D. E. Fitzgerald, J. S. Keates, and D. MacMillan. 1971. The quantitative analysis of occlussive peripheral arterial disease by a non-intrusive ultrasonic technique. Angiology 22:52-55.

Guyton, A. C. 1976. Textbook of medical physiology. 4th ed. W. B. Saunders Co., Philadelphia.

Hale, j. F., D. A. McDonald, and J. R. Womersley. 1955. Velocity profiles of oscillating arterial flow, with some calculations on the viscous drag and the Reynolds number. J. Physiol. 128:629-640.

Iberall, A. S. 1950. Attenuation of oscillatory pressures in instrument lines. J. Res. Nat. Bur. Standards 45:85-108.

Jaron, D., T. W. Moore, and C. Chu. 1984. A cardiovascular model for studying impairment of celebral function during +Gz stress. Aviat. Space Environ. Med. 55(1):24-31.

Ling, S. C., B. H. Atabek, D. L. Fry, D. J. Patel, and J. S. Janicki. 1968. Application of heated-film velocity and shear probes to hemodynamic studies. Circulat. Res. 23:789-801.

McDonald, D. A. 1974. Blood flow in arteries. 2^{nd} ed. Williams and Wilkins Co., Baltimore.

Milnor, W. R. 1982. Hemodynamics. Williams and Wilkins Co., Baltimore.

Morgan, G. W., and J. P. Kiely. 1954. Wave propagation in a viscous liquid contained in a flexible tube. J. Acoust. Soc. Am., 26:323-328.

Mozersky, D. J., D. S. Sumner, D. E. Hokanson, and D. E. Strandness, Jr. 1972. Transcutaneous measurement of the elastic properties of the human femoral artery. Circulation 46:948-955.

Nichols, W. W., C. R. Conti, W. E. Walker, and W. R. Milnor. 1977. Input impedance of the systemic circulation in man. CIrc. Res. 40:451-458

Noordergraaf, A., P. D. Verdouw, and H. B. C. Boom. 1963. The use of an analog computer in a circulation model. Prog. Card. Diseases 5:419-439.

Olsen, J. H., and A. H. Shapiro. 1967. Large-amplitude unsteady flow in liquid-filled elastic tubes. J. Fluid Mech. 29:513-538.

O'Rourke, M. F., and M. G. Taylor. 1966. Vascular impedance of the femoral bed. Circ. Res. 18:126-133.

Porenta, G. P. 1982. A computer based feasibility analysis of assessing arterial flow using pulsatility indices. M.S. Thesis. Iowa State University, Ames.

Porenta, G. P., D. F. Young, and T. R. Rogge. 1986. A finite-element model of blood flow in arteries including taper, branches, and obstructions. J. Biomechanical Eng. 108:161-167.

Raines, J. K. 1972. Diagnosis and analysis of arteriosclerosis in the lower limbs from the arterial pressure pulse. Ph.D. Thesis. Massachusetts Institute of Technology, Cambridge.

Raines, J. K., M. Y. Jaffrin, and A. H. Shapiro. 1974. A computer simulation of arterial dynamics in the human leg. J. Biomechanics 7:77-91.

Rangarajan, N. 1983. Estimation of cardiovascular system parameters using noninvasive measurements. Ph.D. Thesis. Iowa State University, Ames.

Rockwell, R. L., M. Anliker, and J. Elsner. 1974. Model studies of the pressure and flow pulses in viscoelastic arterial conduit. J. Franklin Inst. 297:405-428.

Rooz, E. 1980. A finite element simulation of pulsatile flow in flexible tubes. Ph.D. Thesis. Iowa State University, Ames.

Rooz, E., D. F. Young, and T. R. Rogge. 1982. A finite- element simulation of pulsatile flow in flexible obstructed tubes. J. Biomechanical Eng. 104:119-124.

Rumberger, J. A., and R. M. Nerem. 1977. Method-of- characteristics calculation of coronary blood flow. J. Fluid Mech. 32:429-448.

Sandler, H., S. A. Rositano, and E. P. McCuntheon. 1977. An objective determination of +Gz acceleration tolerance. Acta Astronautica 4:541-553.

Schaaf, B. W., and P. H. Abbrecht. 1972. Digital computer simulation of human systemic arterial pulse transmission: A non- linear model. J. Biomechanics 5:345-364.

Seeley, B. D., and D. F. Young. 1976. Effect of geometry on pressure losses across models of arterial stenoses.. J. Biomechanics 5:345-364.

Shubrooks, S. J., Jr., and S. D. Leverett, Jr. 1973. Effect of the valsava maneuver on tolerance to +Gz acceleration. J. Appl. Physiol. 34:460-466.

Skalak, R. 1972. Synthesis of a complete circulation. Pages 341-376 *in* D. H. Bergel ed. Cardiovascular fluid mechanics. Academic Press, London.

Snyder, M. F., V. C. Rideout, and R. J. Hillestead. 1968. Computer modeling of the human systemic arterial tree. J. Biomechanics 1:341-353.

Streeter, V. L., W. F. Keitzer, and D. F. Bohr. 1963. Pulsatile pressure and flow through distensible vessels. Circ. Res. 13:3-20.

Sud, V. K., and G. S. Sekhon. 1986. Analysis of blood flow through a model of the human arterial system under periodic body acceleration. J. Biomechanics 19:929-941.

Uchida, S. 1956. The pulsating viscous flow superposed on the steady laminar motion of incompressible fluid in a circular pipe. ZAMP 7:403-421.

Vettes, B, H. Vieillefond, and R. Auffret. 1980. Cardivascular responses of man exposed to +Gz accelerations in a centrifuge. Aviat. Space Environ. Med. 51(4):375-378.

Witzig, K. 1984. Uber erzwungene Wellenbuewegungen zäher, inkompressibler Flussigkeitan in ilastischen Röhren. Inaugural Dissertation: Universität Bern. Wyss Erben, Bern.

Weerappuli D. P. V. 1987. Simulation of pulsatile flow in arteries using the finite-element method. Ph.D. Thesis. Iowa State University, Ames.

Wemple, R. R., and L. F. Mockros. 1972. Pressure and flow in the systemic arterial system. J. Biomechanics 5:629-641.

Westerhof, N., F. Bosman, C. J. De Vries, and A. Noordergraaf. 1969. Analog studies of the human systemic arterial tree. J. Biomechanics 2:121-143.

Womersley, J. R. 1955a. Method for the calculation of velocity, rate of flow and viscous drag in arteries when the pressure gradient is known. J. Physiol. 127:553-563.

Womersley, J. R. 1955b. Oscillatory motion of a viscous liquid in a thin-walled elastic tube. I. The linear approximation for long waves. Phil. Mag. 46:199-221.

Womersley, J. R. 1957. The mathematical analysis of the arterial circulation in a state of oscillatory motion. Wright Air Development Center, WADC Technical Report TR 56-614.

Wright, J. L., E. Toscano-Barboza, and R. O. Brandenburg. 1956. Left ventricular and aortic pressure pulses in aortic valvular disease. Proceedings of the Staff

Meetings of the Mayo Clinic 31(5):120-126.

Young, D. F. 1979. Fluid mechanics of arterial stenosis. J. Biomechanical Eng. 101:157-175.

Young, D. F., and F. Y. Tsai. 1973a. Flow characteristics in models of arterial stenoses. I. Steady Flow. J. Biomechanics 6:395-410.

Young, D. F., and F. Y. Tsai. 1973a. Flow characteristics in models of arterial stenoses. II. Unsteady Flow. J. Biomechanics 6:547-559.

Young, D. F., N. R. Cholvin, and A. C. Roth. 1975. Pressure drop across artificially induced stenoses in the femoral arteries of dogs. Circ. Res. 36:735-743.

Young, D. F., N. R. Cholvin, R. L. Kirkeeide, and A. C. Roth. 1977. Hemodynamics of arterial stenoses at elevated flow rates. Circ. Res. 41:99-107.

Young, D. F. T. R. Rogge, T. A. Gray, and E. Rooz. 1980. Indirect evaluation of systemic parameters for pulsatile flow in flexible tubes. J. Biomechanics 5:339-347.

APPENDIX A. FORMULATION OF FINITE ELEMENT EQUATIONS

In Chapter 4 the Galerkin method was applied to continuity and momentum equations to yield the following element equations:

$$\int_{X_i}^{X_j} [N]^T \{\frac{\partial Q}{\partial x} + A^e C_o \frac{\partial p}{\partial t} + A^e C_1 p \frac{\partial p}{\partial t} + Sp\} dx = 0 \tag{A.1}$$

$$\int_{X_i}^{X_j} [N]^T \{c_u \frac{\partial Q}{\partial t} + \frac{\partial}{\partial x}\left(\lambda \frac{Q^2}{A^e}\right) + \frac{A^e}{\rho}\frac{\partial p}{\partial x} + B_1 Q - A^e b_x\} dx = 0 \tag{A.2}$$

To ease the integration procedure the transformation

$$s = \frac{x - X_i}{L} \tag{A.3}$$

is introduced. Then

$$N(s) = [1 - s \qquad s] \tag{A.4}$$

$$x = X_i \Rightarrow s = 0 \tag{A.5}$$

$$x = X_j \Rightarrow s = 1 \tag{A.6}$$

and

$$dx = Lds \tag{A.7}$$

The integration is carried term by term in a straightforward manner. For example the first term in the continuity equation is evaluated as

$$\int_{X_i}^{X_j} [N(x)]^T \frac{\partial Q}{\partial x} dx = \int_{X_i}^{X_j} [N(x)]^T \frac{dN(x)}{dx} \{Q\} dx =$$

$$\left[\int_o^1 [N(s)]^T \left[N_s(s)\frac{ds}{dx}\right]\frac{dx}{ds}\right]\{Q\} = \left[\int_o^1 \begin{bmatrix} 1-s \\ s \end{bmatrix} [-1 \quad 1]\, ds\right]\{Q\} =$$

$$\left[\int_o^1 \begin{bmatrix} -1+s & 1-s \\ -s & s \end{bmatrix} ds\right]\{Q\} = \frac{1}{2}\begin{bmatrix} -1 & 1 \\ -1 & 1 \end{bmatrix}\begin{Bmatrix} Q_i \\ Q_j \end{Bmatrix} \tag{A.8}$$

In a similar fashion, the third, non-linear term of the continuity equation is evaluated as

$$\int_{X_i}^{X_j} [N(x)]^T p\frac{\partial p}{\partial t}dx = L\int_o^1 [N(s)]^T \{p\}^T [N(s)]^T [N(s)]\{\dot{p}\}ds =$$

$$L\left[\int_o^1 \begin{bmatrix} 1-s \\ s \end{bmatrix} \begin{bmatrix} p_i & p_j \end{bmatrix} \begin{bmatrix} 1-s \\ s \end{bmatrix} [1-s \quad s]\, ds\right]\{\dot{p}\} =$$

$$L\left[\int_o^1 \begin{bmatrix} (1-s)^3 p_i + s(1-s)^2 p_j & s(1-s)^2 p_i + s^2(1-s)p_j \\ s(1-s)^2 p_i + s^2(1-s)p_j & s^2(1-s)p_i + s^3 p_j \end{bmatrix} ds\right]\begin{Bmatrix} \dot{p_i} \\ \dot{p_j} \end{Bmatrix} =$$

$$L\begin{bmatrix} \frac{1}{4}p_i + \frac{1}{12}p_j & \frac{1}{12}p_i + \frac{1}{12}p_j \\ \frac{1}{12}p_i + \frac{1}{12}p_j & \frac{1}{12}p_i + \frac{1}{4}p_j \end{bmatrix}\begin{Bmatrix} \dot{p_i} \\ \dot{p_j} \end{Bmatrix} \tag{A.9}$$

After the integration, the element continuity equation is written in matrix form as

$$\frac{1}{2}\begin{bmatrix} -1 & 1 \\ -1 & 1 \end{bmatrix}\begin{Bmatrix} Q_i \\ Q_j \end{Bmatrix} +$$

$$\begin{bmatrix} \frac{2LA^eC_o}{6} + \frac{LA^eC_1}{12}(3p_i + p_j) & \frac{LA^eC_o}{6} + \frac{LA^eC_1}{12}(p_i + p_j) \\ \frac{LA^eC_o}{6} + \frac{LA^eC_1}{12}(p_i + p_j) & \frac{2LA^eC_o}{6} + \frac{LA^eC_1}{12}(p_i + 3p_j) \end{bmatrix}\begin{Bmatrix} \dot{p_i} \\ \dot{p_j} \end{Bmatrix} = 0 \tag{A.10}$$

and the element momentum equation as

$$\frac{c_u L}{6}\begin{bmatrix} 2 & 1 \\ 1 & 2 \end{bmatrix}\begin{Bmatrix} \dot{Q_i} \\ \dot{Q_j} \end{Bmatrix} + \frac{A^e}{2\rho}\begin{bmatrix} -1 & 1 \\ -1 & 1 \end{bmatrix}\begin{Bmatrix} p_i \\ p_j \end{Bmatrix} +$$

$$\begin{bmatrix} -\frac{2Q_i+Q_j}{3A^e}+\frac{2B_1L}{6} & \frac{2Q_i+Q_j}{3A^e}+\frac{B_1L}{6} \\ -\frac{Q_i+2Q_j}{3A^e}+\frac{B_1L}{6} & \frac{Q_i+2Q_j}{3A^e}+\frac{2B_1L}{6} \end{bmatrix} \begin{Bmatrix} Q_i \\ Q_j \end{Bmatrix} \tag{A.11}$$

where

$$B_1 = \frac{8c_v\pi\mu}{\rho A^e} \tag{A.12}$$

Now, the element nodal vector is defined as

$$\{\delta^e\} = \begin{Bmatrix} p_i \\ Q_i \\ p_j \\ Q_j \end{Bmatrix} \tag{A.13}$$

so that the element continuity and momentum equations can be combined in a single matrix equation

$$\begin{bmatrix} \frac{2LA^eC_o}{6}+\frac{LA^eC_1}{12}(3p_i+p_j) & 0 & \frac{LA^eC_o}{6}+\frac{LA^eC_1}{12}(p_i+p_j) & 0 \\ \frac{LA^eC_o}{6}+\frac{LA^eC_1}{12}(p_i+p_j) & 0 & \frac{2LA^eC_o}{6}+\frac{LA^eC_1}{12}(p_i+3p_j) & 0 \\ 0 & \frac{2c_uL}{6} & 0\frac{c_uL}{6} & \\ 0 & \frac{c_uL}{6} & 0\frac{2c_uL}{6} & \end{bmatrix} \begin{Bmatrix} \dot{p}_i \\ \dot{Q}_i \\ \dot{p}_j \\ \dot{Q}_j \end{Bmatrix}$$

$$+ \begin{bmatrix} 0 & -\frac{1}{2} & 0 & \frac{1}{2} \\ 0 & -\frac{1}{2} & 0 & \frac{1}{2} \\ -\frac{A^e}{2\rho} & -\frac{2Q_i+Q_j}{3A^e}+\frac{2B_1L}{6} & \frac{A^e}{2\rho} & \frac{2Q_i+Q_j}{3A^e}+\frac{B_1L}{6} \\ -\frac{A^e}{2\rho} & -\frac{Q_i+2Q_j}{3A^e}+\frac{B_1L}{6} & \frac{A^e}{2\rho} & \frac{Q_i+2Q_j}{3A^e}+\frac{2B_1L}{6} \end{bmatrix} \begin{Bmatrix} p_i \\ Q_i \\ p_j \\ Q_j \end{Bmatrix} = 0 \tag{A.14}$$

which is in the form

$$[A]\{\dot{\delta}^e\} + [B]\{\delta^e\} = 0 \tag{A.15}$$

The objective is to bring the final system of equations into the following form

$$\{\dot{\delta}^e\} = -[A]^{-1}[B]\{\delta^e\} = 0 \tag{A.16}$$

and to evaluate the matrix $[K_e]$, where

$$[K_e] = -[A]^{-1}[B] \tag{A.17}$$

Since some of the quantities in matrices A and B are repeated, the following notation is introduced

$$\begin{aligned}
\lambda &= \frac{LA^eC_o}{6} \\
\eta &= \frac{C_1}{2C_o} \\
\mathcal{A} &= 2 + \eta p_i \left(3 + \frac{p_j}{p_i}\right) \\
\mathcal{B} &= 1 + \eta p_i \left(1 + \frac{p_j}{p_i}\right) \\
\mathcal{C} &= 2 + \eta p_i \left(1 + 3\frac{p_j}{p_i}\right) \\
\beta &= \frac{c_u L}{6} \\
\gamma &= \frac{A^e}{2\rho} \\
Q_A &= \frac{2Q_i + Q_j}{3A^e} \\
Q_B &= \frac{Q_i + 2Q_j}{3A^e} \\
\kappa &= \frac{B_1 L}{6}
\end{aligned}$$

Using the above notation, the element stiffness matrix $[K_e]$ is evaluated as

$$[K_e] = -\frac{adj\,[A]}{det\,[A]}[B] =$$

$$-\frac{1}{3\lambda^2\beta^2\mathcal{D}}\begin{bmatrix} -3\lambda\beta^2\mathcal{C} & 3\lambda\beta^2\mathcal{B} & 0 & 0 \\ 0 & 0 & -2\beta\lambda^2\mathcal{D} & \beta\lambda^2\mathcal{D} \\ 3\lambda\beta^2\mathcal{B} & -3\lambda\beta^2\mathcal{A} & 0 & 0 \\ 0 & 0 & \beta\lambda^2\mathcal{D} & -2\beta\lambda^2\mathcal{D} \end{bmatrix} \otimes \begin{bmatrix} 0 & -\frac{1}{2} & 0 & \frac{1}{2} \\ 0 & -\frac{1}{2} & 0 & \frac{1}{2} \\ -\gamma & -Q_A+2\kappa & \gamma & Q_A+\kappa \\ -\gamma & -Q_B+\kappa & \gamma & Q_B+2\kappa \end{bmatrix} \tag{A.18}$$

where

$$det\,[A] = -3\lambda^2\beta^2\mathcal{D} \tag{A.19}$$

$$\mathcal{D} = \mathcal{A}\mathcal{C} - \mathcal{B}^2 \tag{A.20}$$

After the simplification of terms, the element stiffness matrix becomes

$$[K_e] = \begin{bmatrix} 0 & \frac{1}{2}\frac{\mathcal{C}-\mathcal{B}}{\lambda\mathcal{D}} & 0 & -\frac{1}{2}\frac{\mathcal{C}-\mathcal{B}}{\lambda\mathcal{D}} \\ \frac{\gamma}{3\beta} & \frac{\frac{Q_i}{A^e}-3\kappa}{3\beta} & -\frac{\gamma}{3\beta} & -\frac{Q_i}{3\beta A^e} \\ 0 & \frac{1}{2}\frac{\mathcal{A}-\mathcal{B}}{\lambda\mathcal{D}} & 0 & -\frac{1}{2}\frac{\mathcal{A}-\mathcal{B}}{\lambda\mathcal{D}} \\ \frac{\gamma}{3\beta} & \frac{Q_j}{3\beta A^e} & -\frac{\gamma}{3\beta} & -\frac{\frac{Q_j}{A^e}+3\kappa}{3\beta} \end{bmatrix} \tag{A.21}$$

APPENDIX B. FINITE DIFFERENCE CODE

```
CCCCCCCCCCCCCCCCCCCCCCCCCCCCCCCCCCCCCCCCCCCCCCCCCCCCCCCCCCCCCCCCCCCC
C                                                                     C
C     FINITE ELEMENT PROGRAM FOR THE ANALYSIS OF                      C
C           MULTI-BRANCHED ARTERIAL FLOW                              C
C                                                                     C
C                    MAIN PROGRAM                                     C
C                                                                     C
CCCCCCCCCCCCCCCCCCCCCCCCCCCCCCCCCCCCCCCCCCCCCCCCCCCCCCCCCCCCCCCCCCCC
      IMPLICIT REAL*8(A-H,O-Z)
      CHARACTER*30 FILE,INFILE,OUTFILE,AVGFILE,INF,OUTF,AVGF
C
      COMMON/AREADT/AIN(150),AOUT(150),AVA(500)
      COMMON/BOUND/QBOUN(30,2),PBOUN(30,2)
      COMMON/CONDCT/CONDUCT(150)
      COMMON/COORDN/X(500),DX(500),XLAST(150),COORD(800,2),CLAST(150,2)
      COMMON/FLUPRO/DENS,VISC
      COMMON/FRY/CV,CU
      COMMON/GRAVT/GRAV,GLOAD,GA(2),GZ(500)
      COMMON/ISEGMT/NNODES(150),INDBRA(150),INDPAR(150),INDSTE(150)
      COMMON/NBOUN/NQB,NPB
      COMMON/NDATA/NS,NT,NCYC
      COMMON/NODES/NFIRST(150),NLAST(150)
      COMMON/PEE/PI
      COMMON/SEGDAT/COMPLO(150),COMPL1(150),SLEN(150),SPG(150)
     1             ,DA(150,2)
      COMMON/STENOS/XSTEN(150),STELEN(150),PRC(150)
     1             ,ST1(150),ST2(150),ST3(150)
      COMMON/TERMZ/RES1(150),RES2(150),CT(150)
      COMMON/TDATA/DT,FREQ
```

```
      COMMON/VAINIT/PINIT(500),QINIT(500)
C
*     WRITE(*,'(A \)') ' Enter file name: '
      READ(*,'(A20)') FILE
C
      DO 5 I=20,1,-1
      IF(FILE(I:I).NE.' ') GOTO 7
    5 CONTINUE
    7 CONTINUE
      INFILE=FILE(1:I)//'.DAT'
      OUTFILE=FILE(1:I)//'.OUT'
      AVGFILE=FILE(1:I)//'.AVG'
C
      INF='C:\PHD\FILES\'//INFILE
      OUTF='C:\PHD\FILES\'//OUTFILE
      AVGF='C:\PHD\FILES\'//AVGFILE
      OPEN (UNIT=5,FILE=INF,STATUS='UNKNOWN')
      OPEN (UNIT=6,FILE=OUTF,STATUS='UNKNOWN')
      OPEN (UNIT=7,FILE=AVGF,STATUS='UNKNOWN')
C
      CALL INPUT
      CALL SETUP
      CALL INIVAL
      CALL SOLVE
C
      STOP
      END
C
C
C
      SUBROUTINE INPUT
CCCCCCCCCCCCCCCCCCCCCCCCCCCCCCCCCCCCCCCCCCCCCCCCCCCCCCCCCCCCCCCCCC
C                                                                 C
C     THIS SUBROUTINE READS INPUT DATA                            C
C                                                                 C
CCCCCCCCCCCCCCCCCCCCCCCCCCCCCCCCCCCCCCCCCCCCCCCCCCCCCCCCCCCCCCCCCC
C
C-----INPUT PARAMETERS:
C
C--------------NS: # OF ARTERIAL SEGMENTS
```

```
C-------INDBRA(I): # OF THE FIRST BRANCH OF THE Ith SEGMENT
C                  (0 INDICATES TERMINAL BRANCH)
C-------INDPAR(I): # OF THE PARENT SEGMENT OF THE Ith SEGMENT
C-------INDSTE(I): LOCATION (ELEMENT #) OF STENOSIS (=0, NO STENOSIS)
C---------SLEN(I): SEGMENT LENGTH
C-------NNODES(I): # OF NODES IN EACH SEGMENTS
C----------AIN(I): AREA AT THE BEGINING OF THE SEGMENT
C---------AOUT(I): AREA AT THE END OF THE SEGMENT
C-------COMPL0(I): COMPLIANCE COEFFICIENT OF THE ARTERIAL WALL [C0]
C-------COMPL1(I): COMPLIANCE COEFFICIENT OF THE ARTERIAL WALL [C1]
C----------SPG(I): SEEPAGE OF THE SEGMENT
C-------DA(I,1-2): DIRECTIONAL ANGLES OF THE SEGMENT
C---------RES1(I): TERMINAL RESISTANCE 1
C---------RES2(I): TERMINAL RESISTANCE 2
C-----------CT(I): TERMINAL CAPACITANCE
C--------XSTEN(I): DISTANCE FROM BEGINING OF SEGMENT TO STENOSIS
C-------STELEN(I): LENGTH OF STENOSIS
C----------PRC(I): PERCENT AREA REDUCTION IN STENOSIS
C------------DENS: DENSITY
C------------VISC: VISCOSITY
C------------NCYC: # OF CYCLES
C------------FREQ: BASIC FREQUENCY OF EACH CYCLE
C-------------NQB: # OF FLOW HARMONICS
C-------------NPB: # OF PRESSURE HARMONICS
C----QBOUN(I,1-2): FLOW HARMONICS (INPUT)
C----PBOUN(I,1-2): PRESSURE HARMONICS (INPUT)
C-----------GLOAD: BODY FORCE IN MULTIPLES OF g (ACCL. OF GRAVITY)
C---------GA(1-2): ANGLES OF THE GLOAD VECTOR WRT COORDINATE SYSTEM
C--------------DT: TIME INCREMENT
C
      IMPLICIT REAL*8(A-H,0-Z)
      COMMON/AREADT/AIN(150),AOUT(150),AVA(500)
      COMMON/BOUND/QBOUN(30,2),PBOUN(30,2)
      COMMON/FLUPRO/DENS,VISC
      COMMON/FRY/CV,CU
      COMMON/GRAVT/GRAV,GLOAD,GA(2),GZ(500)
      COMMON/ISEGMT/NNODES(150),INDBRA(150),INDPAR(150),INDSTE(150)
      COMMON/NBOUN/NQB,NPB
      COMMON/NDATA/NS,NT,NCYC
      COMMON/SEGDAT/COMPL0(150),COMPL1(150),SLEN(150),SPG(150)
```

```
     1             ,DA(150,2)
      COMMON/STENOS/XSTEN(150),STELEN(150),PRC(150)
     1             ,ST1(150),ST2(150),ST3(150)
      COMMON/TERMZ/RES1(150),RES2(150),CT(150)
      COMMON/TDATA/DT,FREQ
C
      READ (5,1000) NS
C
      DO 10 I=1,NS
         READ (5,2000) INDBRA(I),INDPAR(I),INDSTE(I),NNODES(I),SLEN(I),
     1                 AIN(I),AOUT(I)
   10 CONTINUE
C
      READ (5,9000)
C
      DO 15 I=1,NS
         READ (5,2500)  COMPL0(I),COMPL1(I),SPG(I),ANGL
         ANGL=ANGL*3.14159D0/180.D0
         DA(I,1)=DCOS(ANGL)
         DA(I,2)=DSIN(ANGL)
   15 CONTINUE
C
      READ (5,9000)
C
      DO 20 I=1,NS
         IF (INDBRA(I).GT.0) GOTO 20
         READ (5,3000) RES1(I),RES2(I),CT(I)
   20 CONTINUE

C
      KS=0
      DO I=1,NS
         KS=KS+INDSTE(I)
      END DO
      IF (KS.EQ.0) GOTO 26
C
      READ (5,9000)
C
      DO 25 I=1,NS
         IF (INDSTE(I).EQ.0) GOTO 25
```

```
         READ (5,3000)  XSTEN(I),STELEN(I),PRC(I)
   25 CONTINUE
   26 CONTINUE
C
      READ (5,4000) DENS,VISC
      READ (5,5000) NCYC,FREQ,DT
      READ (5,4000) CV,CU
C
      READ (5,6000) NPB,NQB
      IF (NPB.GT.0) THEN
         DO 30 I=1,NPB
            READ (5,7000) PBOUN(I,1),PBOUN(I,2)
   30    CONTINUE
      ELSE
         DO 40 I=1,NQB
            READ (5,7000) QBOUN(I,1),QBOUN(I,2)
   40    CONTINUE
      END IF
C
      READ (5,8000) GRAV,GLOAD,GANGL
      GANGL=GANGL*3.14159D0/180.D0
      GA(1)=DCOS(GANGL)
      GA(2)=DSIN(GANGL)
C
C-----CALL VERIPT TO VERIFY INPUT DATA
C
      CALL VERIPT
      RETURN
C
C
 1000 FORMAT(1X/I3//)
 2000 FORMAT(3X,4(2X,I3),3(2X,D12.5))
 2500 FORMAT(3X,4(2X,D12.5))
 3000 FORMAT(3X,3(2X,D12.5))
 4000 FORMAT(//2(2X,D12.5))
 5000 FORMAT(//2X,I3,2(2X,D12.5))
 6000 FORMAT(//2(2X,I3)//)
 7000 FORMAT(2(2X,D12.5))
 8000 FORMAT(//3(2X,D12.5))
 9000 FORMAT(/)
```

```
C
      END
C
C
      SUBROUTINE VERIPT
CCCCCCCCCCCCCCCCCCCCCCCCCCCCCCCCCCCCCCCCCCCCCCCCCCCCCCCCCCCCCCCCCC
C                                                                  C
C      THIS SUBROUTINE VERIFIES INPUT DATA                         C
C                                                                  C
CCCCCCCCCCCCCCCCCCCCCCCCCCCCCCCCCCCCCCCCCCCCCCCCCCCCCCCCCCCCCCCCCC
      IMPLICIT REAL*8(A-H,O-Z)
      COMMON/AREADT/AIN(150),AOUT(150),AVA(500)
      COMMON/BOUND/QBOUN(30,2),PBOUN(30,2)
      COMMON/FLUPRO/DENS,VISC
      COMMON/FRY/CV,CU
      COMMON/GRAVT/GRAV,GLOAD,GA(2),GZ(500)
      COMMON/ISEGMT/NNODES(150),INDBRA(150),INDPAR(150),INDSTE(150)
      COMMON/NBOUN/NQB,NPB
      COMMON/NDATA/NS,NT,NCYC
      COMMON/SEGDAT/COMPLO(150),COMPL1(150),SLEN(150),SPG(150)
     1             ,DA(150,2)
      COMMON/STENOS/XSTEN(150),STELEN(150),PRC(150)
     1             ,ST1(150),ST2(150),ST3(150)
      COMMON/TERMZ/RES1(150),RES2(150),CT(150)
      COMMON/TDATA/DT,FREQ
C
      WRITE (6,500)
      WRITE (6,1000) NS
C
      WRITE (6,1500)
      DO 10 I=1,NS
         WRITE (6,2000) I,INDBRA(I),INDPAR(I),INDSTE(I),NNODES(I),
     1                  SLEN(I),AIN(I),AOUT(I)
   10 CONTINUE
C
      WRITE (6,2100)
      DO 15 I=1,NS
         WRITE (6,2200) I,COMPLO(I),COMPL1(I),SPG(I),DA(I,1),DA(I,2)
   15 CONTINUE
C
```

```
      WRITE (6,2500)
C
      DO 20 I=1,NS
         IF (INDBRA(I).GT.0) GOTO 20
         WRITE (6,3000) I,RES1(I),RES2(I),CT(I)
   20 CONTINUE
C
C
      WRITE (6,3100)
C
      DO 25 I=1,NS
         IF (INDSTE(I).EQ.0) GOTO 25
         WRITE (6,3000) I,XSTEN(I),STELEN(I),PRC(I)
   25 CONTINUE
C
      WRITE (6,3500)
      WRITE (6,4000) DENS,VISC
C
      WRITE (6,4500)
      WRITE (6,5000) NCYC,FREQ,DT
C
      WRITE (6,5200)
      WRITE (6,4000) CV,CU
C
      WRITE (6,5500)
      WRITE (6,6000) NPB,NQB
      IF (NPB.GT.0) THEN
         WRITE (6,6500)
         DO 30 I=1,NPB
            WRITE (6,7000) PBOUN(I,1),PBOUN(I,2)
   30    CONTINUE
      ELSE
         WRITE (6,7500)
         DO 40 I=1,NQB
            WRITE (6,7000) QBOUN(I,1),QBOUN(I,2)
   40    CONTINUE
      END IF
C
      WRITE (6,8500)
      WRITE (6,8000) GRAV,GLOAD,GA(1),GA(2)
```

```
C
      RETURN
C
  500 FORMAT(' NUMBER OF SEGMENTS')
 1000 FORMAT(7X,I4,//)
 1500 FORMAT('  SEG  BRA  PAR  STE  NEL  SEGM. LENGTH  INPUT AREA',
     11X,'   OUTPUT ')
 2000 FORMAT(1X,I3,4(2X,I3),6(2X,D12.5),2(2X,F4.1))
 2100 FORMAT(/'  SEG     COMPLO        COMPL1       SEEPAGE
     1   DIRECTIONAL COSINES')
 2200 FORMAT(1X,I3,5(2X,D12.5))
 2500 FORMAT(/'  SEG      RES1          RES2          CT')
 3000 FORMAT(1X,I3,3(2X,D12.5))
 3100 FORMAT(/'  SEG   X STENOSIS   STENOSIS LNGTH     %')
 3500 FORMAT(/'     DENSITY      VISCOSITY')
 4000 FORMAT(2(2X,D12.5))
 4500 FORMAT(/' # OF CYCLES    FREQUENCY    TIME INCREMENT')
 5000 FORMAT(4X,I3,2(7X,D12.5))
 5200 FORMAT(/'       CV            CU')
 5500 FORMAT(/' # OF PRESSURE FOURIER COEF.   # OF FLOW FOURIER COEF.')
 6000 FORMAT(10X,I3,25X,I3)
 6500 FORMAT(/'   P COS TERM    P SIN TERM')
 7000 FORMAT(2(2X,D12.5))
 7500 FORMAT(/'   Q COS TERM    Q SIN TERM')
 8000 FORMAT(4(2X,D12.5))
 8500 FORMAT(/'  ACCEL. GRAV.    GRAVIT. LOAD        ORIENT. ANGLES')
C
      END
C
C
C
      SUBROUTINE SETUP
CCCCCCCCCCCCCCCCCCCCCCCCCCCCCCCCCCCCCCCCCCCCCCCCCCCCCCCCCCCCCCCCCC
C                                                                 C
C      THIS SUBROUTINE SETS UP THE ELEMENTS,                      C
C      CALCULATES THE ELEMENT LENGTHS AND TYPES                   C
C      ASSIGNS THEIR CHARACTERISTIC VALUES, AND                   C
C      SETS UP A COORDINATE SYSTEM                                C
C                                                                 C
CCCCCCCCCCCCCCCCCCCCCCCCCCCCCCCCCCCCCCCCCCCCCCCCCCCCCCCCCCCCCCCCCC
```

```
      IMPLICIT REAL*8(A-H,O-Z)
      COMMON/AREADT/AIN(150),AOUT(150),AVA(500)
      COMMON/COORDN/X(500),DX(500),XLAST(150),COORD(800,2),CLAST(150,2)
      COMMON/FLUPRO/DENS,VISC
      COMMON/ISEGMT/NNODES(150),INDBRA(150),INDPAR(150),INDSTE(150)
      COMMON/NDATA/NS,NT,NCYC
      COMMON/NODES/NFIRST(150),NLAST(150)
      COMMON/PEE/PI
      COMMON/SEGDAT/COMPLO(150),COMPL1(150),SLEN(150)
     1             ,SPG(150),DA(150,2)
      COMMON/STENOS/XSTEN(150),STELEN(150),PRC(150)
     1             ,ST1(150),ST2(150),ST3(150)
      COMMON/TERMZ/RES1(150),RES2(150),CT(150)
      COMMON/TDATA/DT,FREQ
C
      PI=4.0D0*DATAN(1.0D0)
C
C-----NT: TOTAL # OF NODES
C-----NFIRST(I): THE FIRST NODE OF THE Ith SEGMENT
C-----NLAST(I): THE LAST NODE OF THE Ith SEGMENT
C
      K=0
      DO 10 I=1,NS
         NFIRST(I)=K+1
         K=K+NNODES(I)
         NLAST(I)=K
   10 CONTINUE
      NT=K
C
C-----CALCULATE THE GRID SPACING DX(J) TO THE RIGHT OF EACH NODE
C
      DO 50 I=1,NS
         NF=NFIRST(I)
         NL=NLAST(I)
         IS=INDSTE(I)
         IF(IS.EQ.0) THEN
C-----------NO STENOSES
            DO 20 J=NF,NL-1
               DX(J)=SLEN(I)/(NNODES(I)-1)
   20       CONTINUE
```

```
         ELSE
C-----------THERE ARE STENOSES IN THE SEGMENT
            DO 30 J=NF,NF+IS-2
               DX(J)=XSTEN(I)/(IS-1)
   30       CONTINUE
            DX(NF+IS-1)=STELEN(I)
            DO 40 J=NF+IS,NL-1
               DX(J)=(SLEN(I)-XSTEN(I)-STELEN(I))/(NNODES(I)-IS-1)
   40       CONTINUE
         END IF
   50 CONTINUE
C
C-----CALCULATE THE COORDINATES OF EACH NODE X(I)(ARC-LENGTH),
C-----COORD(I,1) (X-COORDINATE), AND COORD(I,2) (Y-COORDINATE)
C
C-----XLAST(I): THE COORDINATE OF THE LAST NODE OF Ith SEGMENT
C-----CLAST(I,1-2): X AND Y COORDINATES OF LAST NODE OF Ith SEGMENT
C
      X(1)=0.0D00
      COORD(1,1)=0.0D00
      COORD(1,2)=0.0D00
      DO 80 I=1,NS
         NF=NFIRST(I)
         NL=NLAST(I)
         L=INDPAR(I)
         IF (L.EQ.0) GOTO 60
         X(NF)=XLAST(L)
         COORD(NF,1)=CLAST(L,1)
         COORD(NF,2)=CLAST(L,2)
   60    CONTINUE
         DO 70 J=NF+1,NL
            X(J)=X(J-1)+DX(J-1)
            COORD(J,1)=COORD(J-1,1)+DX(J-1)*DA(I,1)
            COORD(J,2)=COORD(J-1,2)+DX(J-1)*DA(I,2)
   70    CONTINUE
         XLAST(I)=X(NL)
         CLAST(I,1)=COORD(NL,1)
         CLAST(I,2)=COORD(NL,2)
   80 CONTINUE
C
```

```
C
C-----CALCULATE THE MEAN AREA FOR EACH ELEMENT
C
      CALL AREA
C
C-----CALCULATE THE BODY FORCE PROJECTION ON EACH SEGMENT
C
      CALL GRAVIT
C
C-----CALCULATE THE STENOSIS COEFFICIENTS SKV(I),SK1(I),SK2(I), AND SK3(I)
C
      CALL STENOSIS
C
C-----PRINT OUT THE FIRST AND LAST NODE OF EACH SEGMENT
C-----AND THE COORDINATES OF THE LAST NODE
C
      WRITE (6,4000)
      DO 110 I=1,NS
         WRITE (6,5000) I,NFIRST(I),NLAST(I),XLAST(I),
     1                  CLAST(I,1),CLAST(I,2)
  110 CONTINUE
C
C-----PRINT OUT THE TOTAL NUMBER OF NODES AND THE
C-----COORDINATES OF EACH NODE
C
      WRITE (6,6000) NT
      WRITE (6,7000)
      DO 120 K=1,NT,5
         L=K+4
         WRITE (6,8000) (I,X(I),I=K,L)
  120 CONTINUE
C
      RETURN
C
 4000 FORMAT(/' SEGMENT  FIRST_NODE  LAST_NODE       LAST_POINT_COORD.')
 5000 FORMAT(2X,I3,2(8X,I3),3(2X,D12.5))
 6000 FORMAT(//' NUMBER OF NODES'/5X,I3)
 7000 FORMAT(/20X,'NODE COORDINATES')
 8000 FORMAT(2X,5(I3,D12.5,1X))
      END
```

```
C
C
      SUBROUTINE AREA
CCCCCCCCCCCCCCCCCCCCCCCCCCCCCCCCCCCCCCCCCCCCCCCCCCCCCCCCCCCC
C                                                             C
C      THIS SUBROUTINE CALCULATES THE ELEMENT AREA            C
C                                                             C
CCCCCCCCCCCCCCCCCCCCCCCCCCCCCCCCCCCCCCCCCCCCCCCCCCCCCCCCCCCC
      IMPLICIT REAL*8(A-H,O-Z)
      COMMON/AREADT/AIN(150),AOUT(150),AVA(500)
      COMMON/COORDN/X(500),DX(500),XLAST(150),COORD(800,2),CLAST(150,2)
      COMMON/ISEGMT/NNODES(150),INDBRA(150),INDPAR(150),INDSTE(150)
      COMMON/NDATA/NS,NT,NCYC
      COMMON/NODES/NFIRST(150),NLAST(150)
      COMMON/SEGDAT/COMPL0(150),COMPL1(150),SLEN(150),SPG(150)
     1             ,DA(150,2)
      COMMON/TERMZ/RES1(150),RES2(150),CT(150)
C
C
      DO 20 I=1,NS
         SLOPE=(AOUT(I)-AIN(I))/SLEN(I)
         KF=NFIRST(I)
         KL=NLAST(I)
         DO 10 J=KF,KL
            AVA(J)=AIN(I)+SLOPE*(X(J)-X(KF))
   10    CONTINUE
   20 CONTINUE
C
      RETURN
      END
C
C
      SUBROUTINE GRAVIT
CCCCCCCCCCCCCCCCCCCCCCCCCCCCCCCCCCCCCCCCCCCCCCCCCCCCCCCCCCCC
C                                                             C
C      THIS SUBROUTINE CALCULATES THE BODY FORCE              C
C      PROJECTION ON EACH SEGMENT                             C
C                                                             C
CCCCCCCCCCCCCCCCCCCCCCCCCCCCCCCCCCCCCCCCCCCCCCCCCCCCCCCCCCCC
      IMPLICIT REAL*8(A-H,O-Z)
```

```
      COMMON/GRAVT/GRAV,GLOAD,GA(2),GZ(500)
      COMMON/NDATA/NS,NT,NCYC
      COMMON/SEGDAT/COMPLO(150),COMPL1(150),SLEN(150),SPG(150)
     1             ,DA(150,2)
C
C
      DO 20 I=1,NS
      PROJ=0.0D0
      DO 10 J=1,2
            PROJ=PROJ+DA(I,J)*GA(J)
   10    CONTINUE
      GZ(I)=PROJ*GLOAD*GRAV
   20 CONTINUE
C
      RETURN
      END
C
C
      SUBROUTINE STENOSIS
CCCCCCCCCCCCCCCCCCCCCCCCCCCCCCCCCCCCCCCCCCCCCCCCCCCCCCCCCCCCCCCCC
C                                                                 C
C     THIS SUBROUTINE CALCULATES THE STENOSIS                     C
C     COEFFICIENTS                                                C
C                                                                 C
CCCCCCCCCCCCCCCCCCCCCCCCCCCCCCCCCCCCCCCCCCCCCCCCCCCCCCCCCCCCCCCCC
      IMPLICIT REAL*8(A-H,O-Z)
      COMMON/AREADT/AIN(150),AOUT(150),AVA(500)
      COMMON/FLUPRO/DENS,VISC
      COMMON/ISEGMT/NNODES(150),INDBRA(150),INDPAR(150),INDSTE(150)
      COMMON/NDATA/NS,NT,NCYC
      COMMON/NODES/NFIRST(150),NLAST(150)
      COMMON/PEE/PI
      COMMON/STENOS/XSTEN(150),STELEN(150),PRC(150)
     1             ,ST1(150),ST2(150),ST3(150)
      COMMON/TDATA/DT,FREQ
C
      REAL*8 KV,KT,KU,LA
C
C
      KU=1.20D00
```

```
      KT=1.52D00
      DO 10 I=1,NS
         KS=INDSTE(I)
         IF(KS.EQ.0) GOTO 10
         J=NFIRST(I)+KS-1
         A1=PRC(I)*AVA(J)
         D1=DSQRT(4.0D00*A1/PI)
         LA=0.83D00*STELEN(I)+1.64D00*D1
         D=DSQRT(4.0D00*AVA(J)/PI)
         KV=3.2D01*(LA/D)*(1.0D00/PRC(I))**2
         ST1(I)=AVA(J)/(DENS*STELEN(I)*KU)
         ST2(I)=-(KV*VISC)/(DENS*STELEN(I)*KU*D)
         ST3(I)=-KT/(2.0D00*KU*STELEN(I)*AVA(J))
     1         *(1.0D00/PRC(I)-1)**2
   10 CONTINUE
C
      RETURN
      END
C
C
      SUBROUTINE INIVAL
CCCCCCCCCCCCCCCCCCCCCCCCCCCCCCCCCCCCCCCCCCCCCCCCCCCCCCCCCCCCCCCCC
C                                                               C
C      THIS SUBROUTINE ASSIGNS INITIAL PRESSURE AND             C
C      FLOW VALUES AT EACH NODE                                 C
C                                                               C
CCCCCCCCCCCCCCCCCCCCCCCCCCCCCCCCCCCCCCCCCCCCCCCCCCCCCCCCCCCCCCCCC
      IMPLICIT REAL*8(A-H,O-Z)
      COMMON/AREADT/AIN(150),AOUT(150),AVA(500)
      COMMON/BOUND/QBOUN(30,2),PBOUN(30,2)
      COMMON/CONDCT/CONDUCT(150)
      COMMON/COORDN/X(500),DX(500),XLAST(150),COORD(800,2),CLAST(150,2)
      COMMON/FLUPRO/DENS,VISC
      COMMON/GRAVT/GRAV,GLOAD,GA(2),GZ(500)
      COMMON/ISEGMT/NNODES(150),INDBRA(150),INDPAR(150),INDSTE(150)
      COMMON/NBOUN/NQB,NPB
      COMMON/NDATA/NS,NT,NCYC
      COMMON/NODES/NFIRST(150),NLAST(150)
      COMMON/PEE/PI
      COMMON/SEGDAT/COMPLO(150),COMPL1(150),SLEN(150),SPG(150)
```

```
     1             ,DA(150,2)
      COMMON/TERMZ/RES1(150),RES2(150),CT(150)
      COMMON/VAINIT/PINIT(500),QINIT(500)
      DIMENSION FL(150),GFL(150)
C
C-----CALCULATE THE TOTAL CONDUCTANCE FIRST (RTOTAL=1/CONDUCTANCE)
C
C--------CALCULATE THE CONDUCTANCE AT THE TERMINAL BRANCHES FIRST
C
      DO 10 I=1,NS
         IF (INDBRA(I).GT.0) GOTO 5
         CONDUCT(I)=1.0D00/(RES1(I)+RES2(I)
     1                      +8.0D00*VISC*SLEN(I)*PI/AOUT(I)**2)
    5    CONTINUE
   10 CONTINUE
C
C--------CALCULATE CONDUCT(I) FOR THE REST OF THE SEGMENTS
C
      DO 20 I=NS,1,-1
         K=INDBRA(I)
         IF (K.EQ.0) GOTO 15
         CONDUCT(I)=1.0D00/(1.0D00/(CONDUCT(K)+CONDUCT(K+1))
     1                      +8.0D00*VISC*PI*SLEN(I)/AOUT(I)**2)
   15    CONTINUE
   20 CONTINUE
C
C--------THE TOTAL RESISTANCE IS THE INVERSE OF THE
C--------CONDUCTIVITY OF THE FIRST SEGMENT
C
      RTOTAL=1.0D00/CONDUCT(1)
C
C
C-----FIX PROXIMAL P AND Q
C
      IF(NPB.GT.0) THEN
         PR=FPRES(0.0D00)
         FL(1)=PBOUN(1,1)/RTOTAL
      ELSE
         FL(1)=FFLOW(0.0D0)
         PR=QBOUN(1,1)*RTOTAL
```

```
      END IF
C
C
C-----ASSIGN INITIAL FLOW VALUES BY DIVIDING Q
C-----ACCORDING TO THE CONDUCTIVITY OF EACH ELEMENT
C
      DO 30 I=1,NS
         IF (INDBRA(I).EQ.0) GOTO 25
         IB1=INDBRA(I)
         IB2=IB1+1
         FL(IB1)=FL(I)*CONDUCT(IB1)/(CONDUCT(IB1)+CONDUCT(IB2))
         FL(IB2)=FL(I)-FL(IB1)
   25    CONTINUE
   30 CONTINUE
C
C-----ADD TO THE INITIAL FLOW VALUES THE PORTION COMING FROM
C-----THE BODY FORCE TERM
C
      DO 40 I=1,NS
         IF(INDBRA(I).GT.0) GOTO 35
            HEAD=CLAST(I,1)*GA(1)+CLAST(I,2)*GA(2)
            GFL(I)=DENS*GRAV*GLOAD*HEAD*CONDUCT(I)
   35    CONTINUE
   40 CONTINUE
      DO 50 I=NS,1,-1
         K=INDBRA(I)
         IF (K.EQ.0) GOTO 50
            GFL(I)=GFL(K)+GFL(K+1)
   50 CONTINUE
C
C-----ASSIGN INITIAL PRESSURE PINIT(I) AND FLOW QINIT(I) VALUES
C     TO ALL NODES
C
      K=0
      DO 70 I=1,NS
         KF=NFIRST(I)
         KL=NLAST(I)
         DO 60 J=KF,KL
            PINIT(J)=PR
            QINIT(J)=FL(I)+GFL(I)
```

```
   60    CONTINUE
   70 CONTINUE
C
C-----PRINT OUT INITIAL VALUES FOR ALL NODES
C
      WRITE (6,1000)
      DO 80 K=1,NT,2
         L=K+1
         WRITE (6,2000) (I,PINIT(I),QINIT(I),I=K,L)
   80 CONTINUE
C
      RETURN
C
 1000 FORMAT(//,15X,'INITIAL PRESSURE AND FLOW VALUES',/)
 2000 FORMAT(2(1X,I3,2X,2(D12.5,1X)))
C
      END
C
C
      SUBROUTINE SOLVE
CCCCCCCCCCCCCCCCCCCCCCCCCCCCCCCCCCCCCCCCCCCCCCCCCCCCCCCCCCCCCCCCCC
C     THIS SUBROUTINE SOLVES THE SYSTEM OF EQUATIONS       C
C     RESULTING FROM THE APPLICATION OF THE IMPLICIT       C
C     FINITE DIFFERENCE METHOD ON THE GOVERNING EQUATIONS. C
C     THE MATRICES ARE FORMED FIRST ARRANGED SO THAT A     C
C     TRIDIAGONAL BLOCK MATRIX SOLVER CAN BE EMPLOYED      C
C     TO SOLVE THE SYSTEM OF EQUATIONS.                    C
CCCCCCCCCCCCCCCCCCCCCCCCCCCCCCCCCCCCCCCCCCCCCCCCCCCCCCCCCCCCCCCCCC
      IMPLICIT REAL*8(A-H,O-Z)
      COMMON/AREADT/AIN(150),AOUT(150),AVA(500)
      COMMON/COORDN/X(500),DX(500),XLAST(150),COORD(800,2),CLAST(150,2)
      COMMON/FLUPRO/DENS,VISC
      COMMON/FRY/CV,CU
      COMMON/GRAVT/GRAV,GLOAD,GA(2),GZ(500)
      COMMON/ISEGMT/NNODES(150),INDBRA(150),INDPAR(150),INDSTE(150)
      COMMON/NBOUN/NQB,NPB
      COMMON/NDATA/NS,NT,NCYC
      COMMON/NODES/NFIRST(150),NLAST(150)
      COMMON/PEE/PI
      COMMON/SEGDAT/COMPLO(150),COMPL1(150),SLEN(150),SPG(150)
```

```
     1             ,DA(150,2)
      COMMON/STENOS/XSTEN(150),STELEN(150),PRC(150)
     1             ,ST1(150),ST2(150),ST3(150)
      COMMON/TERMZ/RES1(150),RES2(150),CT(150)
      COMMON/TDATA/DT,FREQ
      COMMON/VAINIT/PINIT(500),QINIT(500)
C
      DIMENSION P(500),Q(500),PAVG(500),PMAX(500),PMIN(500)
     +                       ,QAVG(500),QMAX(500),QMIN(500)
C
C-----INITIALIZE MAXIMUM AND MINIMUM P AND Q VALUES
C
      DO I=1,NT
         PMAX(I)=0.D0
         QMAX(I)=0.D0
         PMIN(I)=1.D10
         QMIN(I)=1.D10
      END DO
C
C-----NTS: NUMBER OF TIME STEPS
C-----NTSPC: NUMBER OF TIME STEPS PRE CYCLE
C-----NLC: TIME STEP AFTER WIHICH LAST CYCLE BEGINS
C
      NTS=IDNINT(NCYC/(DT*FREQ))
      NTSPC=NTS/NCYC
      NLC=NTS-NTSPC
      IPRN=NTS/NCYC/100
C
C-----COPY THE INITIAL VALUES TO D VECTOR
C-----TO START THE INTEGRATION PROCEDURE
C
      DO 10 J=1,NT
         P(J)=PINIT(J)
         Q(J)=QINIT(J)
   10 CONTINUE
C
C-----START THE SOLUTION - MARCH IN TIME
C
      DO 50 IT=1,NTS
         TIME=IT*DT
```

```
C
      PAR1=8.0D0*CV*PI*VISC*DT/DENS/CU
      DO 30 I=1,NS
C
         NF=NFIRST(I)
         NL=NLAST(I)
C
C-----------WRITE OUT THE EQUATIONS FOR THE FIRST NODE
C
         IF (NF.EQ.1) THEN
C
C--------------PROXIMAL END CONDITION
C
            IF (NPB.GT.0) THEN
C
C-----------------PROXIMAL PRESSURE PRESCRIBED
C
               P(NF)=FPRES(TIME)
               Q(NF)=(1.0D0-PAR1/AVA(NF))*Q(NF)
     1               -DT/(CU*DENS)/DX(NF)*AVA(NF)*
     2               (P(NF+1)-P(NF))
     3              +AVA(NF)*GZ(I)*DT/CU
            ELSE
               Q(NF)=FFLOW(TIME)
               P(NF)=P(NF)-DT/(COMPL0(I)+COMPL1(I)*P(NF))
     1              /DX(NF)/AVA(NF)*(Q(NF+1)-Q(NF))
            END IF
         ELSE
C
C--------------NODE AT BEGINNING OF A BRANCH
C
            P(NF)=P(NLAST(INDPAR(I)))
            Q(NF)=(1.0D0-PAR1/AVA(NF))*Q(NF)
     1            -DT/(CU*DENS)/DX(NF)*AVA(NF)*
     2            (P(NF+1)-P(NF))
     3            +AVA(NF)*GZ(I)*DT/CU
         END IF
C
C-----------WRITE OUT THE EQUATIONS FOR INTERIOR NODES
C-----------(BETWEEN FIRST AND LAST) OF EACH SEGMENT
```

```
C
            IS=INDSTE(I)
            IF(IS.EQ.0) THEN
C--------------NO STENOSES
               DO 20 J=NF+1,NL-1
                  P(J)=P(J)-DT/(COMPLO(I)+COMPL1(I)*P(J))
     1                 /DX(J)/AVA(J)*(Q(J)-Q(J-1))
                  Q(J)=(1.0D0-PAR1/AVA(J))*Q(J)
     1                 -DT/(CU*DENS)/DX(J)*AVA(J)*(P(J+1)-P(J))
     2                 -DT/(CU*DX(J))*(Q(J)**2/AVA(J)
     3                 -Q(J-1)**2/AVA(J-1))
     4                  +AVA(J)*GZ(I)*DT/CU
   20            CONTINUE
            ELSE
C
C--------------STENOSES PRESENT
C
C--------------EQUATIONS FOR NODES BEFORE THE STENOSIS
C
               DO 22 J=NF+1,NF+IS-2
                  P(J)=P(J)-DT/(COMPLO(I)+COMPL1(I)*P(J))
     1                 /DX(J)/AVA(J)*(Q(J)-Q(J-1))
                  Q(J)=(1.0D0-PAR1/AVA(J))*Q(J)
     1                 -DT/(CU*DENS)/DX(J)*AVA(J)*(P(J+1)-P(J))
     2                 -DT/(CU*DX(J))*(Q(J)**2/AVA(J)
     3                 -Q(J-1)**2/AVA(J-1))
     4                  +AVA(J)*GZ(I)*DT/CU
   22            CONTINUE
C
C--------------EQUATIONS FOR PROXIMAL NODE OF STENOSIS
C
               J=NF+IS-1
               P(J)=P(J)-DT/AVA(J)/(COMPLO(I)+COMPL1(I)*P(J))
     1              /DX(J-1)*(Q(J)-Q(J-1))
C
C--------------STENOSIS EQUATION
C
               Q(J)=Q(J)+DT*(ST1(I)*(P(J)-P(J+1))+ST2(I)*Q(J)
     1              +ST3(I)*Q(J)*DABS(Q(J)))
C
```

```
C--------------EQUATIONS FOR DISTAL NODE OF STENOSIS
C
               J=NF+IS
               P(J)=P(J)-DT/AVA(J)/(COMPLO(I)+COMPL1(I)*P(J))
     1              /DX(J)*(Q(J+1)-Q(J))
               Q(J)=Q(J-1)
C
C--------------EQUATIONS FOR NODES DISTAL TO STENOSIS
C
               DO 24 J=NF+IS+1,NL-1
                  P(J)=P(J)-DT/(COMPLO(I)+COMPL1(I)*P(J))
     1                 /DX(J)/AVA(J)*(Q(J)-Q(J-1))
                  Q(J)=(1.0DO-PAR1/AVA(J))*Q(J)
     1                -DT/(CU*DENS)/DX(J)*AVA(J)*(P(J+1)-P(J))
     2                -DT/(CU*DX(J))*(Q(J)**2/AVA(J)
     3                -Q(J-1)**2/AVA(J-1))
     4                 +AVA(J)*GZ(I)*DT/CU
   24          CONTINUE
            END IF
C
C-----------WRITE OUT THE EQUATIONS FOR THE LAST NODE
C
            IF (INDBRA(I).EQ.0) THEN
C
C--------------CASE A. THE SEGMENT ENDS AT A TERMINAL IMPEDANCE
C
               POLD=P(NL)
               IF(CT(I).EQ.0.0DO) THEN
C
C-----------------CASE A.1 SIMPLE RESISTANCE
C
                  P(NL)=P(NL)-DT/(COMPLO(I)+COMPL1(I)*P(NL))
     1                 /DX(NL-1)/AVA(NL)*(Q(NL)-Q(NL-1))
                  Q(NL)=P(NL)/(RES1(I)+RES2(I))
               ELSE
C
C-----------------CASE A.2 WINDKESSEL MODEL
C
                  P(NL)=P(NL)-DT/(COMPLO(I)+COMPL1(I)*P(NL))
     1                 /DX(NL-1)/AVA(NL)*(Q(NL)-Q(NL-1))
```

```
                Q(NL)=Q(NL)+(P(NL)-POLD)/RES1(I)
     1                 +DT/(RES1(I)*RES2(I)*CT(I))*P(NL)
     2                 -DT*(1.0D0+RES1(I)/RES2(I))/(RES1(I)*CT(I))
     3                 *Q(NL)
             END IF
          ELSE
C
C--------------CASE B. THE SEGMENT BIFURCATES
C
                P(NL)=P(NL)-DT/(COMPL0(I)+COMPL1(I)*P(NL))
     1                 /DX(NL-1)/AVA(NL)*(Q(NL)-Q(NL-1))
          END IF
   30    CONTINUE
C
C--------APPLY BRANCH FLOW CONDITION
C
         DO 35 I=1,NS
            NL=NLAST(I)
            NF1=NFIRST(INDBRA(I))
            NF2=NFIRST(INDBRA(I)+1)
            IF(INDBRA(I).NE.0) Q(NL)=Q(NF1)+Q(NF2)
   35    CONTINUE
C
         IF(IT.GT.NLC) THEN
            DO I=1,NT
               PAVG(I)=PAVG(I)+P(I)
               QAVG(I)=QAVG(I)+Q(I)
               IF(P(I).GT.PMAX(I)) PMAX(I)=P(I)
               IF(Q(I).GT.QMAX(I)) QMAX(I)=Q(I)
               IF(P(I).LT.PMIN(I)) PMIN(I)=P(I)
               IF(Q(I).LT.QMIN(I)) QMIN(I)=Q(I)
            END DO
         ELSE
            CONTINUE
         END IF
C
C
C--------PRINT OUT THE NODAL VALUES OF PRESSURE AND FLOW
C--------(PRINT OUT ONLY 100 POINTS PER CYCLE)
C
```

```
         ICHECK=IT/IPRN
         IF(ICHECK*IPRN.NE.IT) GOTO 68
         WRITE (*,'(F7.4)') TIME
         WRITE (6,2000) TIME
         DO 40 J=1,NT,4
            K=J
            K1=K+1
            K2=K+2
            K3=K+3
            Y1=P(J)
            Y2=Q(J)
            Y3=P(J+1)
            Y4=Q(J+1)
            Y5=P(J+2)
            Y6=Q(J+2)
            Y7=P(J+3)
            Y8=Q(J+3)
            WRITE (6,3000) K,Y1,Y2,K1,Y3,Y4,K2,Y5,Y6,K3,Y7,Y8
   40    CONTINUE
   68    CONTINUE
   50 CONTINUE
C
C-----CALCULATE AVERAGE VALUES
C
      DO I=1,NT
         PAVG(I)=PAVG(I)/DFLOAT(NTSPC)
         QAVG(I)=QAVG(I)/DFLOAT(NTSPC)
         WRITE(7,4000) I,PAVG(I),QAVG(I),PMAX(I),QMAX(I),PMIN(I),QMIN(I)
      END DO
      RETURN
C
 2000 FORMAT(//' TIME = ',D10.4)
 3000 FORMAT(1X,4(I3,2X,2(D10.4,2X)))
 4000 FORMAT(1X,I3,6(2X,D10.4))
C
      END
C
C
      FUNCTION FPRES(T1)
CCCCCCCCCCCCCCCCCCCCCCCCCCCCCCCCCCCCCCCCCCCCCCCCCCCCCCCCCCCCCCCCCCCC
```

```
C                                                                       C
C     THIS FUNCTION PROVIDES THE INITIAL VALUE OF                       C
C     THE PRESSURE AT TIME T1                                           C
C                                                                       C
CCCCCCCCCCCCCCCCCCCCCCCCCCCCCCCCCCCCCCCCCCCCCCCCCCCCCCCCCCCCCCCCCCCCCCCC
      IMPLICIT REAL*8(A-H,O-Z)
      COMMON/BOUND/QBOUN(30,2),PBOUN(30,2)
      COMMON/NBOUN/NQB,NPB
      COMMON/PEE/PI
      COMMON/TDATA/DT,FREQ
C
      P=PBOUN(1,1)
      DO 10 I=2,NPB
         ARG=2.0D00*PI*(I-1)*FREQ*T1
         P=P+PBOUN(I,1)*DCOS(ARG)+PBOUN(I,2)*DSIN(ARG)
   10 CONTINUE
      FPRES=P
C
      RETURN
      END
C
C
      FUNCTION FFLOW(T1)
CCCCCCCCCCCCCCCCCCCCCCCCCCCCCCCCCCCCCCCCCCCCCCCCCCCCCCCCCCCCCCCCCCCCCCCC
C                                                                       C
C     THIS FUNCTION PROVIDES THE INITIAL VALUE OF                       C
C     THE FLOW AT TIME T1                                               C
C                                                                       C
CCCCCCCCCCCCCCCCCCCCCCCCCCCCCCCCCCCCCCCCCCCCCCCCCCCCCCCCCCCCCCCCCCCCCCCC
      IMPLICIT REAL*8(A-H,O-Z)
      COMMON/BOUND/QBOUN(30,2),PBOUN(30,2)
      COMMON/NBOUN/NQB,NPB
      COMMON/PEE/PI
      COMMON/TDATA/DT,FREQ
C
      Q=QBOUN(1,1)
      DO 10 I=2,NQB
         ARG=2.0D00*PI*(I-1)*FREQ*T1
         Q=Q+QBOUN(I,1)*DCOS(ARG)+QBOUN(I,2)*DSIN(ARG)
   10 CONTINUE
```

```
      FFLOW=Q
C
      RETURN
      END
```

APPENDIX C. FINITE ELEMENT CODE

```
CCCCCCCCCCCCCCCCCCCCCCCCCCCCCCCCCCCCCCCCCCCCCCCCCCCCCCCCCCCCCCCCCCCC
C                                                                     C
C     FINITE ELEMENT PROGRAM FOR THE ANALYSIS OF                      C
C           MULTI-BRANCHED ARTERIAL FLOW                              C
C                                                                     C
C                    MAIN PROGRAM                                     C
C                                                                     C
CCCCCCCCCCCCCCCCCCCCCCCCCCCCCCCCCCCCCCCCCCCCCCCCCCCCCCCCCCCCCCCCCCCC
      IMPLICIT REAL*8(A-H,O-Z)
      CHARACTER INFILE*20,OUTFILE*20
C
      COMMON/AREADT/AIN(150),AOUT(150),AVA(500)
      COMMON/BOUND/QBOUN(10,2),PBOUN(10,2)
      COMMON/CONDCT/CONDUCT(150)
      COMMON/COORDN/X(500),XLAST(150),COORD(800,2),CLAST(150,2)
      COMMON/FLUPRO/DENS,VISC
      COMMON/FRY/CV,CU
      COMMON/GRAVT/GRAV,GLOAD,GA(2),GZ(500)
      COMMON/ISEGMT/NEL(150),INDBRA(150),INDPAR(150),INDSTE(150)
     1             ,LFIRST(150)
      COMMON/NBOUN/NQB,NPB
      COMMON/NDATA/NS,NUEL,NT,NCYC
      COMMON/NDIMP/SIGMA1,SIGMA2,SIGMA3,PI1,PI2,PI3,PI4
      COMMON/PEE/PI
      COMMON/REFRNC/AREF,XREF,PREF,QREF
      COMMON/SEGDAT/COMPL0(150),COMPL1(150),SLEN(150),SPG(150),DA(150,2)
      COMMON/SODES/RTOL,ATOL
      COMMON/STENOS/XSTEN(150),STELEN(150),PRC(150)
     1             ,ST1(150),ST2(150),ST3(150)
      COMMON/TERMZ/RES1(150),RES2(150),CT(150)
      COMMON/TDATA/TIME,FREQ
```

```
      COMMON/VAINIT/PINIT(500),QINIT(500),YINIT(1600)
C
      10 FORMAT (' Data file: ',$)
*     READ (*,'(A)') INFILE
      I=NCHARS(INFILE)
      OUTFILE=INFILE(1:I)//'.OUT'
      OPEN (UNIT=5,FILE=INFILE,STATUS='UNKNOWN')
      OPEN (UNIT=6,FILE=OUTFILE,STATUS='UNKNOWN')
C
      CALL INPUT
      CALL NONDIM
      CALL SETUP
      CALL INIVAL
      CALL SOLVE
C
      STOP
      END
C
C
C
      SUBROUTINE INPUT
CCCCCCCCCCCCCCCCCCCCCCCCCCCCCCCCCCCCCCCCCCCCCCCCCCCCCCCCCCCCCCCCCC
C                                                                 C
C     THIS SUBROUTINE READS INPUT DATA                            C
C                                                                 C
CCCCCCCCCCCCCCCCCCCCCCCCCCCCCCCCCCCCCCCCCCCCCCCCCCCCCCCCCCCCCCCCCC
C
C-----INPUT PARAMETERS:
C
C--------------NS: # OF ARTERIAL SEGMENTS
C-------INDBRA(I): # OF THE FIRST BRANCH OF THE Ith SEGMENT
C                  (0 INDICATES TERMINAL BRANCH)
C-------INDPAR(I): # OF THE PARENT SEGMENT OF THE Ith SEGMENT
C-------INDSTE(I): LOCATION (ELEMENT #) OF STENOSIS (=0, NO STENOSIS)
C---------SLEN(I): SEGMENT LENGTH
C----------NEL(I): # OF ELEMENTS IN THE SEGMENTS
C----------AIN(I): AREA AT THE BEGINING OF THE SEGMENT
C---------AOUT(I): AREA AT THE END OF THE SEGMENT
C-------COMPL0(I): COMPLIANCE COEFFICIENT OF THE ARTERIAL WALL [C0]
C-------COMPL1(I): COMPLIANCE COEFFICIENT OF THE ARTERIAL WALL [C1]
```

```
C----------SPG(I): SEEPAGE OF THE SEGMENT
C-------DA(I,1-2): DIRECTIONAL ANGLES OF THE SEGMENT
C---------RES1(I): TERMINAL RESISTANCE 1
C---------RES2(I): TERMINAL RESISTANCE 2
C-----------CT(I): TERMINAL CAPACITANCE
C--------XSTEN(I): DISTANCE FROM BEGINING OF SEGMENT TO STENOSIS
C-------STELEN(I): LENGTH OF STENOSIS
C----------PRC(I): PERCENT AREA REDUCTION IN STENOSIS
C------------DENS: DENSITY
C------------VISC: VISCOSITY
C------------NCYC: # OF CYCLES
C------------FREQ: BASIC FREQUENCY OF EACH CYCLE
C-------------NQB: # OF FLOW HARMONICS
C-------------NPB: # OF PRESSURE HARMONICS
C----QBOUN(I,1-2): FLOW HARMONICS (INPUT)
C----PBOUN(I,1-2): PRESSURE HARMONICS (INPUT)
C-----------GLOAD: BODY FORCE IN MULTIPLES OF g (ACCL. OF GRAVITY)
C---------GA(1-2): ANGLES OF THE GLOAD VECTOR WRT COORDINATE SYSTEM
C------------TIME: TIME INCREMENT
C-------RTOL,ATOL: REQUIRED BY LSODES
C
      IMPLICIT REAL*8(A-H,O-Z)
      COMMON/AREADT/AIN(150),AOUT(150),AVA(500)
      COMMON/BOUND/QBOUN(10,2),PBOUN(10,2)
      COMMON/FLUPRO/DENS,VISC
      COMMON/FRY/CV,CU
      COMMON/GRAVT/GRAV,GLOAD,GA(2),GZ(500)
      COMMON/ISEGMT/NEL(150),INDBRA(150),INDPAR(150),INDSTE(150)
     1             ,LFIRST(150)
      COMMON/SODES/RTOL,ATOL
      COMMON/NBOUN/NQB,NPB
      COMMON/NDATA/NS,NUEL,NT,NCYC
      COMMON/SEGDAT/COMPLO(150),COMPL1(150),SLEN(150),SPG(150),DA(150,2)
      COMMON/STENOS/XSTEN(150),STELEN(150),PRC(150)
     1             ,ST1(150),ST2(150),ST3(150)
      COMMON/TERMZ/RES1(150),RES2(150),CT(150)
      COMMON/TDATA/TIME,FREQ
C
      READ (5,1000) NS
C
```

```
      DO 10 I=1,NS
         READ (5,2000) INDBRA(I),INDPAR(I),INDSTE(I),NEL(I),SLEN(I),
     1                 AIN(I),AOUT(I)
   10 CONTINUE
C
      READ (5,9000)
C
      DO 15 I=1,NS
         READ (5,2500)  COMPL0(I),COMPL1(I),SPG(I),DA(I,1),DA(I,2)
   15 CONTINUE
C
      READ (5,9000)
C
      DO 20 I=1,NS
         IF (INDBRA(I).GT.0) GOTO 20
         READ (5,3000) RES1(I),RES2(I),CT(I)
   20 CONTINUE
C
      KS=0
      DO I=1,NS
         KS=KS+INDSTE(I)
      END DO
      IF (KS.EQ.0) GOTO 26
C
      READ (5,9000)
C
      DO 25 I=1,NS
         IF (INDSTE(I).EQ.0) GOTO 25
         READ (5,3000)  XSTEN(I),STELEN(I),PRC(I)
   25 CONTINUE
   26 CONTINUE
C
      READ (5,4000) DENS,VISC
      READ (5,5000) NCYC,FREQ
      READ (5,4000) CV,CU
C
      READ (5,6000) NPB,NQB
      IF (NPB.GT.0) THEN
         DO 30 I=1,NPB
            READ (5,7000) PBOUN(I,1),PBOUN(I,2)
```

```
   30    CONTINUE
         ELSE
            DO 40 I=1,NQB
               READ (5,7000) QBOUN(I,1),QBOUN(I,2)
   40    CONTINUE
         END IF
C
      READ (5,8000) GRAV,GLOAD,GA(1),GA(2)
C
      READ (5,8000) TIME,RTOL,ATOL
C
C-----CALL VERIPT TO VERIFY INPUT DATA
C
      CALL VERIPT
      RETURN
C
C
 1000 FORMAT(1X/I3//)
 2000 FORMAT(3X,4(2X,I3),3(2X,D12.5))
 2500 FORMAT(3X,5(2X,D12.5))
 3000 FORMAT(3X,3(2X,D12.5))
 4000 FORMAT(//2(2X,D12.5))
 5000 FORMAT(//2X,I3,2X,D12.5)
 6000 FORMAT(//2(2X,I3)//)
 7000 FORMAT(2(2X,D12.5))
 8000 FORMAT(//4(2X,D12.5))
 9000 FORMAT(/)
C
      END
C
C
      SUBROUTINE VERIPT
CCCCCCCCCCCCCCCCCCCCCCCCCCCCCCCCCCCCCCCCCCCCCCCCCCCCCCCCCCCCCCCCC
C                                                                 C
C      THIS SUBROUTINE VERIFIES INPUT DATA                        C
C                                                                 C
CCCCCCCCCCCCCCCCCCCCCCCCCCCCCCCCCCCCCCCCCCCCCCCCCCCCCCCCCCCCCCCCC
      IMPLICIT REAL*8(A-H,O-Z)
      COMMON/AREADT/AIN(150),AOUT(150),AVA(500)
      COMMON/BOUND/QBOUN(10,2),PBOUN(10,2)
```

```
      COMMON/FLUPRO/DENS,VISC
      COMMON/FRY/CV,CU
      COMMON/GRAVT/GRAV,GLOAD,GA(2),GZ(500)
      COMMON/ISEGMT/NEL(150),INDBRA(150),INDPAR(150),INDSTE(150)
     1             ,LFIRST(150)
      COMMON/SODES/RTOL,ATOL
      COMMON/NBOUN/NQB,NPB
      COMMON/NDATA/NS,NUEL,NT,NCYC
      COMMON/SEGDAT/COMPLO(150),COMPL1(150),SLEN(150),SPG(150),DA(150,2)
      COMMON/STENOS/XSTEN(150),STELEN(150),PRC(150)
     1             ,ST1(150),ST2(150),ST3(150)
      COMMON/TERMZ/RES1(150),RES2(150),CT(150)
      COMMON/TDATA/TIME,FREQ
C
      WRITE (6,500)
      WRITE (6,1000) NS
C
      WRITE (6,1500)
      DO 10 I=1,NS
         WRITE (6,2000) I,INDBRA(I),INDPAR(I),INDSTE(I),NEL(I),SLEN(I),
     1                  AIN(I),AOUT(I)
   10 CONTINUE
C
      WRITE (6,2100)
      DO 15 I=1,NS
         WRITE (6,2200) I,COMPLO(I),COMPL1(I),SPG(I),DA(I,1),DA(I,2)
   15 CONTINUE
C
      WRITE (6,2500)
C
      DO 20 I=1,NS
         IF (INDBRA(I).GT.0) GOTO 20
         WRITE (6,3000) I,RES1(I),RES2(I),CT(I)
   20 CONTINUE
C
C
      WRITE (6,3100)
C
      DO 25 I=1,NS
         IF (INDSTE(I).EQ.0) GOTO 25
```

```
         WRITE (6,3000) I,XSTEN(I),STELEN(I),PRC(I)
   25 CONTINUE
C
      WRITE (6,3500)
      WRITE (6,4000) DENS,VISC
C
      WRITE (6,4500)
      WRITE (6,5000) NCYC,FREQ
C
      WRITE (6,5200)
      WRITE (6,4000) CV,CU
C
      WRITE (6,5500)
      WRITE (6,6000) NPB,NQB
      IF (NPB.GT.0) THEN
         WRITE (6,6500)
         DO 30 I=1,NPB
            WRITE (6,7000) PBOUN(I,1),PBOUN(I,2)
   30    CONTINUE
      ELSE
         WRITE (6,7500)
         DO 40 I=1,NQB
            WRITE (6,7000) QBOUN(I,1),QBOUN(I,2)
   40    CONTINUE
      END IF
C
      WRITE (6,8500)
      WRITE (6,8000) GRAV,GLOAD,GA(1),GA(2)
C
      WRITE (6,9000)
      WRITE (6,8000) TIME,RTOL,ATOL
C
      RETURN
C
  500 FORMAT(' NUMBER OF SEGMENTS')
 1000 FORMAT(7X,I4,//)
 1500 FORMAT('  SEG  BRA  PAR  STE  NEL  SEGM. LENGTH  INPUT AREA',
     11X,'   OUTPUT ')
 2000 FORMAT(1X,I3,4(2X,I3),6(2X,D12.5),2(2X,F4.1))
 2100 FORMAT(/'  SEG     COMPL0        COMPL1       SEEPAGE
```

```
     1   DIRECTIONAL COSINES')
 2200 FORMAT(1X,I3,5(2X,D12.5))
 2500 FORMAT(/'  SEG      RES1          RES2          CT')
 3000 FORMAT(1X,I3,3(2X,D12.5))
 3100 FORMAT(/'  SEG   X STENOSIS   STENOSIS LNGTH     %')
 3500 FORMAT(/'     DENSITY      VISCOSITY')
 4000 FORMAT(2(2X,D12.5))
 4500 FORMAT(/' # OF CYCLES    FREQUENCY')
 5000 FORMAT(4X,I3,7X,D12.5)
 5200 FORMAT(/'       CV            CU')
 5500 FORMAT(/' # OF PRESSURE FOURIER COEF.   # OF FLOW FOURIER COEF.')
 6000 FORMAT(10X,I3,25X,I3)
 6500 FORMAT(/'   P COS TERM    P SIN TERM')
 7000 FORMAT(2(2X,D12.5))
 7500 FORMAT(/'   Q COS TERM    Q SIN TERM')
 8000 FORMAT(4(2X,D12.5))
 8500 FORMAT(/'  ACCEL. GRAV.    GRAVIT. LOAD        ORIENT. ANGLES')
 9000 FORMAT(/'      TIME          RTOL          ATOL')
C
      END
C
C
      SUBROUTINE NONDIM
CCCCCCCCCCCCCCCCCCCCCCCCCCCCCCCCCCCCCCCCCCCCCCCCCCCCCCCCCCCCCCCCCC
C                                                                 C
C     THIS SUBROUTINE NON-DIMENSIONALIZES INPUT                   C
C     VARIABLES                                                   C
C                                                                 C
CCCCCCCCCCCCCCCCCCCCCCCCCCCCCCCCCCCCCCCCCCCCCCCCCCCCCCCCCCCCCCCCCC
C
C------------AREF: REFERENCE AREA
C------------XREF: REFERENCE LENGTH
C------------PREF: REFERENCE PRESSURE
C------------QREF: REFERENCE FLOW
C
      IMPLICIT REAL*8(A-H,O-Z)
      COMMON/AREADT/AIN(150),AOUT(150),AVA(500)
      COMMON/BOUND/QBOUN(10,2),PBOUN(10,2)
      COMMON/CONDCT/CONDUCT(150)
      COMMON/FLUPRO/DENS,VISC
```

```
      COMMON/FRY/CV,CU
      COMMON/GRAVT/GRAV,GLOAD,GA(2),GZ(500)
      COMMON/ISEGMT/NEL(150),INDBRA(150),INDPAR(150),INDSTE(150)
     1             ,LFIRST(150)
      COMMON/NBOUN/NQB,NPB
      COMMON/NDATA/NS,NUEL,NT,NCYC
      COMMON/NDIMP/SIGMA1,SIGMA2,SIGMA3,PI1,PI2,PI3,PI4
      COMMON/PEE/PI
      COMMON/REFRNC/AREF,XREF,PREF,QREF
      COMMON/SEGDAT/COMPL0(150),COMPL1(150),SLEN(150),SPG(150),DA(150,2)
      COMMON/STENOS/XSTEN(150),STELEN(150),PRC(150)
     1             ,ST1(150),ST2(150),ST3(150)
      COMMON/TDATA/TIME,FREQ
      COMMON/TERMZ/RES1(150),RES2(150),CT(150)
C
      PI=4.0D00*DATAN(1.0D00)
      OMEGA=2.0D00*PI*FREQ
C
C-----TAKE AREF AS THE AREA AT THE BIGINNING OF THE FIRST SEGMENT
C
      AREF=AIN(1)
C
C-----LET XREF BE THE LENGTH OF THE FIRST SEGMENT
C
      XREF=SLEN(1)
C
C-----LET PREF OR QREF BE THE ZERO (MEAN) TERM OF THE FOURIER SERIES
C-----GET QREF OR PREF THEN FROM THE RELATION QREF=PREF/RTOTAL
C-----WHERE RTOTAL IS THE TOTAL STEADY FLOW PERIPHERAL RESISTANCE
C
C-----CALCULATE THE TOTAL CONDUCTANCE FIRST (RTOTAL=1/CONDUCTANCE)
C
C--------CALCULATE THE CONDUCTANCE AT THE TERMINAL BRANCHES FIRST
C
      DO 10 I=1,NS
         IF (INDBRA(I).GT.0) GOTO 10
         CONDUCT(I)=1.0D00/(RES1(I)+RES2(I)
     1                      +8.0D00*VISC*SLEN(I)*PI/AOUT(I)**2)
   10 CONTINUE
C
```

```
C--------CALCULATE CONDUCT(I) FOR THE REST OF THE SEGMENTS
C
      DO 20 I=NS,1,-1
         K=INDBRA(I)
         IF (K.EQ.0) GOTO 20
         CONDUCT(I)=1.0D00/(1.0D00/(CONDUCT(K)+CONDUCT(K+1))
     1                      +8.0D00*VISC*PI*SLEN(I)/AOUT(I)**2)
   20 CONTINUE
C
C--------THE TOTAL RESISTANCE IS THE INVERSE OF THE
C--------CONDUCTIVITY OF THE FIRST SEGMENT
C
      RTOTAL=1.0D00/CONDUCT(1)
C
C-----CALCULATE PREF AND QREF
C
      IF (NPB.GT.0) THEN
         PREF=PBOUN(1,1)
         QREF=PREF/RTOTAL
      ELSE
         QREF=QBOUN(1,1)
         PREF=QREF*RTOTAL
      END IF
C
C-----NON-DIMENSIONALIZE AREAS, LENGTHS, PRESSURES, AND FLOWS
C
      DO 30 I=1,NS
         AIN(I)=AIN(I)/AREF
         AOUT(I)=AOUT(I)/AREF
         SLEN(I)=SLEN(I)/XREF
         IF (INDSTE(I).EQ.0) GOTO 30
            XSTEN(I)=XSTEN(I)/XREF
            STELEN(I)=STELEN(I)/XREF
   30 CONTINUE
C
      IF (NPB.GT.0) THEN
         DO 40 I=1,NPB
            DO 40 J=1,2
               PBOUN(I,J)=PBOUN(I,J)/PREF
   40    CONTINUE
```

```
      ELSE
         DO 50 I=1,NQB
            DO 50 J=1,2
               QBOUN(I,J)=QBOUN(I,J)/QREF
   50    CONTINUE
      END IF
C
C-----PRINT THE REFERENCE VALUES AREF,XREF,PREF, AND QREF
C
      WRITE (6,1000)
      WRITE (6,2000) AREF,XREF,PREF,QREF
C
C-----CALCULATE THE CONSTANT PARAMETERS INVOLVED IN THE
C-----NON-DIMENSIONALIZATION PROCESS
C
      B1=8.0D00*CV*PI*VISC/(DENS*AREF)
C
      SIGMA1=XREF*AREF*PREF*FREQ/QREF
      SIGMA2=XREF*AREF*(PREF**2)*FREQ/QREF
      SIGMA3=XREF*PREF/QREF
C
      PI1=2.0D00*QREF/(CU*FREQ*AREF*XREF)
      PI2=AREF*PREF/(DENS*CU*QREF*FREQ*XREF)
      PI3=B1/(CU*FREQ)
      PI4=-AREF*GRAV/(CU*QREF*FREQ)
C
      RETURN
C
 1000 FORMAT(/'     AREF          XREF          PREF         QREF')
 2000 FORMAT(4(2X,D12.5))
      END
C
C
      SUBROUTINE SETUP
CCCCCCCCCCCCCCCCCCCCCCCCCCCCCCCCCCCCCCCCCCCCCCCCCCCCCCCCCCCCCCCCC
C                                                               C
C      THIS SUBROUTINE SETS UP THE ELEMENTS,                    C
C      CALCULATES THE ELEMENT LEGTHS AND TYPES                  C
C      ASSIGNS THEIR CHARACTERISTIC VALUES, AND                 C
C      SETS UP A COORDINATE SYSTEM                              C
```

```
C                                                                       C
CCCCCCCCCCCCCCCCCCCCCCCCCCCCCCCCCCCCCCCCCCCCCCCCCCCCCCCCCCCCCCCCCCCCCCC
      IMPLICIT REAL*8(A-H,O-Z)
      COMMON/AREADT/AIN(150),AOUT(150),AVA(500)
      COMMON/COORDN/X(500),XLAST(150),COORD(800,2),CLAST(150,2)
      COMMON/ELEDAT/ELEN(500),ERES(500),EFLI(500)
      COMMON/FLUPRO/DENS,VISC
      COMMON/IELEMT/INDEL(500)
      COMMON/ISEGMT/NEL(150),INDBRA(150),INDPAR(150),INDSTE(150)
     1             ,LFIRST(150)
      COMMON/NDATA/NS,NUEL,NT,NCYC
      COMMON/NODES/NFIRST(150),NLAST(150)
      COMMON/PEE/PI
      COMMON/SEGDAT/COMPL0(150),COMPL1(150),SLEN(150),SPG(150),DA(150,2)
      COMMON/STENOS/XSTEN(150),STELEN(150),PRC(150)
     1             ,ST1(150),ST2(150),ST3(150)
      COMMON/TERMZ/RES1(150),RES2(150),CT(150)
      COMMON/TDATA/TIME,FREQ
C
C-----CALCULATE THE LENGTH FOR EACH ELEMENT ELEN(I) AND
C-----CHARACTERIZE THE ELEMENT TYPE INDEL(I)
C
C-----INDEL(0)=0: DUMMY ELEMENT
C-----INDEL(I)=1: "NORMAL ELEMENT"
C-----INDEL(I)=2: ELEMENT AT THE BEGINING OF A SEGMENT
C-----INDEL(I)=3: ELEMENT AT THE END OF A TERMINAL BRANCH
C-----INDEL(I)=4: ELEMENT PRECEDING A STENOSIS
C-----INDEL(I)=5: STENOSIS ELEMENT
C-----INDEL(I)=6: ELEMENT FOLLOWING A STENOSIS
C
C-----ELEN(I): LENGTH OF Ith ELEMENT
C-----LFIRST(I): FIRST ELEMENT OF THE Ith SEGMENT
C-----NUEL: TOTAL # OF ELEMENTS
C
      K=0
      NUEL=0

      DO 50 I=1,NS
         LFIRST(I)=K+1
         IF(INDSTE(I).EQ.0) THEN
```

```
C
C--------THERE IS NO STENOSIS IN THE SEGMENT
C
            DO 30 J=1,NEL(I)
               ELEN(J+K)=SLEN(I)/NEL(I)
               IF (J.EQ.1) THEN
                  INDEL(J+K)=2
               ELSE
                  INDEL(J+K)=1
               END IF
               NUEL=NUEL+1
   30       CONTINUE
         ELSE
C
C--------THERE IS A STENOSIS IN THE SEGMENT
C
            KPRES=INDSTE(I)-1
            KPOSTS=NEL(I)-INDSTE(I)
C
C-----------MARK ELEMENTS PRECEDING THE STENOSIS
C
            DO 35 J=1,KPRES
               ELEN(J+K)=XSTEN(I)/KPRES
               IF(J.EQ.1) THEN
                  INDEL(J+K)=2
               ELSE IF (J.EQ.KPRES) THEN
                  INDEL(J+K)=4
               ELSE
                  INDEL(J+K)=1
               END IF
   35       CONTINUE
C
C-----------STENOSIS ELEMENT
C
            J=INDSTE(I)
            ELEN(J+K)=STELEN(I)
            INDEL(J+K)=5
C
C-----------MARK ELEMENTS FOLLOWING THE STENOSIS
C
```

```
            DO 40 J=INDSTE(I)+1,NEL(I)
               ELEN(J+K)=(SLEN(I)-XSTEN(I)-STELEN(I))/KPOSTS
               IF(J.EQ.INDSTE(I)+1) THEN
                  INDEL(J+K)=6
               ELSE
                  INDEL(J+K)=1
               END IF
   40       CONTINUE
         END IF
         K=K+NEL(I)
C
C--------PUT A DUMMY ELEMENT AT THE END OF A BRANCHING SEGMENT
C
         IF (INDBRA(I).GT.0) THEN
            K=K+1
            ELEN(K)=0.0D00
            INDEL(K)=0
            NUEL=NUEL+1
         ELSE
            INDEL(K)=3
         END IF
   50 CONTINUE
C
C-----NT: TOTAL # OF NODES
C-----NFIRST(I): THE FIRST NODE OF THE Ith SEGMENT
C-----NLAST(I): THE LAST NODE OF THE Ith SEGMENT
C
C-----CALCULATE THE COORDINATES OF EACH NODE X(I)(ARC-LENGTH),
C-----COORD(I,1) (X-COORDINATE), AND COORD(I,2) (Y-COORDINATE)
C
C-----XLAST(I): THE COORDINATE OF THE LAST NODE OF Ith SEGMENT
C-----CLAST(I,1-2): X AND Y COORDINATES OF LAST NODE OF Ith SEGMENT
C
      K=0
      X(1)=0.0D00
      COORD(1,1)=0.0D00
      COORD(1,2)=0.0D00
      DO 80 I=1,NS
         NFIRST(I)=K+1
         L=INDPAR(I)
```

```
            IF (L.EQ.0) GOTO 60
            X(K+1)=XLAST(L)
            COORD(K+1,1)=CLAST(L,1)
            COORD(K+1,2)=CLAST(L,2)
   60       CONTINUE
            M=LFIRST(I)
            DO 70 J=1,NEL(I)
               X(K+J+1)=X(K+J)+ELEN(M+J-1)
               COORD(K+J+1,1)=COORD(K+J,1)+ELEN(M+J-1)*DA(I,1)
               COORD(K+J+1,2)=COORD(K+J,2)+ELEN(M+J-1)*DA(I,2)
   70       CONTINUE
            K=K+NEL(I)+1
            NLAST(I)=K
            XLAST(I)=X(K)
            CLAST(I,1)=COORD(K,1)
            CLAST(I,2)=COORD(K,2)
   80    CONTINUE
C
         NT=K
C
C
C-----CALCULATE THE MEAN AREA FOR EACH ELEMENT
C
         CALL AREA
C
C-----CALCULATE THE BODY FORCE PROJECTION ON EACH ELEMENT
C
         CALL GRAVIT
C
C-----CALCULATE THE STENOSIS COEFFICIENTS SKV(I),SK1(I),SK2(I), AND SK3(I)
C
         CALL STENOSIS
C
C-----PRINT OUT THE TOTAL NUMBER OF ELEMENTS, THE ELEMENT TYPE,
C-----THE ELEMENT LENGTH, AND THE ELEMENT AVERAGE AREA
C
         WRITE (6,1000) NUEL
         WRITE (6,2000)
         DO 100 I=1,NUEL
            WRITE (6,3000) I,INDEL(I),ELEN(I),AVA(I)
```

```
  100 CONTINUE
C
C-----PRINT OUT THE FIRST AND LAST NODE OF EACH SEGMENT
C-----AND THE COORDINATES OF THE LAST NODE
C
      WRITE (6,4000)
      DO 110 I=1,NS
         WRITE (6,5000) I,NFIRST(I),NLAST(I),XLAST(I),
     1                  CLAST(I,1),CLAST(I,2)
  110 CONTINUE
C
C-----PRINT OUT THE TOTAL NUMBER OF NODES AND THE
C-----COORDINATES OF EACH NODE
C
      WRITE (6,6000) NT
      WRITE (6,7000)
      DO 120 K=1,NT,5
         L=K+4
         WRITE (6,8000) (I,X(I),I=K,L)
  120 CONTINUE
C
      RETURN
C
 1000 FORMAT(//' NUMBER OF ELEMENTS'/8X,I3)
 2000 FORMAT(/' ELEMENT  TYPE    LENGTH       AVRG AREA')
 3000 FORMAT(2X,I3,5X,I3,2(2X,D12.5))
 4000 FORMAT(/' SEGMENT  FIRST_NODE  LAST_NODE       LAST_POINT_COORD.')
 5000 FORMAT(2X,I3,2(8X,I3),3(2X,D12.5))
 6000 FORMAT(//' NUMBER OF NODES'/5X,I3)
 7000 FORMAT(/20X,'NODE COORDINATES')
 8000 FORMAT(2X,5(I3,D12.5,1X))
      END
C
C
      SUBROUTINE AREA
CCCCCCCCCCCCCCCCCCCCCCCCCCCCCCCCCCCCCCCCCCCCCCCCCCCCCCCCCCCCCCCCCC
C                                                                  C
C      THIS SUBROUTINE CALCULATES THE ELEMENT AREA                 C
C                                                                  C
CCCCCCCCCCCCCCCCCCCCCCCCCCCCCCCCCCCCCCCCCCCCCCCCCCCCCCCCCCCCCCCCCC
```

```
      IMPLICIT REAL*8(A-H,O-Z)
      COMMON/AREADT/AIN(150),AOUT(150),AVA(500)
      COMMON/COORDN/X(500),XLAST(150),COORD(800,2),CLAST(150,2)
      COMMON/ISEGMT/NEL(150),INDBRA(150),INDPAR(150),INDSTE(150)
     1             ,LFIRST(150)
      COMMON/NDATA/NS,NUEL,NT,NCYC
      COMMON/NODES/NFIRST(150),NLAST(150)
      COMMON/SEGDAT/COMPLO(150),COMPL1(150),SLEN(150),SPG(150),DA(150,2)
      COMMON/TERMZ/RES1(150),RES2(150),CT(150)
C
C
      DO 20 I=1,NS
         SLOPE=(AOUT(I)-AIN(I))/SLEN(I)
         KF=NFIRST(I)
         KL=NLAST(I)
         KE=LFIRST(I)-1
         DO 10 J=KF,KL-1
            XM=(X(J+1)+X(J))/2.0D00
            KE=KE+1
            AVA(KE)=AIN(I)+SLOPE*(XM-X(KF))
   10    CONTINUE
   20 CONTINUE
C
      RETURN
      END
C
C
      SUBROUTINE STENOSIS
CCCCCCCCCCCCCCCCCCCCCCCCCCCCCCCCCCCCCCCCCCCCCCCCCCCCCCCCCCCCCCCCCC
C                                                                 C
C     THIS SUBROUTINE CALCULATES THE STENOSIS                     C
C     COEFFICIENTS                                                C
C                                                                 C
CCCCCCCCCCCCCCCCCCCCCCCCCCCCCCCCCCCCCCCCCCCCCCCCCCCCCCCCCCCCCCCCCC
      IMPLICIT REAL*8(A-H,O-Z)
      COMMON/AREADT/AIN(150),AOUT(150),AVA(500)
      COMMON/ISEGMT/NEL(150),INDBRA(150),INDPAR(150),INDSTE(150)
     1             ,LFIRST(150)
      COMMON/NDATA/NS,NUEL,NT,NCYC
      COMMON/FLUPRO/DENS,VISC
```

```
      COMMON/PEE/PI
      COMMON/REFRNC/AREF,XREF,PREF,QREF
      COMMON/STENOS/XSTEN(150),STELEN(150),PRC(150)
     1             ,ST1(150),ST2(150),ST3(150)
      COMMON/TDATA/TIME,FREQ
C
      REAL*8 KV,KT,KU,LA
C
C
      KU=1.20D00
      KT=1.52D00
      DO 10 I=1,NS
         KS=INDSTE(I)
         IF(KS.EQ.0) GOTO 10
         J=LFIRST(I)+KS-1
         A1=PRC(I)*AVA(J)*AREF
         D1=DSQRT(4.0D00*A1/PI)
         LA=0.83D00*STELEN(I)*XREF+1.64D00*D1
         D=DSQRT(4.0D00*AVA(J)*AREF/PI)
         KV=3.2D01*(LA/D)*(1.0D00/PRC(I))**2
         ST1(I)=(AVA(I)/(DENS*STELEN(I)*KU))*(AREF*PREF/QREF/FREQ/XREF)
         ST2(I)=-(KV*VISC)/(DENS*STELEN(I)*XREF*KU*D*FREQ)
         ST3(I)=-KT/(2.0D00*KU*STELEN(I)*AVA(J))
     1         *(1.0D00/PRC(I)-1)**2*(QREF/FREQ/AREF/XREF)
   10 CONTINUE
C
      RETURN
      END
C
C
      SUBROUTINE GRAVIT
CCCCCCCCCCCCCCCCCCCCCCCCCCCCCCCCCCCCCCCCCCCCCCCCCCCCCCCCCCCCCCCCCC
C                                                                 C
C      THIS SUBROUTINE CALCULATES THE BODY FORCE                  C
C      PROJECTION ON EACH ELEMENT                                 C
C                                                                 C
CCCCCCCCCCCCCCCCCCCCCCCCCCCCCCCCCCCCCCCCCCCCCCCCCCCCCCCCCCCCCCCCCC
      IMPLICIT REAL*8(A-H,O-Z)
      COMMON/GRAVT/GRAV,GLOAD,GA(2),GZ(500)
      COMMON/ISEGMT/NEL(150),INDBRA(150),INDPAR(150),INDSTE(150)
```

```
     1             ,LFIRST(150)
      COMMON/NDATA/NS,NUEL,NT,NCYC
      COMMON/NODES/NFIRST(150),NLAST(150)
      COMMON/PEE/PI
      COMMON/SEGDAT/COMPLO(150),COMPL1(150),SLEN(150),SPG(150),DA(150,2)
C
C
      DO 30 I=1,NS
         PROJ=0.0D00
         DO 10 J=1,2
            PROJ=PROJ+DA(I,J)*GA(J)
   10    CONTINUE
         KF=NFIRST(I)
         KL=NLAST(I)
         KE=LFIRST(I)-1
         DO 20 J=KF,KL-1
            KE=KE+1
            GZ(KE)=PROJ*GLOAD
   20    CONTINUE
   30 CONTINUE
C
      RETURN
      END
C
C
      SUBROUTINE INIVAL
CCCCCCCCCCCCCCCCCCCCCCCCCCCCCCCCCCCCCCCCCCCCCCCCCCCCCCCCCCCCCCCCC
C                                                               C
C      THIS SUBROUTINE ASSIGNS INITIAL PRESSURE AND             C
C      FLOW VALUES AT EACH NODE                                 C
C                                                               C
CCCCCCCCCCCCCCCCCCCCCCCCCCCCCCCCCCCCCCCCCCCCCCCCCCCCCCCCCCCCCCCCC
      IMPLICIT REAL*8(A-H,O-Z)
      COMMON/BOUND/QBOUN(10,2),PBOUN(10,2)
      COMMON/CONDCT/CONDUCT(150)
      COMMON/COORDN/X(500),XLAST(150),COORD(800,2),CLAST(150,2)
      COMMON/FLUPRO/DENS,VISC
      COMMON/GRAVT/GRAV,GLOAD,GA(2),GZ(500)
      COMMON/ISEGMT/NEL(150),INDBRA(150),INDPAR(150),INDSTE(150)
     1             ,LFIRST(150)
```

```
      COMMON/NBOUN/NQB,NPB
      COMMON/NDATA/NS,NUEL,NT,NCYC
      COMMON/NODES/NFIRST(150),NLAST(150)
      COMMON/REFRNC/AREF,XREF,PREF,QREF
      COMMON/SEGDAT/COMPL0(150),COMPL1(150),SLEN(150),SPG(150),DA(150,2)
      COMMON/TERMZ/RES1(150),RES2(150),CT(150)
      COMMON/VAINIT/PINIT(500),QINIT(500),YINIT(1600)
      DIMENSION FL(150),GFL(150)
C
C-----ASSUME CONSTANT PRESSURE PR AT EVERY SEGMENT
C-----(PR = PRESSURE AT TIME=0.)
C
      PR=FPRES(0.0D00)
C
C
C-----ASSIGN INITIAL FLOW VALUES BY DIVIDING Q
C-----ACCORDING TO THE CONDUCTIVITY OF EACH ELEMENT
C
      FL(1)=PR*CONDUCT(1)*(PREF/QREF)
      DO 10 I=1,NS
         IF (INDBRA(I).EQ.0) GOTO 10
         IB1=INDBRA(I)
         IB2=IB1+1
         FL(IB1)=FL(I)*CONDUCT(IB1)/(CONDUCT(IB1)+CONDUCT(IB2))
         FL(IB2)=FL(I)-FL(IB1)
   10 CONTINUE
C
C-----ADD TO THE INITIAL FLOW VALUES THE PORTION COMING FROM
C-----THE BODY FORCE TERM
C
      DO 20 I=1,NS
         IF(INDBRA(I).GT.0) GOTO 20
            HEAD=CLAST(I,1)*GA(1)+CLAST(I,2)*GA(2)
            GFL(I)=DENS*GRAV*GLOAD*HEAD*CONDUCT(I)*(XREF/QREF)
   20 CONTINUE
      DO 25 I=NS,1,-1
         K=INDBRA(I)
         IF (K.EQ.0) GOTO 25
            GFL(I)=GFL(K)+GFL(K+1)
   25 CONTINUE
```

```
C
C-----ASSIGN INITIAL PRESSURE PINIT(I) AND FLOW QINIT(I) VALUES
C-----TO ALL NODES
C
      K=0
      DO 40 I=1,NS
         KF=NFIRST(I)
         KL=NLAST(I)
         DO 30 J=KF,KL
            PINIT(J)=PR
            QINIT(J)=FL(I)+GFL(I)
   30    CONTINUE
   40 CONTINUE
C
C-----SUBSTITUTE THE PINIT AND QINIT VALUES TO THE YINIT VECTOR
C
      DO 50 I=1,NT
         IP=2*I-1
         IQ=2*I
         YINIT(IP)=PINIT(I)
         YINIT(IQ)=QINIT(I)
   50 CONTINUE
C
C-----PRINT OUT INITIAL VALUES FOR ALL NODES
C
      WRITE (6,1000)
      DO 60 K=1,NT,2
         L=K+1
         WRITE (6,2000) (I,PINIT(I),QINIT(I),I=K,L)
   60 CONTINUE
C
      RETURN
C
 1000 FORMAT(//,15X,'INITIAL PRESSURE AND FLOW VALUES',/)
 2000 FORMAT(2(1X,I3,2X,2(D12.5,1X)))
C
      END
C
C
      SUBROUTINE SOLVE
```

```
CCCCCCCCCCCCCCCCCCCCCCCCCCCCCCCCCCCCCCCCCCCCCCCCCCCCCCCCCCCCCCCCCCC
C                                                                    C
C     THIS SUBROUTINE MAKES USE OF THE SYSTEM ROUTINE                C
C     LSODES TO SOLVE THE SYSTEM OF ORDINARY                         C
C     DIFFERENTIAL EQUATIONS DEFINED BY FEX.                         C
C     IT PRINTS OUT THE PRESSURE AND FLOW WAVEFORMS                  C
C     OBTAINED.                                                      C
C                                                                    C
CCCCCCCCCCCCCCCCCCCCCCCCCCCCCCCCCCCCCCCCCCCCCCCCCCCCCCCCCCCCCCCCCCCC
C
      IMPLICIT REAL*8(A-H,O-Z)
      COMMON/NDATA/NS,NUEL,NT,NCYC
      COMMON/PEE/PI
      COMMON/REFRNC/AREF,XREF,PREF,QREF
      COMMON/SODES/RTOL,ATOL
      COMMON/VAINIT/PINIT(500),QINIT(500),YINIT(1600)
      COMMON/TDATA/TIME,FREQ
C
      DIMENSION Y(1600),RWORK(200000),IWORK(3200)
C
      EXTERNAL FEX
C
C-----ND=THE TOTAL # OF DEGREES OF FREEDOM
C
      ND=2*NT
C
C
C-----COPY YINIT TO Y TO START THE SOLUTION
C
      DO 5 I=1,ND
         Y(I)=YINIT(I)
    5 CONTINUE
C
C-----DEFINE THE PARAMETERS REQUIRED BY LSODES
C
C-----ITASK=1 FOR NORMAL COMPUTATION OF OUTPUT VALUES AT T=TOUT
C-----ISTATE=1 INTEGER FLAG
C-----IOPT=0 FOR NO OPTIONAL INPUT
C-----ITOL=1 FOR SCALAR ATOL
C-----MF=222 FOR STIFF MATRIX - INTERNALLY GENERATED JACOBIAN
```

```
C
      ITASK=1
      ISTATE=1
      IOPT=0
      ITOL=1
      MF=222
C
C-----NTS: NUMBER OF TIME STEPS
C
      DT=TIME*FREQ
      NTS=NCYC/DT+1
C     IPRN=NTS/100
C
C-----SOLVE THE SYSTEM OF DIFFERENTIAL EQUATIONS AT EACH TIME STEP
C
      T=0.0D0
      TOUT=0.0D0
      DO 30 I=1,NTS
         TOUT=TOUT+DT
C
C-----CALL LSODES TO SOLVE FOR THE VALUES AT T=TOUT
C
         CALL LSODES(FEX,ND,Y,T,TOUT,ITOL,RTOL,ATOL,ITASK,ISTATE,
     1               IOPT,RWORK,200000,IWORK,3200,JDUM,MF)
C
C-----FOR ISTATE NOT EQUAL TO 2 THERE IS AN ERROR IN THE SYSTEM
C
         IF (ISTATE.EQ.2) GOTO 10
            WRITE(6,1000) ISTATE
         STOP
   10    CONTINUE
C
C-----PRINT OUT ONLY 100 POINTS PER CYCLE
C
C     ICHECK=I/IPRN
C     IF(ICHECK*IPRN.NE.I) GOTO 25
C
C-----PRINT OUT THE NODAL VALUES OF PRESSURE AND FLOW AT T=TOUT
C
C        TYPE *, TOUT/FREQ
```

```
         WRITE (6,2000) TOUT/FREQ,IWORK(11)
         DO 20 J=1,ND,8
            K=J/2+1
            K1=K+1
            K2=K+2
            K3=K+3
            Y1=Y(J)*PREF
            Y2=Y(J+1)*QREF
            Y3=Y(J+2)*PREF
            Y4=Y(J+3)*QREF
            Y5=Y(J+4)*PREF
            Y6=Y(J+5)*QREF
            Y7=Y(J+6)*PREF
            Y8=Y(J+7)*QREF
            WRITE (6,3000) K,Y1,Y2,K1,Y3,Y4,K2,Y5,Y6,K3,Y7,Y8
   20    CONTINUE
   25    CONTINUE
   30 CONTINUE
      RETURN
C
  500 FORMAT(I2)
 1000 FORMAT(//' ISTATE=',I3//)
 2000 FORMAT(/' TIME = ',D12.6,'   NST = ',I5)
 3000 FORMAT(1X,4(I3,2X,2(D10.4,2X)))
C
      END
C
C
      SUBROUTINE FEX(ND,T,Y,YDOT)
CCCCCCCCCCCCCCCCCCCCCCCCCCCCCCCCCCCCCCCCCCCCCCCCCCCCCCCCCCCCCCCCCC
C                                                                  C
C     THIS SUBROUTINE PROVIDES LSODES WITH THE SET OF              C
C     ORDINARY DIFFERENTIAL EQUATIONS DY/DT=F(Pn,Qn)               C
C                                                                  C
CCCCCCCCCCCCCCCCCCCCCCCCCCCCCCCCCCCCCCCCCCCCCCCCCCCCCCCCCCCCCCCCCC
      IMPLICIT REAL*8(A-H,O-Z)
      COMMON/ELEDAT/ELEN(500),ERES(500),EFLI(500)
      COMMON/FLUPRO/DENS,VISC
      COMMON/IELEMT/INDEL(500)
      COMMON/ISEGMT/NEL(150),INDBRA(150),INDPAR(150),INDSTE(150)
```

```
     1             ,LFIRST(150)
      COMMON/NDATA/NS,NUEL,NT,NCYC
      COMMON/NODES/NFIRST(150),NLAST(150)
      COMMON/REFRNC/AREF,XREF,PREF,QREF
      COMMON/SEGDAT/COMPL0(150),COMPL1(150),SLEN(150),SPG(150),DA(150,2)
      COMMON/STENOS/XSTEN(150),STELEN(150),PRC(150)
     1             ,ST1(150),ST2(150),ST3(150)
      COMMON/TERMZ/RES1(150),RES2(150),CT(150)
      COMMON/TDATA/TIME,FREQ
C
      DIMENSION Y(ND),YDOT(ND),SKI(16),SKJ(16)
C
C-----PHASE 1.
C-----WRITE THE GENERAL EXPRESSIONS FOR YDOT
C-----FOR EACH DEGREE OF FREEDOM
C-----(INITIAL AND BOUNDARY CONDITIONS ARE GIVEN IN PHASE 2.)
C
      DO 20 I=1,NS
         NF=NFIRST(I)
         NL=NLAST(I)
         LF=LFIRST(I)
C
C--------WRITE THE EQUATIONS FOR THE FIRST NODE
C
         NP=2*NF-1
         NQ=2*NF
         CALL ELEMAT (LF,I,NP,NQ,ND,SKI,Y)
         YDOT(NQ)=SKI(5)*Y(NP)+SKI(6)*Y(NQ)
     1           +SKI(7)*Y(NP+2)+SKI(8)*Y(NQ+2)
C
C--------WRITE THE EQUATIONS BETWEEN THE FIRST AND LAST NODE
C--------OF EACH SEGMENT
C
         DO 10 J=NF+1,NL-1
            NP=2*J-1
            NQ=2*J
            LF=LF+1
            CALL ELEMAT (LF,I,NP,NQ,ND,SKJ,Y)
            IF(INDEL(LF).EQ.5) THEN
C
```

```
C--------------THE ELEMENT IS A STENOSIS
C--------------WRITE THE EQUATIONS FOR THE FIRST NODE OF STENOSIS
C
               YDOT(NP)=SKI(9)*Y(NP-2)+SKI(10)*Y(NQ-2)
     1                 +SKI(11)*Y(NP)+SKI(12)*Y(NQ)
C
C--------------STENOSIS EQUATION
C
               YDOT(NQ)=ST1(I)*(Y(NP)-Y(NP+2))+ST2(I)*Y(NQ)
     1                 +ST3(I)*Y(NQ)*DABS(Y(NQ))
            ELSE IF (INDEL(LF).EQ.6) THEN
C
C--------------ELEMENT FOLLOWING THE STENOSIS
C
               YDOT(NP)=SKJ(1)*Y(NP)+SKJ(2)*Y(NQ)
     1                 +SKJ(3)*Y(NP+2)+SKJ(4)*Y(NQ+2)
               YDOT(NQ)=YDOT(NQ-2)
            ELSE
C
C--------------"NORMAL ELEMENT
C
               YDOT(NP)=0.5D00*(SKI(9)*Y(NP-2)+SKI(10)*Y(NQ-2)
     1                 +(SKI(11)+SKJ(1))*Y(NP)+(SKI(12)+SKJ(2))*Y(NQ)
     2                 +SKJ(3)*Y(NP+2)+SKJ(4)*Y(NQ+2))
               YDOT(NQ)=0.5D00*(SKI(13)*Y(NP-2)+SKI(14)*Y(NQ-2)
     1                 +(SKI(15)+SKJ(5))*Y(NP)+(SKI(16)+SKJ(6))*Y(NQ)
     2                 +SKJ(7)*Y(NP+2)+SKJ(8)*Y(NQ+2))
            END IF
            DO 7 K=1,16
               SKI(K)=SKJ(K)
    7       CONTINUE
   10    CONTINUE
C
C--------WRITE THE EQUATIONS FOR THE LAST NODE
C
         NP=NL*2-1
         NQ=NL*2
         YDOT(NP)=SKI(9)*Y(NP-2)+SKI(10)*Y(NQ-2)
     1           +SKI(11)*Y(NP)+SKI(12)*Y(NQ)
C
```

```
   20 CONTINUE
C
C-----PHASE 2.
C-----APPLY THE INITIAL AND BOUNDARY CONDITIONS
C
      DO 30 I=1,NS
         NF=NFIRST(I)
         NL=NLAST(I)
         LF=LFIRST(I)
         IF (NF.EQ.1) THEN
C
C-----------APPLY THE INITIAL CONDITION
C
            YDOT(1)=FPRESD(T)
         ELSE
C
C-----------APPLY THE CONDITION AT THE BEGINNING OF A SEGMENT
C
            NP=2*NF-1
            IPAR=INDPAR(I)
            LPAR=NLAST(IPAR)
            NPL=2*LPAR-1
            YDOT(NP)=YDOT(NPL)
         END IF
C
C--------APPLY THE CONDITIONS AT THE DISTAL END OF THE SEGMENT
C
         NP=2*NL-1
         NQ=2*NL
         IF (INDBRA(I).EQ.0) THEN
C
C-----------CASE A. THE SEGMENT ENDS AT A TERMINAL IMPEDANCE
C
            IF (CT(I).GT.0.0D00) THEN
C
C--------------CASE A.1 WINDKESSEL MODEL
C
               YDOT(NQ)=YDOT(NP)*(1.0D00/RES1(I))*(PREF/QREF)
     1            +Y(NP)*(PREF/(RES1(I)*RES2(I)*CT(I)*QREF*FREQ))
     2            -Y(NQ)*(1.0D00+RES1(I)/RES2(I))/(RES1(I)*CT(I)*FREQ)
```

```
            ELSE
C
C--------------CASE A.2 SIMPLE RESISTANCE
C
               YDOT(NQ)=YDOT(NP)/(RES1(I)+RES2(I))*(PREF/QREF)
            END IF
         ELSE
C
C-----------CASE B. THE SEGMENT BIFURCATES
C
            IB=INDBRA(I)
            NF1=2*NFIRST(IB)
            NF2=2*NFIRST(IB+1)
            YDOT(NQ)=YDOT(NF1)+YDOT(NF2)
         END IF
C
   30 CONTINUE
C
C
      RETURN
      END
C
C
      SUBROUTINE ELEMAT (L,IS,NP,NQ,ND,SK,Y)
CCCCCCCCCCCCCCCCCCCCCCCCCCCCCCCCCCCCCCCCCCCCCCCCCCCCCCCCCCCCCCCCCC
C                                                                 C
C      THIS SUBROUTINE COMPUTES THE ELEMENT MATRIX                C
C                                                                 C
CCCCCCCCCCCCCCCCCCCCCCCCCCCCCCCCCCCCCCCCCCCCCCCCCCCCCCCCCCCCCCCCCC
      IMPLICIT REAL*8(A-H,O-Z)
      REAL*8 K1,K2,K3,M1,M2,M3,M4,LAMDA
C
      COMMON/AREADT/AIN(150),AOUT(150),AVA(500)
      COMMON/CONDCT/CONDUCT(150)
      COMMON/ELEDAT/ELEN(500),ERES(500),EFLI(500)
      COMMON/GRAVT/GRAV,GLOAD,GA(2),GZ(500)
      COMMON/NDATA/NS,NUEL,NT,NCYC
      COMMON/NDIMP/SIGMA1,SIGMA2,SIGMA3,PI1,PI2,PI3,PI4
      COMMON/REFRNC/AREF,XREF,PREF,QREF
      COMMON/SEGDAT/COMPL0(150),COMPL1(150),SLEN(150),SPG(150),DA(150,2)
```

```
      COMMON/TERMZ/RES1(150),RES2(150),CT(150)
C
      DIMENSION Y(ND),SK(16)
C
C-----CALCULATE THE ELEMENT COEFFICIENTS K1,K2,K3,M1,M2,M3, AND M4
C
      K1=SIGMA1*AVA(L)*COMPLO(IS)
      K2=SIGMA2*AVA(L)*COMPL1(IS)
      K3=SIGMA3*SPG(L)
C
      M1=PI1/(AVA(L))
      M2=PI2*AVA(L)
      M3=PI3/AVA(L)
      M4=PI4*AVA(L)*GZ(L)
C
C-----CALCULATE THE PARAMETERS APPEARING IN THE ELEMENT EQUATIONS
C
      PRATIO=Y(NP+2)/Y(NP)
      ETA=K2/(2.0D00*K1)
      AA=2.0D00+ETA*Y(NP)*(3.0D00+PRATIO)
      AB=1.0D00+ETA*Y(NP)*(1.0D00+PRATIO)
      AC=2.0D00+ETA*Y(NP)*(1.0D00+3.0D00*PRATIO)
C
      LAMDA=ELEN(L)*K1/6.0D00
      BETA=ELEN(L)/6.0D00
      DET=AA*AC-AB**2
      SIGMA=ELEN(L)*K3/6.0D00
      GAMMA=M2/2.0D00
C     QA=M1*(2.0D00*Y(NQ)+Y(NQ+2))/6.0D00
C     QB=M1*(Y(NQ)+2.0D00*Y(NQ+2))/6.0D00
      QA=0.0D0
      QB=0.0D0
      BA=ELEN(L)*M4/(2.0D00*Y(NP))
      BB=ELEN(L)*M4/(2.0D00*Y(NP+2))
      CAPK=ELEN(L)*M3/6.0D00
      DELTA=1.0D00/(LAMDA*DET)
C
C-----CALCULATE THE ELEMENT MATRIX SK(16) OF ELEMENT L
C
      SK(1)=SIGMA*DELTA*(AB-2.0D00*AC)
```

```
      SK(2)=0.5D00*DELTA*(AC-AB)
      SK(3)=SIGMA*DELTA*(2.0D00*AB-AC)
      SK(4)=-SK(2)
      SK(5)=(GAMMA-2.0D00*BA)/(3.0D00*BETA)
      SK(6)=(2.0D00*QA-QB-3.0D00*CAPK)/(3.0D00*BETA)
      SK(7)=(BB-GAMMA)/(3.0D00*BETA)
      SK(8)=(QB-2.0D00*QA)/(3.0D00*BETA)
      SK(9)=SIGMA*DELTA*(2.0D00*AB-AA)
      SK(10)=0.5D00*DELTA*(AA-AB)
      SK(11)=SIGMA*DELTA*(AB-2.0D00*AA)
      SK(12)=-SK(10)
      SK(13)=(GAMMA+BA)/(3.0D00*BETA)
      SK(14)=(2.0D00*QB-QA)/(3.0D00*BETA)
      SK(15)=(-GAMMA-2.0D00*BB)/(3.0D00*BETA)
      SK(16)=(QA-2.0D00*QB-3.0D00*CAPK)/(3.0D00*BETA)
C
C     WRITE(6,1000) ND,NP,NQ,Y(NP),Y(NP+2)
 1000 FORMAT(1X,' ND=',I3,'   NP=',I3,'   NQ=',I3,
     1   '    Y(NP)=',D12.5,'    Y(NP+2)=',D12.5)
      RETURN
      END
C
C
      FUNCTION FPRES(T1)
CCCCCCCCCCCCCCCCCCCCCCCCCCCCCCCCCCCCCCCCCCCCCCCCCCCCCCCCCCCCCCCCCC
C                                                                  C
C     THIS FUNCTION PROVIDES THE INITIAL VALUE OF                  C
C     THE PRESSURE AT TIME T1                                      C
C                                                                  C
CCCCCCCCCCCCCCCCCCCCCCCCCCCCCCCCCCCCCCCCCCCCCCCCCCCCCCCCCCCCCCCCCC
      IMPLICIT REAL*8(A-H,O-Z)
      COMMON/BOUND/QBOUN(10,2),PBOUN(10,2)
      COMMON/NBOUN/NQB,NPB
      COMMON/PEE/PI
      COMMON/TDATA/TIME,FREQ
C
      P=PBOUN(1,1)
      DO 10 I=2,NPB
         ARG=2.0D00*PI*(I-1)*T1
         P=P+PBOUN(I,1)*DCOS(ARG)+PBOUN(I,2)*DSIN(ARG)
```

```
   10 CONTINUE
      FPRES=P
C
      RETURN
      END
C
C
      FUNCTION FPRESD(T1)
CCCCCCCCCCCCCCCCCCCCCCCCCCCCCCCCCCCCCCCCCCCCCCCCCCCCCCCCCCCCCCCCCC
C                                                                 C
C     THIS FUNCTION PROVIDES THE INITIAL VALUE OF                 C
C     THE TIME DERIVATIVE OF PRESSURE AT TIME T1                  C
C                                                                 C
CCCCCCCCCCCCCCCCCCCCCCCCCCCCCCCCCCCCCCCCCCCCCCCCCCCCCCCCCCCCCCCCCC
      IMPLICIT REAL*8(A-H,O-Z)
      COMMON/BOUND/QBOUN(10,2),PBOUN(10,2)
      COMMON/NBOUN/NQB,NPB
      COMMON/PEE/PI
      COMMON/TDATA/TIME,FREQ
C
      PD=0.0D00
      DO 10 I=2,NPB
         ARGD=2.0D00*PI*(I-1)
         ARG=ARGD*T1
         PD=PD-PBOUN(I,1)*ARGD*DSIN(ARG)+PBOUN(I,2)*ARGD*DCOS(ARG)
   10 CONTINUE
      FPRESD=PD
C
      RETURN
      END
C
C
      FUNCTION FFLOW(T1)
CCCCCCCCCCCCCCCCCCCCCCCCCCCCCCCCCCCCCCCCCCCCCCCCCCCCCCCCCCCCCCCCCC
C                                                                 C
C     THIS FUNCTION PROVIDES THE INITIAL VALUE OF                 C
C     THE FLOW AT TIME T1                                         C
C                                                                 C
CCCCCCCCCCCCCCCCCCCCCCCCCCCCCCCCCCCCCCCCCCCCCCCCCCCCCCCCCCCCCCCCCC
      IMPLICIT REAL*8(A-H,O-Z)
```

```
      COMMON/BOUND/QBOUN(10,2),PBOUN(10,2)
      COMMON/NBOUN/NQB,NPB
      COMMON/PEE/PI
      COMMON/TDATA/TIME,FREQ
C
      Q=QBOUN(1,1)
      DO 10 I=2,NQB
         ARG=2.0D00*PI*(I-1)*T1
         Q=Q+QBOUN(I,1)*DCOS(ARG)+QBOUN(I,2)*DSIN(ARG)
   10 CONTINUE
      FFLOW=Q
C
      RETURN
      END
      FUNCTION FFLOWD(T1)
CCCCCCCCCCCCCCCCCCCCCCCCCCCCCCCCCCCCCCCCCCCCCCCCCCCCCCCCCCCCCCCCCC
C                                                                  C
C     THIS FUNCTION PROVIDES THE INITIAL VALUE OF                  C
C     THE TIME DERIVATIVE OF FLOW AT TIME T1                       C
C                                                                  C
CCCCCCCCCCCCCCCCCCCCCCCCCCCCCCCCCCCCCCCCCCCCCCCCCCCCCCCCCCCCCCCCCC
      IMPLICIT REAL*8(A-H,O-Z)
      COMMON/BOUND/QBOUN(10,2),PBOUN(10,2)
      COMMON/NBOUN/NQB,NPB
      COMMON/PEE/PI
      COMMON/TDATA/TIME,FREQ
C
      QD=0.0D00
      DO 10 I=2,NQB
         ARGD=2.0D00*PI*(I-1)
         ARG=ARGD*T1
         QD=QD-QBOUN(I,1)*ARGD*DSIN(ARG)+QBOUN(I,2)*ARGD*DCOS(ARG)
   10 CONTINUE
      FFLOWD=QD
C
      RETURN
      END
```

APPENDIX D. INPUT DATA FILE

NUMBER OF SEGMENTS
55

SEG#	BRAN	PARNT	STN	#NOD	SEGMT LENGTH	INPUT AREA	OUTPUT AREA
1	2	0	0	2	4.00000E-2	6.78866E-4	6.51440E-4
2	14	1	0	2	2.00000E-2	3.94081E-4	3.94081E-4
3	4	1	0	3	3.40000E-2	1.20763E-4	1.20763E-4
4	6	3	0	3	3.40000E-2	5.62122E-5	5.62122E-5
5	12	3	0	5	1.77000E-1	4.30084E-5	4.30084E-5
6	0	4	0	5	1.48000E-1	1.11036E-5	1.05209E-5
7	8	4	0	9	4.22000E-1	5.10222E-5	1.74974E-5
8	0	7	0	6	2.35000E-1	9.51148E-6	6.33470E-6
9	10	7	0	4	6.70000E-2	1.45220E-5	1.45220E-5
10	0	9	0	4	7.90000E-2	2.60155E-6	2.60155E-6
11	0	9	0	5	1.71000E-1	1.29462E-5	1.05209E-5
12	0	5	0	5	1.77000E-1	9.84229E-6	2.16424E-6
13	0	5	0	5	1.77000E-1	9.84229E-6	2.16424E-6
14	18	2	0	2	3.90000E-2	3.59681E-4	3.59681E-4
15	16	2	0	6	2.08000E-1	4.30084E-5	4.30084E-5
16	0	15	0	5	1.77000E-1	9.84229E-6	2.16424E-6
17	0	15	0	5	1.77000E-1	9.84229E-6	2.16424E-6
18	26	14	0	3	5.20000E-2	3.13531E-4	3.13531E-4
19	20	14	0	2	3.40000E-2	5.62122E-5	5.62122E-5
20	0	19	0	5	1.48000E-1	1.11036E-5	1.05209E-5
21	22	19	0	9	4.22000E-1	5.10222E-5	1.74974E-5
22	0	21	0	6	2.35000E-1	9.51148E-6	6.33470E-6
23	24	21	0	4	6.70000E-2	1.45220E-5	1.45220E-5
24	0	23	0	4	7.90000E-2	2.60155E-6	2.60155E-6
25	0	23	0	5	1.71000E-1	1.29462E-5	1.05209E-5
26	0	18	0	4	8.00000E-2	1.25664E-5	7.06858E-6
27	28	18	0	5	1.04000E-1	1.43139E-4	1.30698E-4

28	34	27	0	3	5.30000E-2	1.16899E-4	1.16899E-4
29	30	27	0	2	1.00000E-2	4.77836E-5	4.77836E-5
30	32	29	0	2	1.00000E-2	1.25664E-5	1.25664E-5
31	0	29	0	3	6.60000E-2	1.52053E-5	1.52053E-5
32	0	30	0	3	7.10000E-2	1.01788E-5	1.01788E-5
33	0	30	0	3	6.30000E-2	2.37583E-5	2.37583E-5
34	0	28	0	4	5.90000E-2	5.94467E-5	5.94467E-5
35	36	28	0	2	1.00000E-2	1.13097E-4	1.13097E-4
36	0	35	0	2	3.20000E-2	2.12371E-5	2.12371E-5
37	38	35	0	2	1.00000E-2	1.09359E-4	1.09359E-4
38	0	37	0	2	3.20000E-2	2.12371E-5	2.12371E-5
39	40	37	0	5	1.06000E-1	1.05683E-4	9.43432E-5
40	0	39	0	3	5.00000E-2	8.04247E-6	8.04247E-6
41	42	39	0	2	1.00000E-2	8.49486E-5	8.49486E-5
42	44	41	0	3	5.82000E-2	4.25447E-5	3.85000E-5
43	50	41	0	3	5.82000E-2	4.25447E-5	3.85000E-5
44	46	42	0	4	1.44000E-1	3.21700E-5	2.29022E-5
45	0	42	0	3	5.00000E-2	1.25660E-5	1.25660E-5
46	48	44	0	9	4.43000E-1	2.10741E-5	1.13411E-5
47	0	44	0	4	1.26000E-1	2.04282E-5	1.08686E-5
48	0	46	0	8	3.21000E-1	1.91665E-5	6.24580E-6
49	0	46	0	8	3.43000E-1	5.30929E-6	5.30929E-6
50	52	43	0	4	1.44000E-1	3.21700E-5	2.29022E-5
51	0	43	0	3	5.00000E-2	1.25660E-5	1.25660E-5
52	54	50	0	9	4.43000E-1	2.10741E-5	1.13411E-5
53	0	50	0	4	1.26000E-1	2.04282E-5	1.08686E-5
54	0	52	0	8	3.21000E-1	1.91665E-5	6.24580E-6
55	0	52	0	8	3.43000E-1	5.30929E-6	5.30929E-6

SEG#	COMPLO	COMPL1	SEEPAGE	ORIENTATION ANGLE
1	-.48530E-6	3.0794E-09	0.00000D+0	0.09000D+3
2	1.16650E-6	2.8208E-09	0.00000D+0	0.00000D+3
3	4.98820E-6	2.1620E-09	0.00000D+0	0.13500D+3
4	7.15050E-6	1.7170E-09	0.00000D+0	0.18000D+3
5	7.74630E-6	1.5746E-09	0.00000D+0	0.09000D+3
6	7.66060E-6	2.2096E-10	0.00000D+0	0.12000D+3
7	9.26730E-6	1.0976E-09	0.00000D+0	0.24000D+3
8	7.45900E-6	2.0325E-10	0.00000D+0	0.24000D+3
9	8.05040E-6	2.6030E-10	0.00000D+0	0.24000D+3
10	3.88430E-6	3.8352E-11	0.00000D+0	0.24000D+3

11	7.88450E-6	2.4264E-10	0.00000D+0	0.24000D+3
12	6.84260E-6	1.5751E-10	0.00000D+0	0.09000D+3
13	6.84260E-6	1.5751E-10	0.00000D+0	0.13500D+3
14	1.55090E-6	2.7589E-09	0.00000D+0	0.00000D+3
15	7.74680E-6	1.5745E-09	0.00000D+0	0.06000D+3
16	6.84260E-6	1.5751E-10	0.00000D+0	0.09000D+3
17	6.84260E-6	1.5751E-10	0.00000D+0	0.04500D+3
18	2.02360E-6	2.6817E-09	0.00000D+0	0.27000D+3
19	7.15050E-6	1.7170E-09	0.00000D+0	0.04500D+3
20	7.66060E-6	2.2096E-10	0.00000D+0	0.06000D+3
21	9.26730E-6	1.0976E-09	0.00000D+0	0.30000D+3
22	7.45900E-6	2.0325E-10	0.00000D+0	0.30000D+3
23	8.05040E-6	2.6030E-10	0.00000D+0	0.30000D+3
24	3.88430E-6	3.8352E-11	0.00000D+0	0.30000D+3
25	7.88450E-6	2.4264E-10	0.00000D+0	0.30000D+3
26	5.54300E-7	2.9180E-09	0.00000D+0	0.00000D+3
27	4.59810E-6	2.2348E-09	0.00000D+0	0.27000D+3
28	4.95530E-6	2.1683E-09	0.00000D+0	0.27000D+3
29	7.56190E-6	1.6201E-09	0.00000D+0	0.00000D+3
30	8.38010E-6	1.2662E-09	0.00000D+0	0.00000D+3
31	9.36680E-6	1.0505E-09	0.00000D+0	0.31500D+3
32	9.63070E-6	8.7312E-10	0.00000D+0	0.45000D+3
33	8.87870E-6	1.2487E-09	0.00000D+0	0.00000D+3
34	6.96760E-6	1.7584E-09	0.00000D+0	0.22500D+3
35	3.09500E-6	2.5017E-09	0.00000D+0	0.27000D+3
36	8.99390E-6	1.2077E-09	0.00000D+0	0.00000D+3
37	3.59640E-6	2.4148E-09	0.00000D+0	0.27000D+3
38	8.99390E-6	1.2077E-09	0.00000D+0	0.00000D+3
39	5.59580E-6	2.0450E-09	0.00000D+0	0.27000D+3
40	9.68730E-6	7.7582E-10	0.00000D+0	0.27000D+3
41	-.25920E-5	3.3951E-09	0.00000D+0	0.27000D+3
42	9.68961E-6	7.59771-10	0.00000D+0	0.31500D+3
43	9.68961E-6	7.59771-10	0.00000D+0	0.22500D+3
44	-.64348E-6	3.10359-09	0.00000D+0	0.31500D+3
45	-.18647E-4	5.51695-09	0.00000D+0	0.27000D+3
46	9.68610E-6	7.2179E-10	0.00000D+0	0.27000D+3
47	4.88360E-6	6.5690E-11	0.00000D+0	0.31500D+3
48	4.65380E-6	5.8506E-11	0.00000D+0	0.27000D+3
49	4.07200E-6	4.2755E-11	0.00000D+0	0.27000D+3
50	-.64348E-6	3.10359-09	0.00000D+0	0.22500D+3

51	-.18647E-4	5.51695-09	0.00000D+0	0.27000D+3
52	9.68610E-6	7.2179E-10	0.00000D+0	0.27000D+3
53	4.88360E-6	6.5690E-11	0.00000D+0	0.22500D+3
54	4.65380E-6	5.8506E-11	0.00000D+0	0.27000D+3
55	4.07200E-6	4.2755E-11	0.00000D+0	0.27000D+3

SEG	RES1	RES2	CT
6	.12020E+10	.48080E+10	.30955E-10
8	.10560E+10	.42240E+10	.35235E-10
10	.16860E+11	.67440E+11	.22069E-11
11	.10560E+10	.42240E+10	.35235E-10
12	.27800E+10	.11120E+11	.13384E-10
13	.27800E+10	.11120E+11	.13384E-10
16	.27800E+10	.11120E+11	.13384E-10
17	.27800E+10	.11120E+11	.13384E-10
20	.12020E+10	.48080E+10	.30955E-10
22	.10560E+10	.42240E+10	.35235E-10
24	.16860E+11	.67440E+11	.22069E-11
25	.10560E+10	.42240E+10	.35235E-10
26	.27800E+09	.11120E+10	.13384E-09
31	.72600E+09	.29040E+10	.51251E-10
32	.10820E+10	.43280E+10	.34389E-10
33	.46400E+09	.18560E+10	.80191E-10
34	.18600E+09	.74400E+09	.20005E-09
36	.22600E+09	.90400E+09	.16464E-09
38	.22600E+09	.90400E+09	.16464E-09
40	.13760E+10	.55040E+10	.27041E-10
45	.15872E+10	.63488E+10	.23443E-10
47	.95400E+09	.38160E+10	.39003E-10
48	.95400E+09	.38160E+10	.39003E-10
49	.11180E+10	.44720E+10	.33281E-10
51	.15872E+10	.63488E+10	.23443E-10
53	.95400E+09	.38160E+10	.39003E-10
54	.95400E+09	.38160E+10	.39003E-10
55	.11180E+10	.44720E+10	.33281E-10

DENSITY	VISCOSITY
0.10500D+4	0.45000D-2

CYCLES FREQUENCY TIME INCREMENT

```
 2     1.00000D00     0.50000D-3

     CV             CU
 1.00000D00     1.00000D00

NPB  NQB
 0   21

 Q COS TERM      Q SIN TERM
 0.86393E-4     0.00000E+0
 -.88455E-4     0.13368E-3
 -.52515E-4     -.12280E-3
 0.86471E-4     0.22459E-4
 -.26395E-4     0.22693E-4
 -.12987E-4     0.22398E-5
 0.20133E-5     -.22315E-4
 0.70896E-5     0.10065E-4
 0.32577E-5     -.21066E-5
 -.56573E-5     0.90633E-5
 -.19302E-5     -.85422E-5
 0.22387E-5     0.14770E-5
 0.23050E-5     -.32397E-5
 0.11909E-5     0.59775E-5
 -.39818E-5     -.18464E-5
 0.58176E-6     -.14751E-5
 0.19556E-5     -.12112E-5
 0.48907E-6     0.24434E-5
 -.66338E-6     0.50967E-6
 -.21719E-5     -.23241E-6
 0.19705E-5     -.20190E-5

 ACC. GRAV.     GRAV. LOAD      ANGLE
 9.81000D00     2.00000D+0     0.27000D+3
```